ISSN No. 0737-5352-78

A STUDY OF TROPICAL CYCLONE STRUCTURAL EVOLUTION

Katherine S. Maclay
Thomas H. Vonder Haar

Funding for this research was sponsored by CIRA activities and participation in the GOES Improved Measurement Product Assurance Plan (GIMPAP) under NOAA cooperative agreement NA17RJ1.

CIRA Cooperative Institute for Research in the Atmosphere

Colorado State University

THESIS

A STUDY OF TROPICAL CYCLONE STRUCTURAL EVOLUTION

Submitted By

Katherine S. Maclay

Department of Atmospheric Science

In partial fulfillment of the requirements
For the Degree of Master of Science
Colorado State University
Fort Collins, CO
Fall 2006

ABSTRACT OF THESIS

A STUDY OF TROPICAL CYCLONE STRUCTURAL EVOLUTION

The destructive potential of a tropical cyclone is highly dependent on both the intensity and size of the storm. There has been extensive research done on intensity and intensity change, but far less work has focused on tropical cyclone structure and structural changes. The recent highly active Atlantic tropical seasons reemphasize the need for a better understanding of tropical cyclone structural evolution. This is particularly true of the 2005 season which produced a number of storms, such as Katrina, Rita, and Wilma, that not only became extremely intense, but also grew substantially in size during intensification. In contrast to these giants are the storms such as Hurricanes Charley (2004) and Emily (2005), which reached equal intensity, but remained fairly small in size. The goal of this study is to gain a better understanding of what causes these different structural evolutions in tropical cyclones.

The inner core (0-200 km) wind-fields of Atlantic and Eastern Pacific tropical cyclones from 1995-2005 from aircraft reconnaissance flight-level data is used to calculate the low-level inner core kinetic energy. An inner core kinetic energy-intensity relationship is defined which describes the general trend of tropical cyclone inner core kinetic energy (KE) with respect to intensity. However, this mean KE/intensity relationship does not define the evolution of an individual storm. The KE deviations from the mean relationship for each storm are used to determine the cases where a storm is experiencing significant structural changes. The evolution of the KE deviations from the mean with respect to intensity indicates that hurricanes generally either grow and weaken or maintain their intensity, or strengthen but do not grow at the same time. The

data is sorted by the state of intensification (intensifying, weakening, or maintaining intensity) and structure change (growing or non-growing), defining six sub-groups. The dynamic, thermodynamic, and internal conditions for the storm sub-groups are analyzed with the aid of statistical testing in order to determine what conditions are significantly different for growing versus non-growing storms in each intensification regime. These results reveal that there two primary types of growth processes. The first is through eyewall replacement cycles, an internally dominated process, and the second via external forcing from the synoptic environment.

As a supplement to this study, a new tropical cyclone classification system based on inner core KE is presented as a complement to the Saffir-Simpson hurricane scale.

Katherine S. Maclay
Department of Atmospheric Science
Colorado State University
Fort Collins, CO 80523
Fall 2006

ACKNOWLEDGEMENTS

First and foremost I would like to thank my advisor Dr. Vonder Haar and my mentor Mark DeMaria for all the support and guidance they provided in the past two years. I would also like to thank my other committee members Dr. Schubert and Dr. Krueger for their comments and reviews of this work.

There are a number of people who were helpful to me throughout this research. From CIRA I would like to thank John Knaff, Ray Zehr and Jack Dostalek for the guidance and help they provided. I would like to recognize the Schubert Group "Hurricane Specialists" Brian McNoldy, Chris Rozoff, and Jonathan Vigh for always being willing and eager to discuss anything hurricane related. I would also like to thank fellow Vonder Haar students Rebecca Mazur, Kevin Donofrio, and Dustin Rapp for all their support. Lastly, but most importantly, I would like to thank all of my friends and family for their love and encouragement!

Funding for this research was sponsored by CIRA activities and participation in the GOES Improved Measurement Product Assurance Plan (GIMPAP) under NOAA cooperative agreement NA17RJ1228.

TABLE OF CONTENTS

CHAPTER 1 – INTRODUCTION

There is a large amount of variation in the size, intensity and structure of tropical cyclones. Much research has focused on the area of tropical cyclone intensity; however, far less work has been done on the problem of size and structure change. The terminology used to describe the characteristics of tropical cyclones has varied in the literature, so in order to avoid confusion, the following terms and definitions will be used for this work.

- *Intensity*: Tropical cyclone intensity is traditionally based on either maximum sustained surface wind speed or minimum central pressure. Intensification is indicated by either an increase in the maximum sustained wind or a decrease in the minimum central pressure.
- *Size*: This refers to the horizontal dimension of the cyclone circulation. In forecasting this has often been measured by the extent of gale-force winds (17 ms^{-1}), or as the average radius of the outer closed isobar. Growth refers to an expansion of the cyclone circulation. In this study the inner core, low-level kinetic energy is used as an indicator of growth.
- *Strength*: This parameter is a measure of a cyclone's combined intensity and size. A storm's strength can change while the maximum wind and extent of gale-force winds remain constant. The definitions of strength have varied considerably in past studies. Merrill (1984) measured strength as the average wind speed in the cyclone circulation. Weatherford and Gray (1988a) defined and measured outer-core strength as an area-weighted average storm relative tangential wind speed

from 1° to 2.5° (111-278 km) radius. Holland and Merrill (1984) defined strength as the average relative angular momentum of the low-level inner circulation (within the 300 km radius). In this study, strength is only considered conceptually and not quantitatively.

Fig. 1.1, from Holland and Merrill (1984), illustrates changes in intensity, size and strength from an initial azimuthally averaged tangential wind profile. Note that changes in intensity, size or strength can occur independently of the other two components.

The structure and size of a tropical cyclone is a significant component of a storm's destructive potential. For a large storm with hurricane force winds extending out over a large area compared to a small storm of equal intensity not only will the wind damage be great, but such a storm will also generate a larger storm surge. Storm surge is a very serious threat to coastal regions and the damage it causes is often greater than that of the winds. This was dramatically demonstrated by Hurricane Katrina (2005), which caused unprecedented storm surge damage to portions of Louisiana and Mississippi. Therefore, it is important to understand and forecast a storm's structural evolution. This study will use the maximum sustained wind as a measure of storm intensity and intensification; and changes in the inner core, low-level kinetic energy, which relates to strength, will be used as an indicator of growth.

The typical life cycle of a tropical cyclone, as described by Dunn and Miller (1960) and Riehl (1979), is given by four stages:

1) *The formative stage* – a period from the development of the initial vortex to the first occurrence of hurricane-force winds. The cyclone typically contracts slightly and develops its characteristic high-energy core during this stage.

2) *The immature stage* – a time of rapid intensification with only a very slight change in size. Generally, the cyclone will achieve its maximum wind at the end of this stage.

3) *The mature stage* – the cyclone begins to grow during this stage, but no longer increases in intensity.

4) *The decaying stage* – a period when the cyclone reaches its greatest size and beings to collapse, while the maximum winds diminish.

This life cycle generally describes the evolution of a tropical cyclone, including its size development. However, historical evidence shows that some storms experience relatively small growth during their life cycle while others grow substantially. Hurricanes Charley 2004 and Emily 2005 are two storms which grew very little in size, as shown by the plots of their respective wind swaths during their lifetimes (Figs. 1.2 and 1.3). In contrast, Hurricanes Katrina and Wilma from the 2005 season represent storms that grew significantly in size through the course of their evolution, as is well illustrated in Figs. 1.4 and 1.5 by the respective wind swath plots for Katrina and Wilma. In the case of intense hurricanes in particular, size change is a critical feature to understand and forecast.

Consider more closely the structural evolution of Hurricanes Charley 2004 and Wilma 2005, both of which formed in the Caribbean Sea and made land-fall in similar locations in southwest Florida. Hurricane Charley 2004 formed in the Caribbean off the coast of Jamaica as a small storm and traveled north over Cuba into the Gulf of Mexico. It made land-fall on the west coast of Florida as a category 4 hurricane on the Saffir-Simpson Hurricane Scale. The storm intensified from a category 2 to a category 4 within a time span of approximately 5 hours shortly before making land-fall in Florida, but it

remained small throughout this intensification. At land-fall the extreme 125 knot winds were confined to a very small area within six nautical miles of the center of the storm. A wind swath plot of Hurricane Charley shows that the storm gained very little size throughout its lifetime.

A far different development occurred with Hurricane Wilma 2005, which formed farther southwest in the Caribbean as a small, intense storm. Observations from Air Force reconnaissance indicated that at the storm's peak intensity (160 kt winds with a minimum sea level pressure of 882 mb) its eye was a remarkable 2 nautical miles in diameter. The hurricane then grew substantially in size, with its record breaking tiny eye being replaced by a much larger 40 nautical mile diameter eye. It remained a large storm as it traveled up over the Yucatan peninsula and into the Gulf of Mexico before turning sharply eastward towards Florida and finally making land-fall just north of the Everglades as a category 3 hurricane. The hurricane force winds for Wilma extended over a much larger area of Florida than for Charley, as is illustrated by the wind swath plots of hurricane and tropical storm force winds. Infrared satellite images of Hurricanes Charley and Wilma at the time of the respective Florida land-falls are shown in Figs. 1.6 and 1.7. The difference in size of these storms is clearly evident. These storms, while unique in their own right, are not anomalies with respect to their structure changes. The focus of this study is to gain a better understanding of what causes variability in tropical cyclone size.

1.1 Background Information on the Structural Evolution of Tropical Cyclones

Tropical cyclone structure and structural evolution was investigated by Weatherford and Gray (1988a-b) using U.S. Air Force aircraft reconnaissance data of

northwest Pacific tropical cyclones from 1980 to 1982. Recognizing the great value of the aircraft reconnaissance data, Weatherford and Gray (hereafter, W-G) documented and stratified the minimum sea level pressure and outer core wind strength with respect to the location, time of year and day, and the speed and direction of storm motion. W-G found that tropical cyclones generally have greater outer core wind circulations at higher latitudes, which was shown previously by Merrill (1984). Both Merrill and W-G found that the relationship between tropical cyclone intensity change and size change is weak. However, W-G noted that typically inner core intensification precedes increased winds in the outer core, and furthermore, inner core filling usually precedes outer core weakening. In other words, generally both intensification and weakening in tropical cyclones occurs from the inner core outwards. W-G further noted that increased wind speeds in the outer core result in an increased inertial stability in the outer core thereby decreasing the inflow. Decreasing the inflow lessens the angular momentum transport into the inner core of the storm inhibiting further intensification. Finally, W-G hypothesized that the outer core is more influenced by the lower tropospheric environmental flow conditions than the concentration of inner core convection.

Results from a study of large, medium, and small sized Western North Pacific typhoons by Cocks and Gray (2002) suggest that the synoptic environment may be a key factor in determining tropical cyclone size. They also found that generally small tropical cyclones were smaller than the medium and large storms early in their life cycle. Additionally, the large tropical cyclones were generally significantly larger than small and medium storms by a quarter of the way through their life cycle.

A number of studies have investigated the effects of various environments on the structure and intensity of tropical cyclones with the specific emphasis on the effects of heat and angular momentum sources. Challa and Pfeffer (1980) carried out a numerical modeling study, using Sundqvist's (1970) axisymmetric model, on the effects environmental forcing has on tropical cyclone intensification. They found that an upper-level axisymmetric forcing produced intensification but little size change. However, a low-level forcing produced a considerable size change, which led to intensity change, and hence, a much stronger storm. Even with sub-critical sea surface temperatures (< 26°C) they found intensification could be maintained by the environmental forcing.

Shapiro and Willoughby (1982) studied the response of a balanced symmetric vortex to heat and momentum sources using a diagnostic technique developed by Eliassen (1951). Their results suggest that heat and momentum sources may contribute equally to the intensification process. The intensification effects caused by a momentum source support the previous results of Challa and Pfeffer (1980). Furthermore, they found that while the heat source primarily increased the tangential winds inwards from the source there was also a notable increase in the winds outwards from the source. This effect could extend to great distances from the heat source.

Holland and Merrill (1984) found that inner core convection along with upper tropospheric environmental forcing can result in intensity and strength changes, but has little effect on size. For a size or large strength change a substantial import of angular momentum is necessary (Holland 1983a). This can be provided by lower tropospheric environmental forcing. Low-level forcing is not likely to directly affect the inner core of

the storm because of the high inertial stability in the outer core regions which inhibits inflow and the transport of angular momentum into the inner core.

These studies have provided some useful insights into the possible mechanisms for intensity and structure change in tropical cyclones. However, the models are greatly simplified which should be taken into account when considering the accuracy of these findings.

1.2 Focus of this Study

In this study the inner core (0-200 km) wind-fields of tropical cyclones from 1995 to 2005, derived from the aircraft flight level data, are used to calculate the low level inner core kinetic energy. Note that the definition of inner core differs from that of W-G. W-G define the inner core as the region 0-1° or 0-111 km radius and the outer core as the region 1°-2.5° or 111-278 km radius. The inner core defined in this study incorporates W-G's inner core as well as a portion of what they consider outer core. The kinetic energy is used as a measure of storm growth, since it takes into account the inner core area integrated winds. The kinetic energies for the entire dataset are plotted against the intensities revealing a general trend of mean kinetic energy (KE) compared to intensity. Intensity is defined in this study by the maximum wind in the storm. The deviations from this mean KE/maximum wind relationship are used to identify cases that are undergoing significant structural changes.

Although, in the mean, KE increases as maximum wind increases, significant changes in storm size and intensity usually do not occur simultaneously, as was found in previous studies. The data is sorted into six groups which are defined by the storm's state of intensification and growth. In an effort to determine possible factors leading to these

intensification-growth cases, a statistical analysis of GOES infrared data is carried out to determine the convective profiles of heating for each group. The environmental conditions and synoptic environments most significant for each group are analyzed using NCEP reanalysis fields. Special emphasis is given to the anomalous cases where a storm intensifies and grows, or weakens and does not grow. Previous studies highlight convective heating and angular momentum sources from the surrounding synoptic environment as possible factors for storm growth. The combination of an 11-year sample of reconnaissance data, GOES observations and reanalysis fields will shed further light on the mechanisms that lead to storm size change, since both the inner core and environmental effects are examined for the same cases.

As an offshoot of this research, a new hurricane scale based on inner core KE is proposed. The highly active hurricane seasons of 2004 and 2005 and the devastation caused by Hurricane Katrina 2005 to Louisiana and Mississippi, and specifically New Orleans, have sparked increased concern over the effectiveness of the Saffir-Simpson Hurricane Scale (hereafter, SSHS or SS scale) in alerting the public accurately to the potential danger of a storm. Kantha (2006) proposed replacing the SSHS with a dynamic-based, continuous scale similar to that which is used for earthquakes. While such a scale would have the benefit of improved accuracy, it adds a large element of complication. Much of the beauty and success of the SSHS is in its simplicity. A simpler classification designed to complement the SSHS can be determined using the inner core KE. The advantage of using KE in a hurricane scaling system is that it takes into account both intensity and size of the storm, whereas the SSHS only uses the storm's

intensity. Incorporating size should give a better estimate of the potential damage by severe winds, intense rain, and storm surge.

The data sets used for this study are described in Chapter 2. This includes the aircraft reconnaissance data, satellite data (GOES IR and SSM/I/SSMIS microwave data), and the environmental condition data (SHIPS predictor variables and NCEP reanalysis data). Chapter 3 contains a description of the methodology used to create the inner core kinetic energy climatology, as well as a proposed new hurricane scale based on KE. The KE scale and SS scale are compared by looking at all U.S. land-falling hurricanes from 1995 through 2005. An analysis of storm KE evolution and six intensification/growth cases are also defined in Chapter 3. The results of the statistical analysis of the convective profiles, environmental conditions, and synoptic environments associated with the cases are given in Chapter 4. Finally, Chapter 5 provides a summary of the results of this study as well as a discussion of future work.

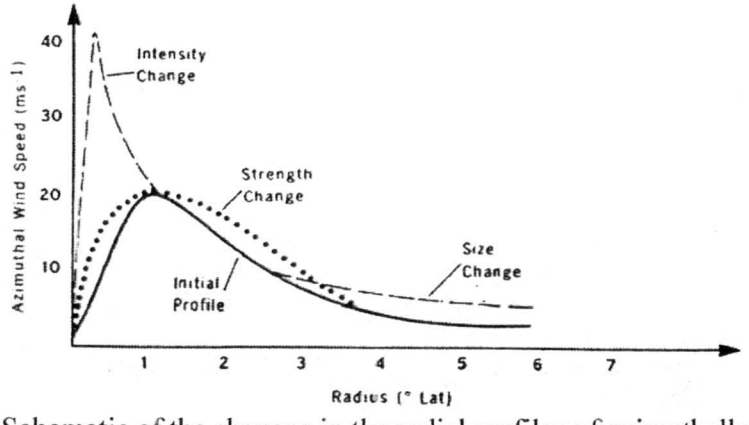

Figure 1.1: Schematic of the changes in the radial profiles of azimuthally averaged tangential wind speed (ms^{-1}) for intensity, strength, and size changes (Holland and Merrill (1984)).

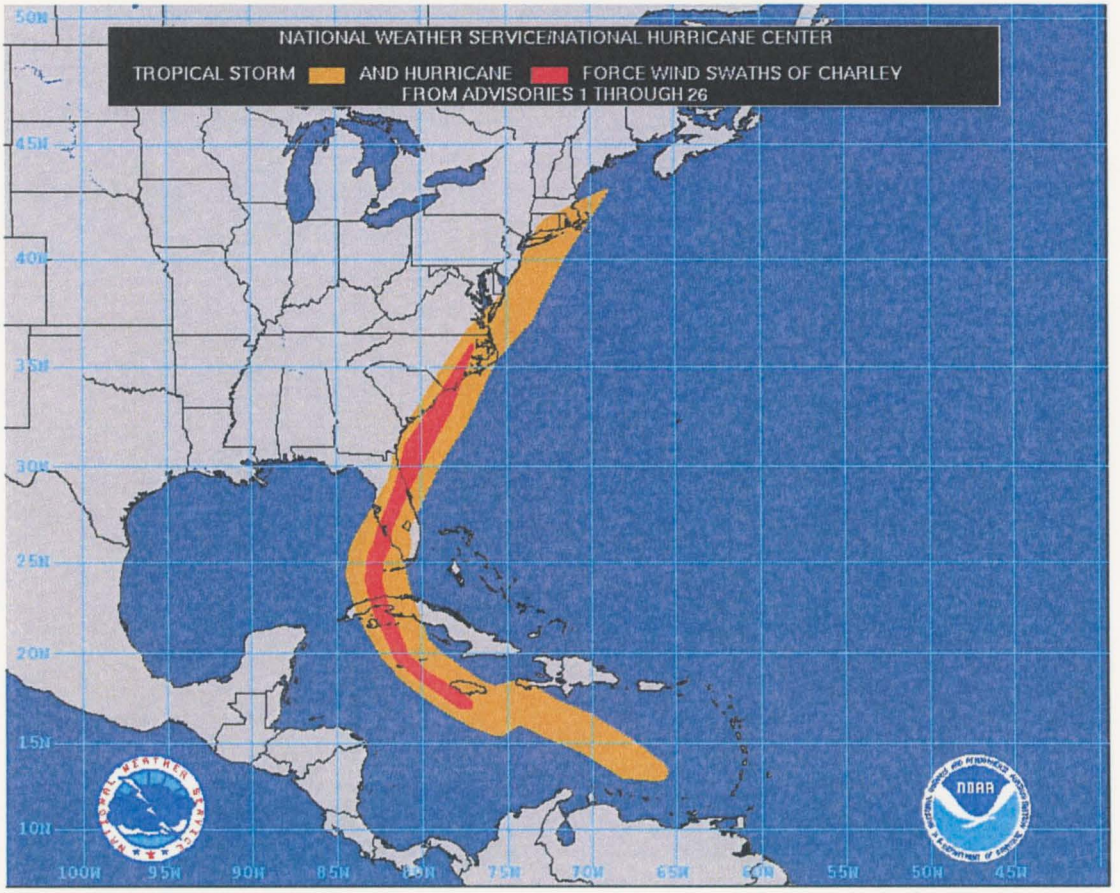

Figure 1.2: Wind swath plot of tropical storm and hurricane force winds for Hurricane Charley 2004 (NHC archived data).

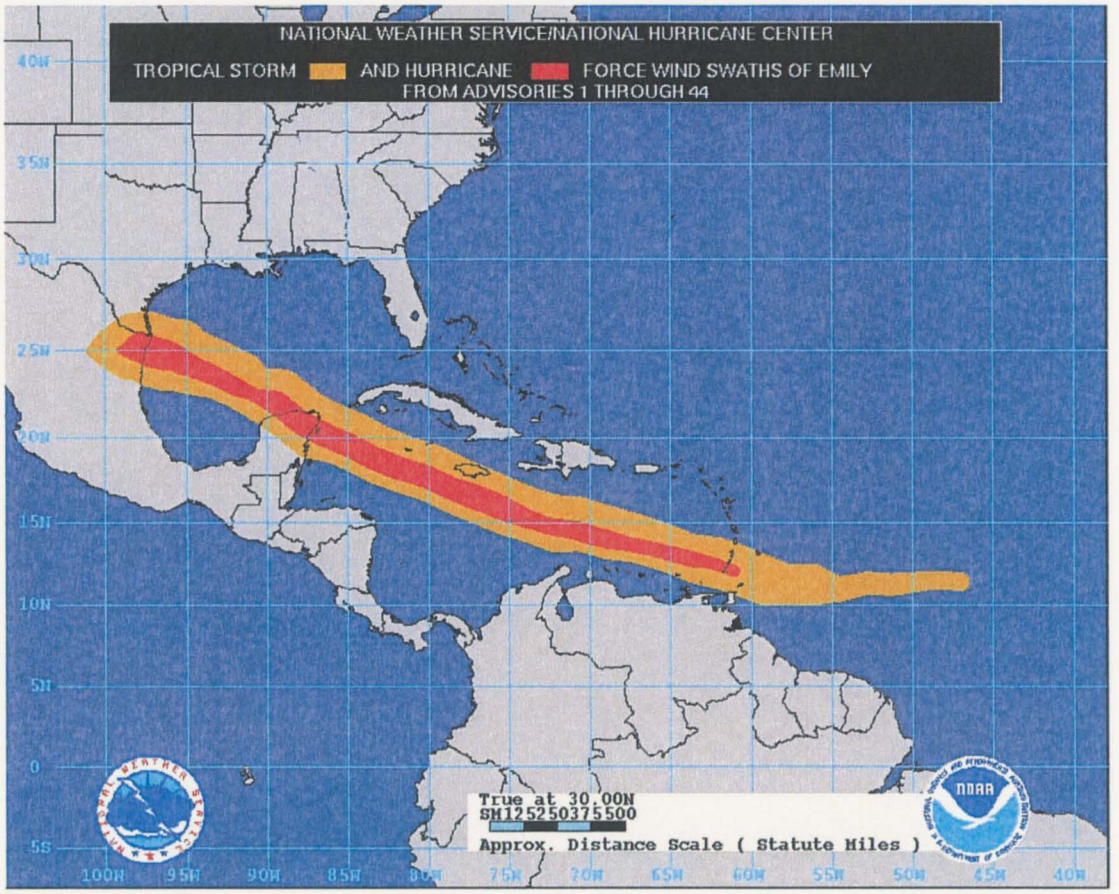

Figure 1.3: Wind swath plot of tropical storm and hurricane force winds for Hurricane Emily 2005 (NHC archived data).

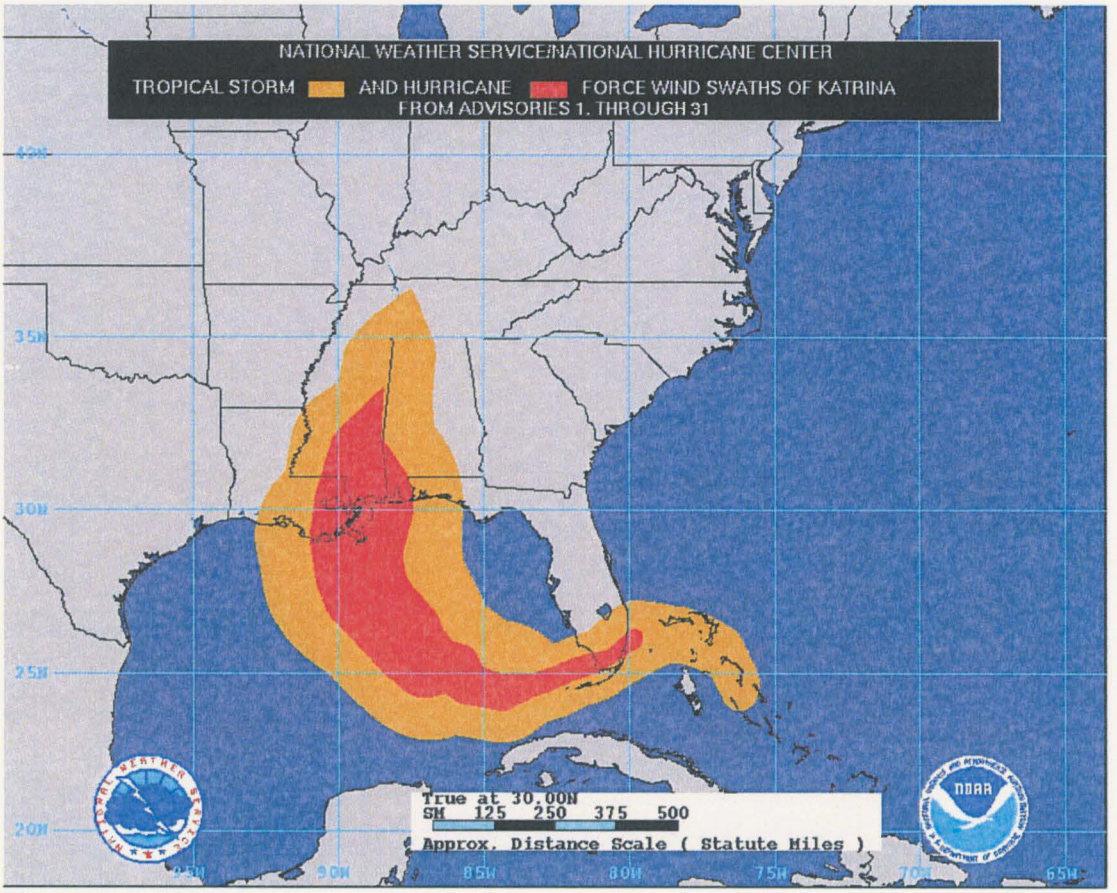

Figure 1.4: Wind swath plot of tropical storm and hurricane force winds for Hurricane Katrina 2005 (NHC archived data).

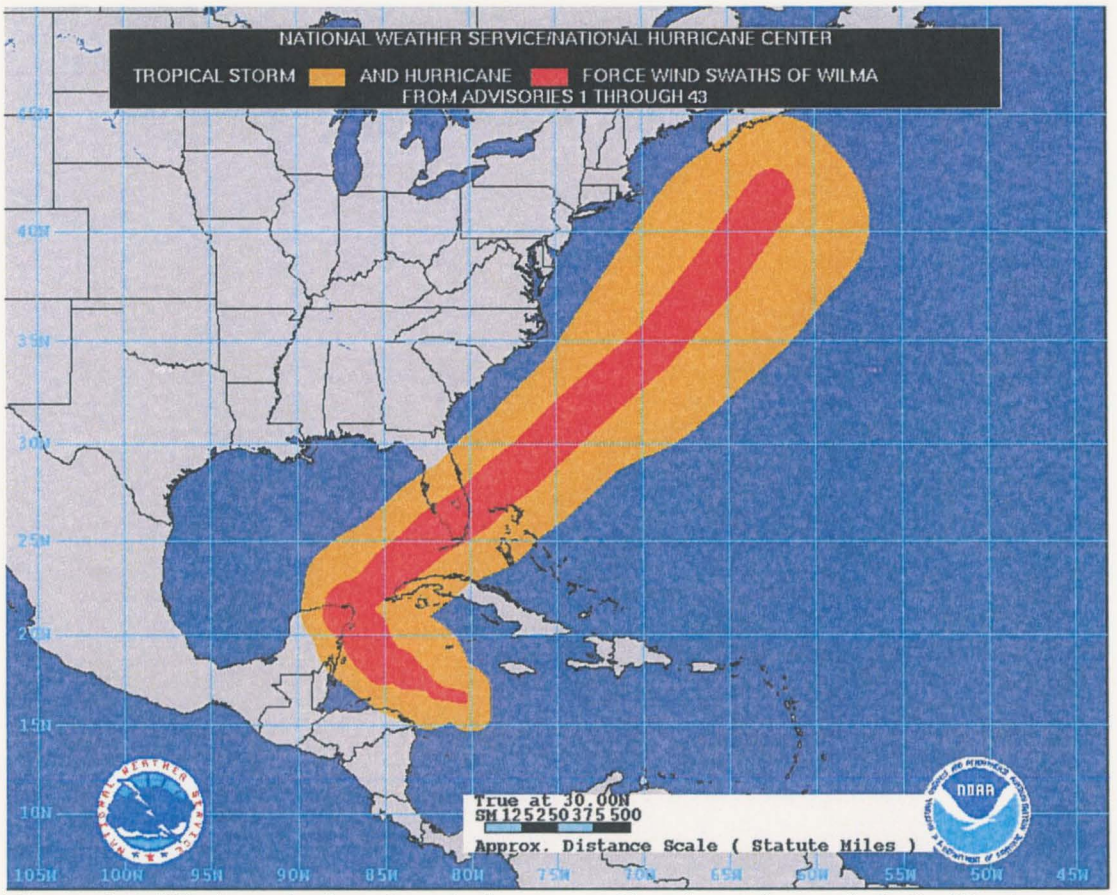

Figure 1.5: Wind swath plot of tropical storm and hurricane force winds for Hurricane Wilma 2005 (NHC archived data).

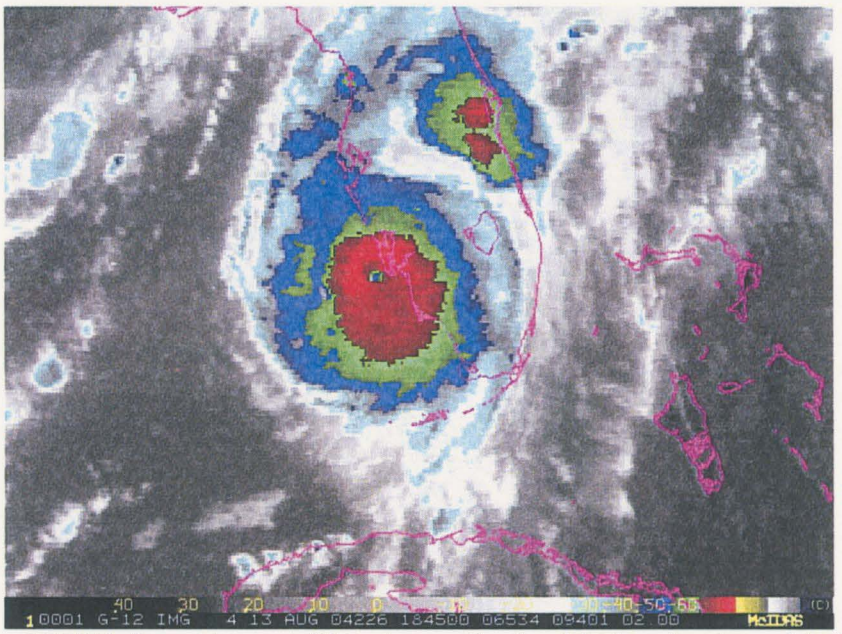

Figure 1.6: GOES infrared image of Hurricane Charley 2004 at the time of its Florida land-fall.

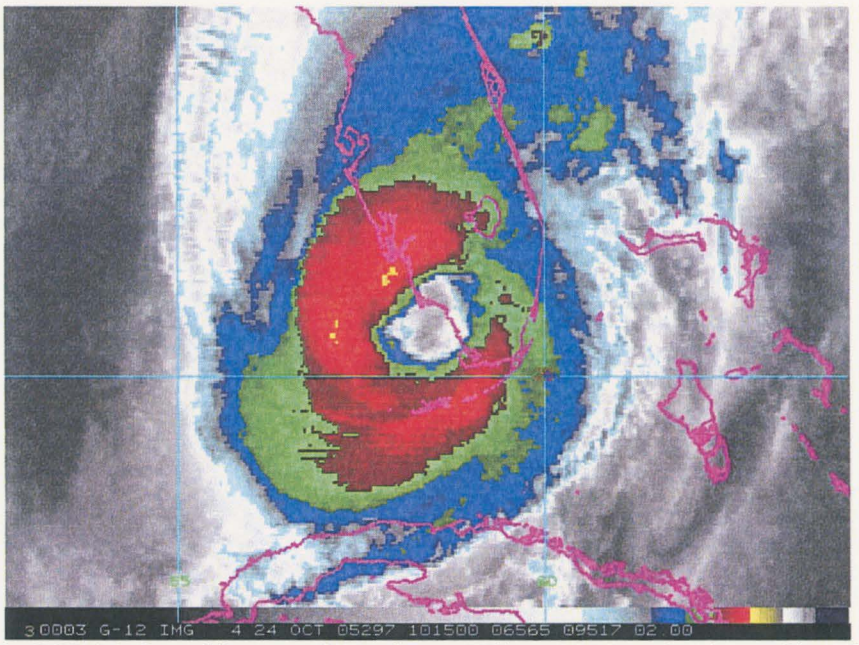

Figure 1.7: GOES infrared image of Hurricane Wilma 2005 at the time of its Florida land-fall.

CHAPTER 2 – DATA SOURCES

In this chapter the various data sets used in this study are presented. The raw and objectively analyzed aircraft reconnaissance data, which is used to calculate the inner core KE, is described in Section 2.1. Section 2.2 goes over the satellite products. This includes the Geostationary Operational Environmental Satellite (GOES) infrared measurements, and the Special Sensor Microwave/Imager (SSM/I) and Special Sensor Microwave Imager/Sounder (SSMIS) microwave imagery. Section 2.3 briefly describes the National Centers for Environmental Prediction (NCEP) reanalysis data, which provide the synoptic environmental conditions associated with the storms analyzed in this study. Finally, the assorted integrated storm and storm environment variables are described in Section 2.4. These variables provide a description of a variety of attributes of the storm and its environment.

2.1 Aircraft Reconnaissance Data

A. The Basic Aircraft Reconnaissance Data

The National Oceanic and Atmospheric Administration (NOAA) maintains two WP-3D Orion aircraft which are reserved for hurricane research 120 days each year (Aberson et al. 2006). However, the bulk of hurricane aircraft reconnaissance in the Atlantic and Eastern Pacific basins is carried out by the U.S. Air Force 53rd Weather Reconnaissance Squadron stationed at Keesler Air Force Base, Mississippi. This division, more commonly known as the "Hurricane Hunters," uses ten WC-130 aircraft for these missions.

During each mission, the aircraft flies through the hurricane at an altitude of 10,000 feet, or approximately 700 hPa. Aircraft may be flown at lower altitudes in the early developmental stages of the storm when conditions are less severe. A typical flight pattern starts at the northwest corner of the storm, extends diagonally to the southeast corner passing through the storm center, then makes a left turn to fly with the winds to the northeast corner, and finally completes a second diagonal pass through the center to the southwest quadrant (Fig. 2.1). This flight pattern is termed the "Alpha Pattern." Each leg extends out at least 105 miles from the center of the storm, and a pass through the center is made every two hours. This flight pattern is designed to capture a good representation of the wind structure of the storm. Data is archived every 10 seconds, and a complete weather observation (temperature, dewpoint, pressure, altitude, winds, and position) is taken every 30 seconds from measurements obtained from instrumentation attached to and within the aircraft. The winds are calculated using data from pressure change measurements from two probes, which give the true airspeed and side-slip, and data from the onboard navigation system, which supplies ground speed and heading (http://www.hurricanehunters.com/fact.htm).

B. Objective Analysis of the Aircraft Reconnaissance Data

An objective analysis, as described by Mueller et al (2006), of the aircraft reconnaissance data acquired from the National Hurricane Center (NHC) Air Force reconnaissance archive is carried out. The data used for this study encompasses Atlantic and Eastern Pacific tropical cyclones from the 1995-2005 seasons. This includes a total

of 124 storms. For each storm, the aircraft data is composited over 6 hour intervals in order to best capture the time evolution of the KE.

The data is adjusted to storm relative coordinates to eliminate the issue of storm movement over the 6 hour analysis period. The NHC best track data is used to locate the storm center. The best track data provides a best estimate of the position and intensity every 6 hours throughout the lifetime of the storm. It is derived using all available data on the tropical cyclone. Linear interpolation is used to determine the center location at the time of each wind observation. The distance east and north of the center is then calculated for each observation. An analysis is not carried out if the best track data is unavailable for the end time of the analysis. The storm relative data is assumed to be representative of the wind structure at the end of the 6 hour interval.

Extensive error checking is done to ensure a good quality data set. The data is checked for unrealistic values in wind speed, wind direction, and plane altitude (an approximate 700 hPa flight altitude is required for measurement consistency). The error checked winds are then converted from a Cartesian to a cylindrical coordinate system.

While the "Alpha Pattern" discussed earlier is the standard flight plan of aircraft reconnaissance missions, occasionally there are significant deviations from this pattern or only a portion of the pattern is flown. Therefore, a check is done to guarantee that there is sufficient data to create an accurate analysis of the wind-field. Any data set with an 180° or greater azimuthal data gap for four or more adjacent radii is discarded. The error-checked data is now objectively analyzed to an evenly spaced grid of 50 radial data points at 4 km increments, and 16 azimuthal data points at 22.5° increments. The

objective analysis routine uses smoothing constraints to minimize the difference between the winds on the analysis grid interpolated to the observations points and the original observations. A final error check is now carried out to identify regions where there is a 75 knot or greater difference in the observed value and the analyzed value. If this occurs, it simply indicates that the observed value at that grid point is significantly different than the surrounding observed grid point values. To correct this, the observation grid point is given zero weight. If more than 10% of the grid points are determined to be bad, then that data set is discarded. Otherwise, a final objective analysis is completed using the correctly weighted grid points for the interpolation. Fig. 2.2 shows the resulting wind analysis corresponding to the aircraft reconnaissance wind-field shown in Fig. 2.1. The 124 storms for this study yield a total of 1244 wind-field analyses.

2.2 Satellite Data

A. GOES Satellite Data

Satellite remote sensing instruments are a unique tool for the observation and measurement of atmospheric phenomena such as tropical cyclones. Visual and infrared (IR) radiation imagery from the Geostationary Operational Environmental Satellite (GOES) provide cloud-top measurements. The visual imagery (0.4-0.7 μm spectral range) is available only during daylight hours, whereas IR imagery (10-12.5 μm spectral range) is available continuously. A further benefit of the IR imagery is that it supplies a measure of the emission temperatures of the cloud-tops. Given that the troposphere generally decreases in temperature with height, a colder cloud-top emission temperature indicates a higher cloud-top. With a tropical cyclone, the coldest cloud-tops indicate

where the strongest convection is occurring in the storm, and the GOES IR imagery has the necessary resolution to accurately locate these intense updrafts.

The Cooperative Institute for Research in the Atmosphere (CIRA) IR archive contains digital satellite imagery for tropical cyclones since the 1995 hurricane season. The data is MCIDAS formatted 4 km resolution Mercator remaps generally in 30 minute intervals (Zehr 2000). The data encompasses the lifetime of each storm from its initial designation as a tropical depression to the time of its last advisory. The archive data for Atlantic and Eastern Pacific storms uses imagery from GOES east (currently GOES-12) and west (currently GOES-11). In order to capture the entire storm circulation, the location of the sector is altered to keep the storm center no less than 4 degrees latitude from the edge of the 640 element by 480 element image. This data is utilized to study the convective profiles of various types of storm evolution in Chapter 4.

B. SSM/I and SSMIS Satellite Data

Imagery from the Special Sensor Microwave/Imager (SSM/I) 85 GHz and Special Sensor Microwave Imager/Sounder (SSMIS) 91 GHz horizontally polarized channels are used to verify the occurrence of eyewall replacement cycles in select storms in Chapter 3. These instruments are onboard sun-synchronous polar orbiting satellites with an orbital period of approximately 101 minutes. At the equator the satellite makes a pass over the same location once every 12 hours. Microwave satellite imagery, unlike visual and infrared imagery, can penetrate the cirrus clouds that often form over portions of tropical cyclones obscuring the cloud structures below. The microwave spectral range encompasses wavelengths of 1 millimeter to 1 meter. In regions of convection there is significant scattering of radiation in the 85 and 91 GHz frequency ranges by large

precipitation particles, especially by ice particles above the freezing level. This causes a decrease in the measured 85/91 GHz brightness temperatures. As convection becomes more intense, more ice particles will be present in the upper atmosphere resulting in even lower 85/91 GHz brightness temperatures. Thus, the 85 and 91 GHz channels are well-suited for depicting the eyewall and rainband structures of tropical cyclones. The primary difficulty in using microwave imagery to observe tropical cyclone structure is the substantial limitation in data availability. There are currently no satellites with microwave instrumentation that provide constant monitoring of the tropics.

2.3 Synoptic Environment Data

In order to analyze the two-dimensional synoptic environment in which a storm resides the National Centers for Environmental Prediction (NCEP) reanalysis data is utilized. NCEP reanalysis fields are generated through assimilation of observations from upper-air temperature, horizontal wind, and specific humidity rawinsonde observations; operational Television Infrared Observation Satellite (TIROS) Operational Vertical Sounder (TOVS) vertical temperature soundings from NOAA polar orbiters over ocean with microwave retrievals excluded between 20°N and 20°S due to rain contamination; TOVS temperature soundings over land only above 100hPa; cloud-tracked winds from geostationary satellites; aircraft observations of wind and temperature; land surface reports of surface pressure and oceanic reports of surface pressure, temperature, horizontal winds, and specific humidity (Kistler et al. 2001). This study uses 31° by 41° storm centered grids of the horizontal wind and temperature fields at various pressure levels in order to obtain a better idea of the overall environmental conditions associated with the different stages of tropical cyclone evolution.

2.4 Integrated Storm and Storm Environment Variables

A broad selection of integrated variables encompassing information about the storm and storm environment are used in a statistical analysis in order to determine what factors may contribute to tropical cyclone structure change. These variables include the Statistical Hurricane Intensity Prediction Scheme (SHIPS) predictor variables, which are comprised of climatological, persistence and synoptic variables, ocean heat content, a set of variables derived from GOES infrared (channel 4) imagery, and variables derived from the reconnaissance data objective analysis. Table 2.1 shows a list of the variables along with a brief description for each.

The standard SHIPS predictor variables are horizontally averaged values over a given radial distance. Primarily, the area average is calculated for radii 200-800 km from the storm center. Exceptions are for the divergence, vorticity and momentum flux variables. The divergence and vorticity variables are an average over radii 0-1000 km; the momentum flux is an average over radii 0-600 km. The GOES channel 4 brightness temperatures and standard deviations in brightness temperature are azimuthally averaged on a 4-km, storm-centered radial grid. The reconnaissance data objective analysis variables are retrieved from the objectively analyzed aircraft reconnaissance data described earlier.

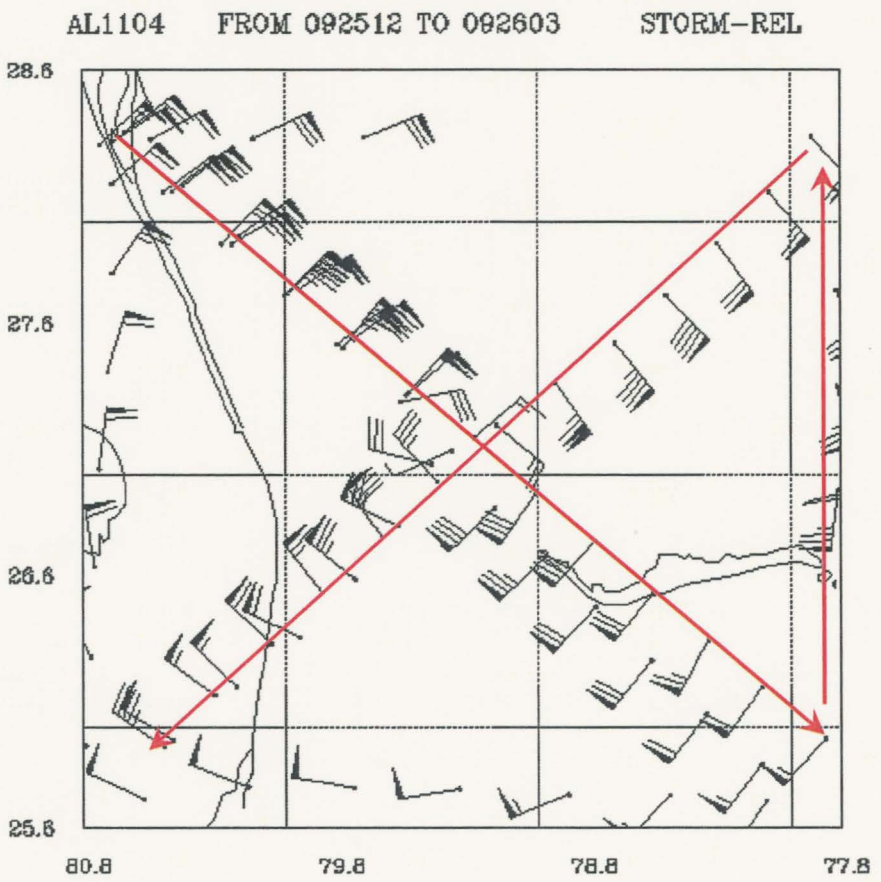

Figure 2.1: Aircraft reconnaissance flight-level winds for Hurricane Jeanne 25 September 2004. The red arrows denote the signature "Alpha Pattern."

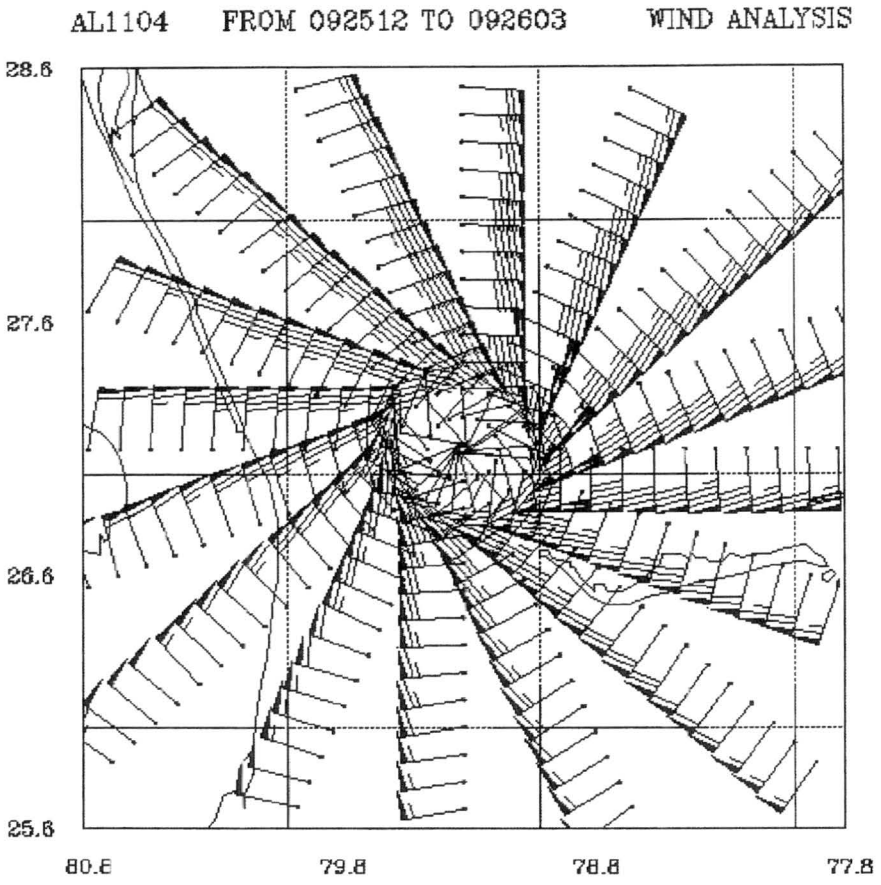

Figure 2.2: Objectively analyzed wind analysis for Hurricane Jeanne 25 September 2004.

Table 2.1: The extended SHIPS Variables, GOES IR variables, and aircraft reconnaissance variables used in this study

Variable Name	Description	Units and Scaling	
VMAX	Maximum winds	ms^{-1}	Extended SHIPS Variables
RSST	Reynolds Sea Surface Temperature	°C *10	
T150	150 mb Temperature	°C *10	
T200	200 mb Temperature	°C *10	
T250	250 mb Temperature	°C *10	
DTL	Distance to nearest major land mass	km	
LAT	Latitude	°N*10	
LON	Longitude	°W*10	
INCV	6 hour intensity change	kt	
U200	200 mb zonal wind	kt*10	
EPOS	Average theta-e difference between a parcel lifted from the surface and its environment (only positive differences are included)	°C *10	
ENEG	Same as EPOS, but only negative differences are included	°C *10	
RHLO	850-700 mb relative humidity	%	
RHMD	700-500 mb relative humidity	%	
RHHI	500-300 mb relative humidity	%	
SHRD	850-200 mb shear magnitude	kt*10	
SHTD	Heading of above shear vector	degrees	
SHRS	850-500 mb shear magnitude	kt*10	
SHTS	Heading of above shear vector	degrees	
PSLV	Pressure of the center of mass of the layer where storm motion best matches environmental flow	mb	
Z850	850 mb vorticity	sec^{-1} * 10**5	
D200	200 mb divergence	sec^{-1} * 10**5	
REFC	Relative eddy momentum flux convergence	m/sec/day, 100-600 km avg	

RHCN	Ocean heat content derived from satellite altimetry	kJ/cm^2	
IR0	Age of the GOES imagery relative to the storm case time	10*hr	GOES IR Variables
IR1	0-200 km radially averaged TB	°C *10	
IR2	0-200 km radially averaged TB std deviation	°C *10	
IR3	100-300 km radially averaged TB	°C *10	
IR4	100-300 km radially averaged TB std deviation	°C *10	
IR5	Percent area from r = 50 to 200 km with TB < -10 C	%	
IR6	Same as IR5 with TB < -20 C	%	
IR7	Same as IR5 with TB < -30 C	%	
IR8	Same as IR5 with TB < -40 C	%	
IR9	Same as IR5 with TB < -50 C	%	
IR10	Same as IR5 with TB < -60 C	%	
IR11	Maximum TB from 0-30 km radius	°C *10	
IR12	Average TB from 0-30 km radius	°C *10	
IR13	Radius of maximum TB	km	
IR14	Minimum TB from 20-120 km radius	°C *10	
IR15	Average TB from 20-120 km radius	°C *10	
IR16	Radius of minimum TB	km	
REC0	Age of the analysis relative to the storm case time	10*hr	Aircraft Reconnaissance Variables
REC1	Radius of maximum symmetric tangential wind	km	
REC2	Value of maximum symmetric tangential wind	kt	
REC3	Radius of maximum total wind	km	
REC4	Value of maximum total wind	kt	
REC5	Azimuth of maximum total wind	°CCW from east	
REC6	Tangential wind gradient outside the RMW	100*kt/km	

REC7	100-180 km average radial wind	10*kt
REC8	100-180 km average tangential wind	10*kt
REC9	Average radial wind from r = +/- 20 km from rmstw	10*kt
REC10	Average tangential wind from r = +/- 20 km from rmstw	10*kt
REC11	0-200 km integrated KE	1.0e-15*J
REC12	Climatological 0-200 km integrated KE for given V_{max}	1.0e-15*J

CHAPTER 3 - KINETIC ENERGY CLIMATOLOGY, SCALE, AND EVOLUTION

In this chapter the details of the inner core kinetic energy (KE) calculations from the aircraft data are presented. As described previously, the KE will be used as a measure of storm structure. The kinetic energies for all of the analyses are also used to establish a KE climatology. A new hurricane scale is proposed that is based on hurricane KE which serves to complement the SSHS. The evolution in the KE for individual storms is then investigated and a frequently occurring progression is identified. One notable feature in the KE evolution is the occurrence of eyewall replacement cycles, and examples of this are presented. Finally, the aircraft analyses are classified by their state of intensification and growth, thus defining six regimes into which the analyses are partitioned. These regimes are utilized in the remaining portions of this study.

3.1 Inner Core Kinetic Energy Calculation

From physics, the definition of the kinetic energy, in Joules, of an object is

$$E_k = \frac{1}{2}mv^2 \tag{3.1}$$

where m represents the mass of the object in kilograms and v is the speed with which the object is moving in meters per second. Consider a unit volume ($V = 1\text{m}^3$) parcel of air of density ρ (kgm^{-3}) moving at a total velocity $\vec{v}$. The mass of the air parcel is simply

$$m = \rho V . \tag{3.2}$$

Assuming a cylindrical coordinate system and neglecting vertical velocities ($w\hat{k} = 0$), the velocity of the air parcel can be broken down into its radial u and tangential v components:

$$\vec{v} = u\hat{i} + v\hat{j}\,. \tag{3.3}$$

Therefore, the kinetic energy of a unit volume air parcel becomes

$$E_k = \frac{1}{2}\rho(u^2 + v^2)\,. \tag{3.4}$$

However, for this study, the total inner core kinetic energy of a hurricane is desired. The inner core can simply be considered as a thin disk of set radius and depth (Fig. 3.1). The total kinetic energy within the disk is found by integrating the kinetic energy for a single air parcel over the volume (radius, azimuth and height) of the disk

$$KE = \int_{z_1}^{z_2}\int_{0}^{2\pi}\int_{0}^{R}\frac{1}{2}\rho(u^2 + v^2)r\,dr\,d\theta\,dz\,, \tag{3.5}$$

where r is the radius, θ is the azimuth, and z is the height. Furthermore, it is assumed that the aircraft reconnaissance flight-level winds, which are the source of the winds for this KE calculation, are representative of the storm structure over a one kilometer depth. The variation in the air density within this volume is small and thus a constant density can be assumed. Taking into account these assumptions, the total inner core kinetic energy equation becomes

$$KE = \frac{\rho_o \Delta z}{2}\int_{0}^{2\pi}\int_{0}^{R}(u^2 + v^2)r\,dr\,d\theta \tag{3.6}$$

where ρ_o is assigned a value of 0.9 kgm^{-3} (a typical air density at 700 hPa). Using Equation 3.6 the KE is calculated for 1244 analyses of aircraft reconnaissance flight-level derived wind-fields for the124 Atlantic and East Pacific tropical cyclones from 1995 through 2005 in the data set.

To determine how storm inner core energy evolves as storms intensify the inner core kinetic energies (J) are plotted versus the maximum wind (ms^{-1}) in the storm in Fig.

3.2. This plot clearly demonstrates that, in the broad scheme, KE increases nonlinearly with increasing intensity. From the basic definition of kinetic energy one would expect a storm's kinetic energy to increase with the square of the winds (illustrated by the blue line). A best-fit applied to the data reveals a power series relationship

$$KE = 3 * 10^{13} (V_{\max})^{1.872} \quad , \tag{3.7}$$

as is illustrated by the red line in Fig. 3.2. The variance explained R^2 for this best-fit is 0.8217. Thus, KE increases with nearly the square of the maximum winds. It should be noted that the mean KE-intensity relationship does not describe the evolution of inner core kinetic energy for a single storm. The KE evolution through the life cycle of a single storm is investigated more thoroughly in Section 3.3.

3.2 Kinetic Energy Hurricane Scale

Before investigating the evolution of KE, the KE climatology is first described. This hurricane KE climatology will be used to formulate a new hurricane scale based on kinetic energy. While the SSHS is simple and well-established, it has substantial shortcomings. Arguably, its primary problem is that it is based solely on intensity and neglects the size of the storm. Combining both intensity and size into a simple scale should yield an improved measurement tool for the destructive potential of a tropical cyclone. The inner core kinetic energy measure described above incorporates both the size and intensity of a storm thus making it a good candidate as a basis for a new scale.

Using the SSHS as a guide, a new hurricane scale based on the inner core kinetic energy is now defined. So that it may complement the SSHS, a system of six categories is defined ranging from 0 to 5, where category 0 represents tropical storms on the SSHS. The percentages of storms corresponding to each of the SSHS categories are determined

from the NHC best-track data for storms from 1947 through 2004. The thresholds for the KE hurricane scale categories are chosen by applying these same percentages to the KE climatology data set. Table 3.1 outlines the SSHS categories, their corresponding historical distributions (as a percentage), and the analogous KE hurricane scale categories.

To compare these scales, consider the U.S. land-falling hurricanes from 1995 through 2005. Table 3.2 shows each of the storms, the KE value from the analyses nearest the time of official land-fall, the NHC official intensity at land-fall, the location of land-fall and the estimated *total* U.S. damage from the storm. These KE values are plotted against the official NHC intensities in Fig. 3.3. The vertical dotted lines mark the thresholds for the SSHS categories and the horizontal dotted lines mark the thresholds for the KE hurricane scale categories.

Observe first the data points for Hurricane Katrina (2005) and Hurricane Ivan (2004). On the SS scale Hurricane Katrina made land-fall on the Louisiana/Mississippi border as a category 3, however, the KE scale measures the storm as an impressive category 5. Similarly, Hurricane Ivan was very nearly a KE category 5 at land-fall, and it too was a SSHS category 3. Table 3.2 reveals that Katrina and Ivan are estimated to have been the two most costly storms in the United States during the period of 1995-2005, yet they were not the most intense storms to make U.S. land-fall for this period. The damages resulting from these storms are highly dependent on factors unrelated to the actual storm dynamics, so it is not wise to attempt to draw definitive conclusions about a storm based solely on the damage. However, it should be noted that much of the damage from these storms was caused by storm surge. From this evidence it appears that the KE

hurricane scale is a reasonably good indicator of a hurricane's potential for damage that is not available by using only the maximum wind.

The main weakness of the KE scale is that it does not accurately represent the destructive potential of small, intense storms. Hurricane Charley (2004) is a perfect example of this. At its first land-fall in Punta Gorda, Florida the storm measured an impressive category 4 on the SSHS, but it was a category 0 in terms of its KE. At its second land-fall in Myrtle Beach, South Carolina it had weakened to barely a SSHS category 1, yet increased to a category 1 on the KE scale. This phenomenon relates to the fact that at first land-fall the storm was an extremely intense, compact system. While it contained very strong winds, they were confined to within 6 nautical miles of the center of the storm. For a storm to have a high value of KE, high winds over a large area are necessary. At Charley's second land-fall this storm had weakened with respect to its maximum sustained winds, but had become a larger system with fairly high winds covering a greater area, resulting in an increased KE. The most significant damage occurred during initial land-fall and was caused by extreme winds. There was very little storm surge associated with Hurricane Charley. This demonstrates precisely why the KE scale cannot replace the SS scale, but it can certainly be used to complement it.

3.3 Hurricane Kinetic Energy Evolution

While the overall evolution in storm KE with respect to intensity is generally defined by the power series curve, individual storms do not evolve in this manner. This can best be illustrated by looking at individual storm's kinetic energy deviations from the mean curve as a function of intensity. The kinetic energy deviations (KE') are calculated by taking the difference between the measured KE and the expected KE for the storm's

intensity from Equation 3.7. A zero value in KE' indicates that the storm has the expected KE for its intensity and lies upon the mean curve described by Equation 3.7 and shown in Fig. 3.2. Therefore, positive KE' values denote storms which have higher KE than expected for their intensity and negative values indicate lower KE than expected. Increasing KE' implies storm growth and decreasing KE' implies that the storm is not growing in size. These plots were created for all storms which have at least three associated aircraft analyses, of which there are 97.

A. "Horizontal Question Mark" Evolution

While there is a large amount of variability in the KE' evolution plots, extensive review of these plots reveal some common characteristics. Most notably, during the life cycle of a storm it is much more common to see intensification with a simultaneous decrease in KE', which indicates that the storm is not increasing in size; or a decrease in intensity with a simultaneous increase in KE', which signifies an increase in storm size. The opposite scenarios occur less frequently. In fact, a unique evolution in intensity and structure is apparent, which will be referred to as the "horizontal question mark" evolution. Good examples of this are shown in the plots for Hurricanes Katrina (Fig. 3.4) and Wilma (Fig. 3.5) from the 2005 season. This question mark storm evolution suggests that as a storm begins to intensify there is often a modest decrease in KE', but as the storm reaches a stage of more rapid intensification the KE' decreases substantially. However, once the storm has reached peak intensity and begins to weaken the KE' will often increase. These findings are in agreement with the previous studies of W-G discussed earlier.

B. Eyewall Replacement Cycles

Eyewall replacement cycles occasionally occur in major hurricanes (category 3 or greater on the SSHS) and can be easily identified in the KE'-V_{max} plots. Once a hurricane reaches an intensity of category 3 or higher, a relatively small eye and radius of maximum winds may form and the outer rainbands may begin to become more organized and form a secondary eyewall. When this occurs, the inertial stability in the secondary eyewall impedes the radial inflow of momentum and moisture to the inner eyewall (Willoughby et al, 1982). Having lost or greatly decreased its energy source, the inner eye breaks down yielding a weakening in intensity as the maximum winds from the inner eye are lost. The secondary eyewall now becomes the new primary eyewall, and while its maximum winds are not as high as the former eyewall its larger size results in an increase in the KE'. The new, larger eye may then become more organized, and intensify and contract. Thus, an increase in V_{max} and decrease in KE' should be seen. The following analysis of Hurricanes Ivan (2004) and Wilma (2005), which both experienced eyewall replacement cycles during their evolution, reveals that these cycles are indeed evident in the KE'-V_{max} plots.

Consider first Hurricane Ivan (2004) which underwent several eyewall replacement cycles during its passage through the Caribbean and Gulf of Mexico, some of which were captured by SSM/I microwave imagery. In Fig. 3.6(a), as the storm passed to the south of Jamaica, a small, well-defined eye surrounded by rainbands began to form a secondary eyewall. In Fig. 3.6(b) the secondary eyewall is seen to have strengthened and become more organized, and the inner eyewall has begun to break down. Finally, Fig. 3.6(c) shows that the small eye has been replaced by a much larger

eye that formed from the rainbands and has begun to intensify and contract. The KE' evolution with respect to intensity for Ivan is shown in Fig. 3.7, and the points that correspond most closely to the microwave imagery in Fig. 3.6(a-c) are labeled accordingly.

Ivan then began to intensify again as the new eye contracts and another eyewall replacement cycle began to take place, as is shown in Fig. 3.8(a-d). This eyewall replacement cycle, however, appears to be somewhat disrupted by interactions with the Cuban landmass. The secondary eyewall had begun to form and strengthen, but did not wrap entirely around the existing eye, as is represented by the KE' increase and slight decrease in intensity shown in Fig. 3.7 points D and E. Hence, the inner eye was able to hold together and the storm intensified further (Fig. 3.8(b)), which is indicated by the progression from point E to F in Fig. 3.7. The eyewall replacement did finally occur, as is seen in Figs. 3.8(c) and (d), resulting in a decrease in intensity, and an increase in the KE' (Fig. 3.7 points F-G). Both of these eyewall replacement cycles have the expected development in KE' and intensity.

Hurricane Wilma (2005) had a dramatic eyewall replacement cycle early in the storm's lifetime. Wilma formed in the Caribbean (Fig. 3.9(a)) and very quickly intensified into an extremely small and intense hurricane (Fig. 3.9(b)). At this time its tiny eye became encompassed by a much larger secondary eyewall. The small eye broke down leaving the larger eye in its place (Fig. 3.9(c)). The new eyewall then proceeded to become more organized and intensified (Fig. 3.9(d)). The KE' evolution with respect to intensity for Hurricane Wilma is shown in Fig. 3.10 with the points corresponding mostly closely to the imagery in Fig. 3.9(a-d) labeled appropriately. The storm's development,

as shown in the microwave imagery, is clearly evident in the evolution of the KE' and V_{max}. From Fig. 3.10 point A to B the storm developed to its peak intensity with a simultaneous decrease in the KE.' Then an eyewall replacement cycle occurred (Fig. 3.10 point B to C) causing a decrease in intensity, but, with the formation of the new larger eye, the KE' increases. Finally, Fig. 3.10 point C to D shows the moderate intensification and a decrease in the KE' as the storms new, large eye contracts.

The eyewall replacement cycles of Hurricane Ivan and Wilma illustrate a discrete growth process common to the structural evolution of strong hurricanes. During the eyewall replacement cycle the storm initially loses intensity as the inner eyewall breaks down and is replaced by an existing secondary eyewall. The new larger eye may contract as the storm re-intensifies, but generally remains larger than the previous eye. This is one of the primary ways for a storm to grow in size.

C. Intensity Change/Size Change Regimes

To confirm the prevalence of the evolutional tendencies which have been presented, and to facilitate further analysis of storm structural evolution, the time tendencies of intensity (V_{max}) and kinetic energy deviation (KE') were calculated. For each analysis of each storm the average change in KE' and V_{max}, normalized to a 24 hour period, is determined. These values are found by computing the normalized difference in the values for the current analysis with those of the analyses before and after. The differences are then averaged and the results assigned to the current analysis. These calculations are summarized by the general Equation 3.9, which can be used to find either the KE' or V_{max} tendency.

$$\Delta X_A = \frac{1}{2}\left(\frac{X_A - X_{before}}{t_A - t_{before}} + \frac{X_{after} - X_A}{t_{after} - t_A} \right), \tag{3.9}$$

where ΔX_A is the time tendency of the variable for each analysis, A, t is the time, and the subscripts *before* and *after* indicate values for the previous and next available analyses, respectively. For the special cases of the first and last available analyses for a given storm the ΔKE' and ΔV_{max} values are computed using only the averaged differences between the first analysis and the following (*after*) analysis, and, similarly, between the last analysis and the previous (*before*) analysis. Also, ΔKE' and ΔV_{max} values are only used for analyses at least three hours, but less than 24 hours, apart. This is done to avoid unrealistic values for the 24 hour intensification or growth when the aircraft reconnaissance analyses were too close together or far apart.

The averaged ΔV_{max} and ΔKE' values are sorted based on the intensity change, and three groups are defined: the lower third represents weakening storms, the upper third represents intensifying storms, and the middle third represents storms that approximately maintain their intensity (i.e., neither greatly increasing nor decreasing in intensity). The ΔKE' distributions for these three groups are shown in a histogram in Fig. 3.11. The weakening ΔKE' distribution is more heavily weighted in the positive indicating that weakening storms tend to grow relative to the mean intensity/size relationship. The intensifying ΔKE' distribution is more heavily weighted in the negative, thus storms which are intensifying do not tend to grow relative to the mean relationship. The maintaining ΔKE' distribution does not show a significant tendency towards the positive or negative, although there is a slight bias towards growth. To specifically quantify these observations, the weakening, maintaining and intensifying groups are each split into growing (positive ΔKE') and non-growing (negative ΔKE') subgroups. The number of values for each of the six sub-groups is shown in Table 3.3. These numbers support not

only previous studies, but also the observations presented in the initial investigation of the KE'-V_{max} evolution ('Horizontal Question Mark'), where storms typically first intensify and then grow. The synoptic scale data will be partitioned into these six sub-groups to help identify the physical processes associated with storm growth, or lack of growth.

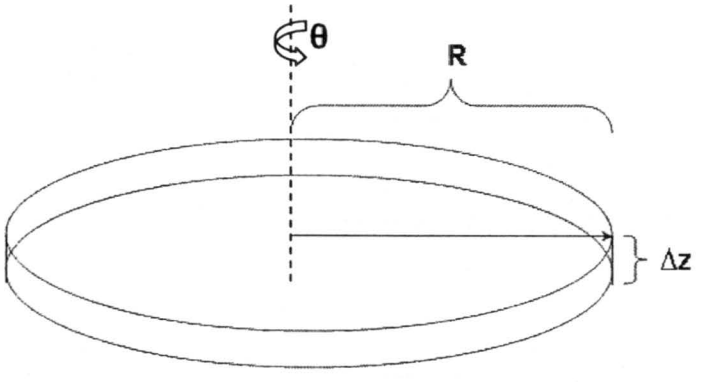

Figure 3.1: Schematic of the thin disk within a hurricane for which the KE is calculated.

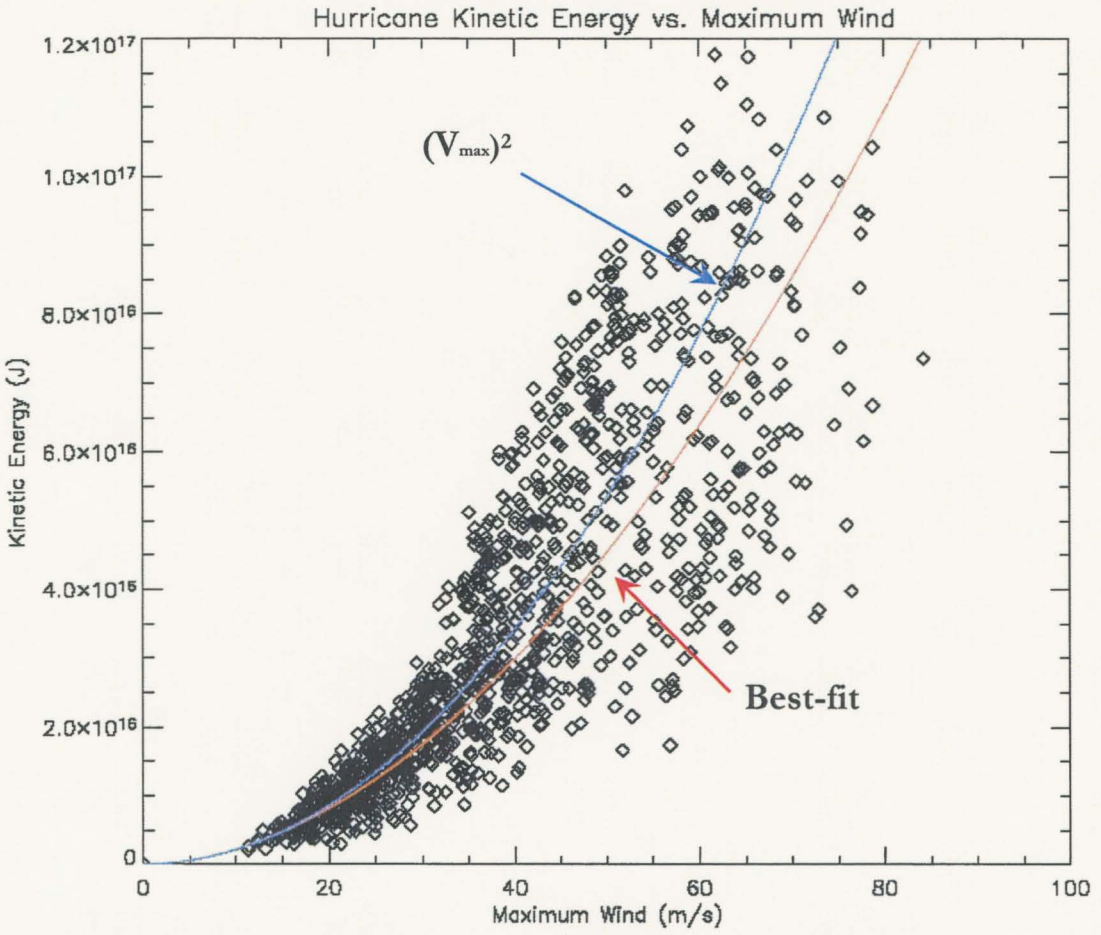

Figure 3.2: KE [J] versus intensity (V_{max} [ms^{-1}] from the aircraft reconnaissance analyses).

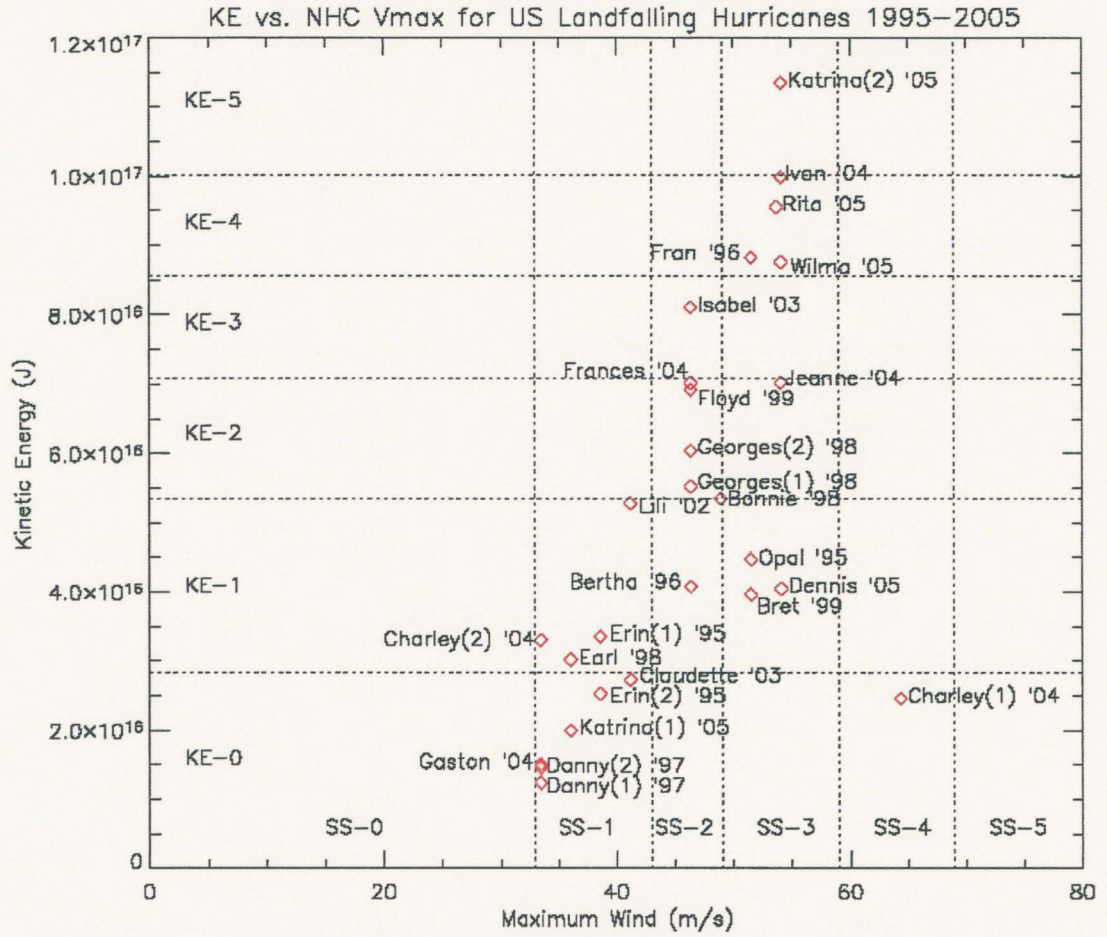

Figure 3.3: The approximate KE versus the intensity as reported by NHC at land-fall for all U.S. land-falling hurricanes from 1995-2005.

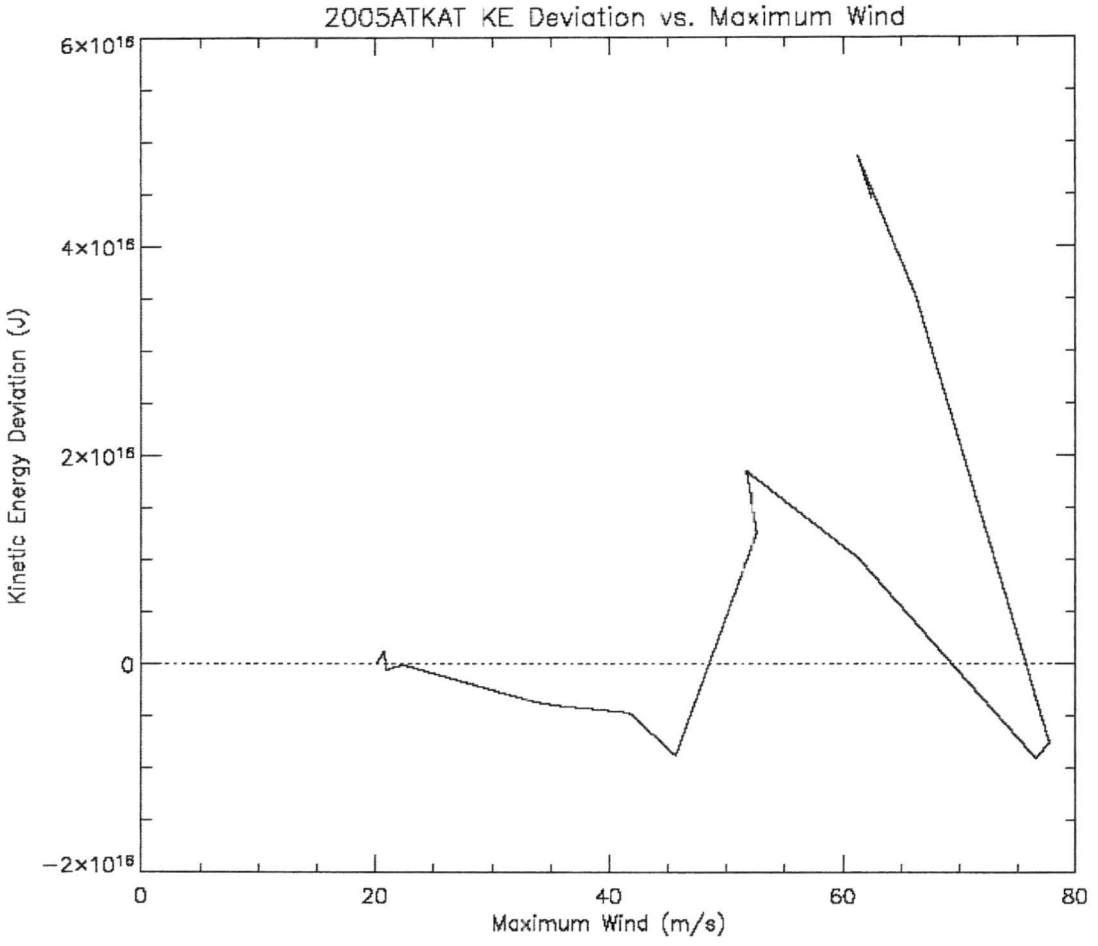

Figure 3.4: KE deviations from the mean curve versus intensity for Hurricane Katrina (2005).

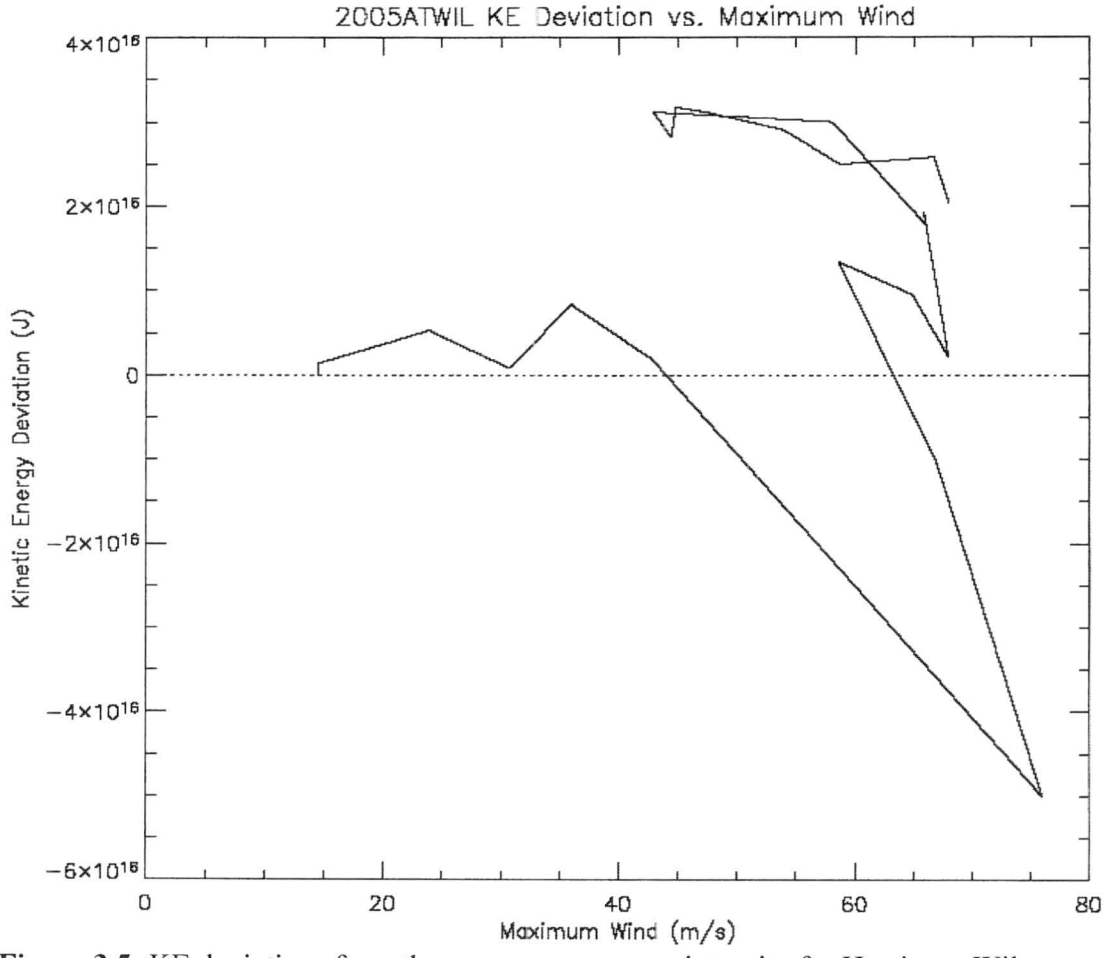

Figure 3.5: KE deviations from the mean curve versus intensity for Hurricane Wilma (2005).

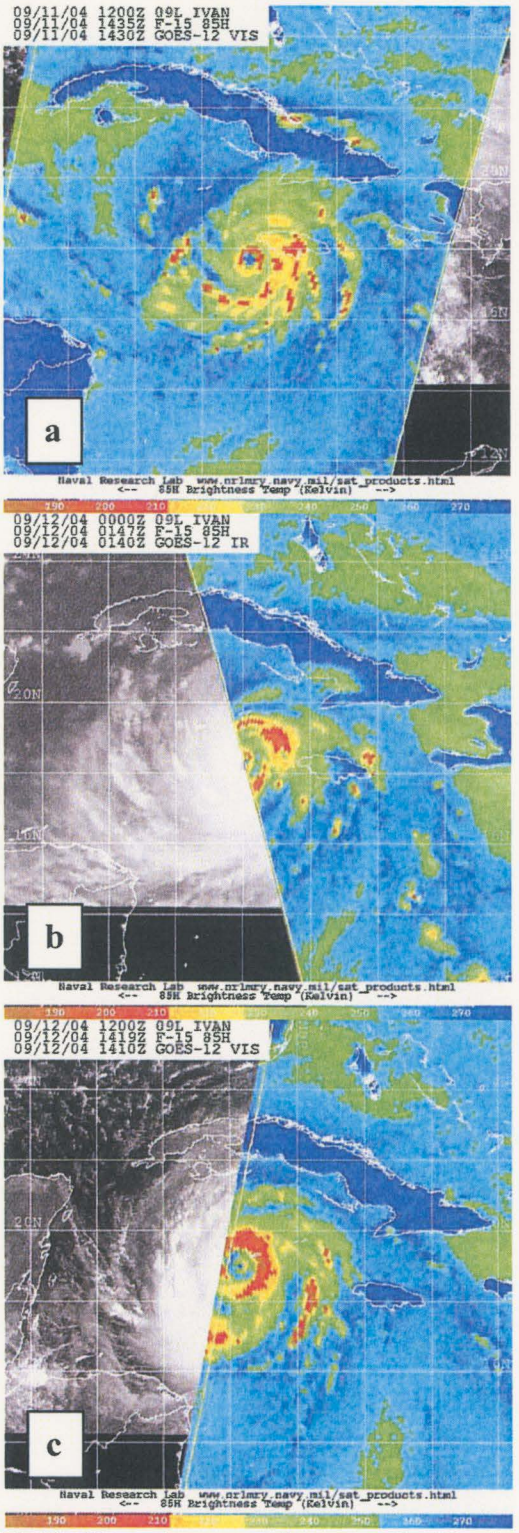

Figure 3.6 (a-c): SSM/I 85H GHz microwave imagery for Hurricane Ivan (2004) illustrating an eyewall replacement cycle.

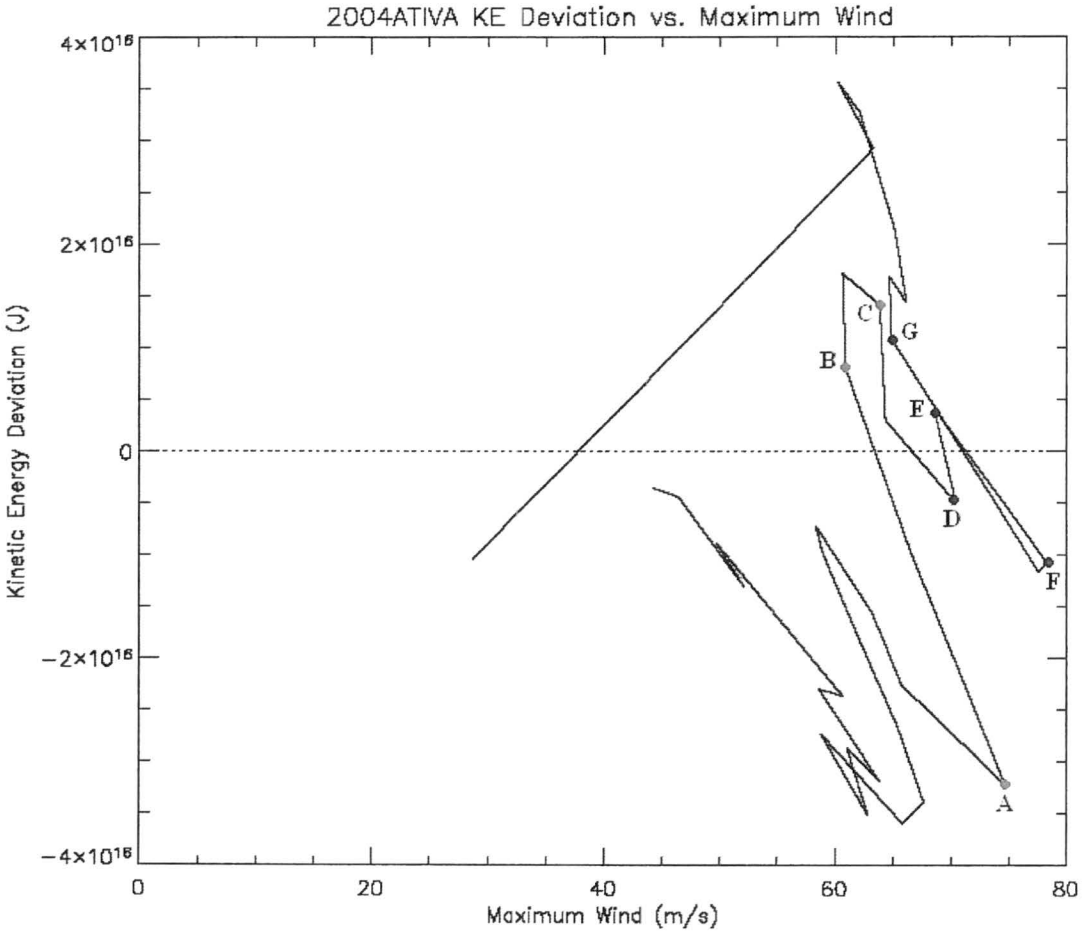

Figure 3.7: The KE deviations from the mean curve versus intensity evolution for Hurricane Ivan (2004). The labeled points A-C and D-G correspond to the storm's structure and intensity changes during two separate eyewall replacement cycles.

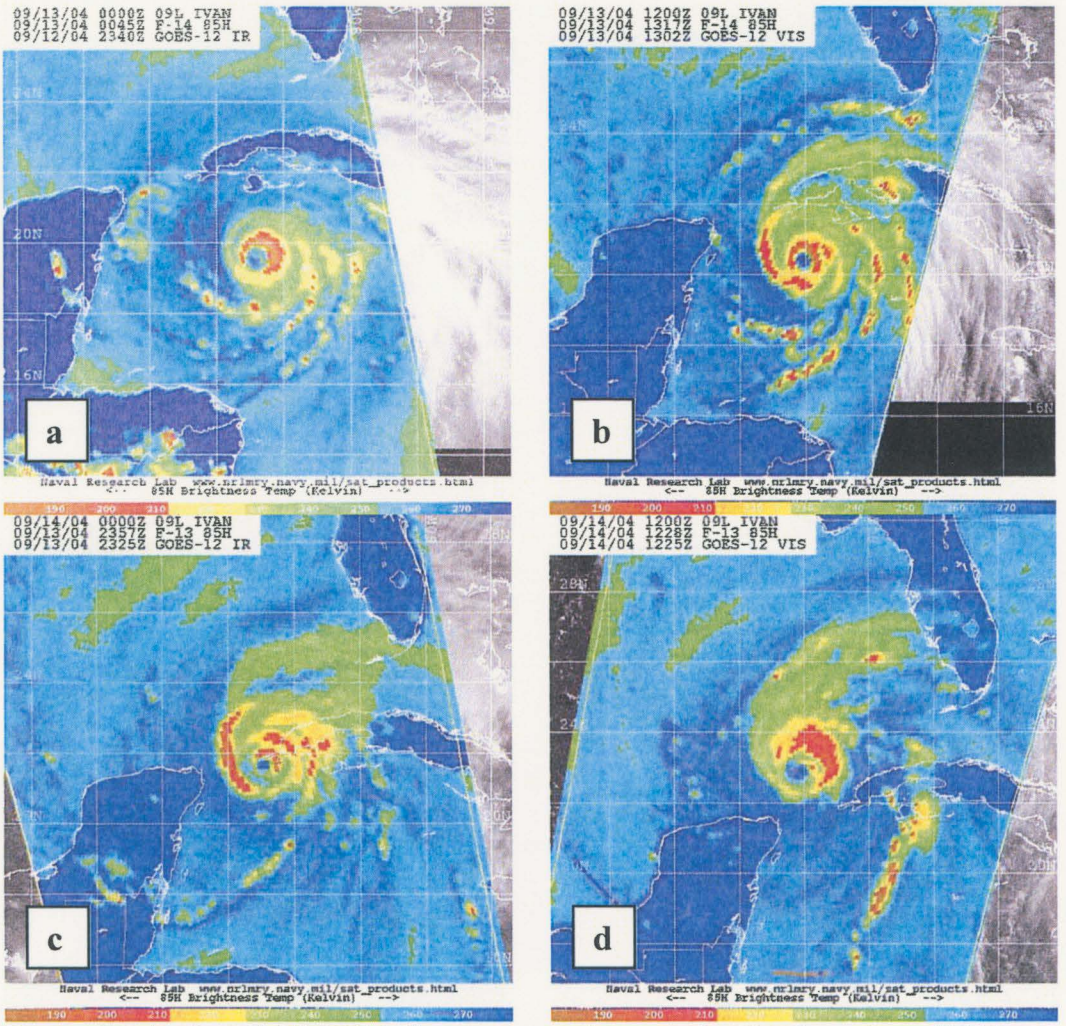

Figure 3.8 (a-d): SSM/I 85H GHz microwave imagery for Hurricane Ivan (2004) illustrating a second eyewall replacement cycle.

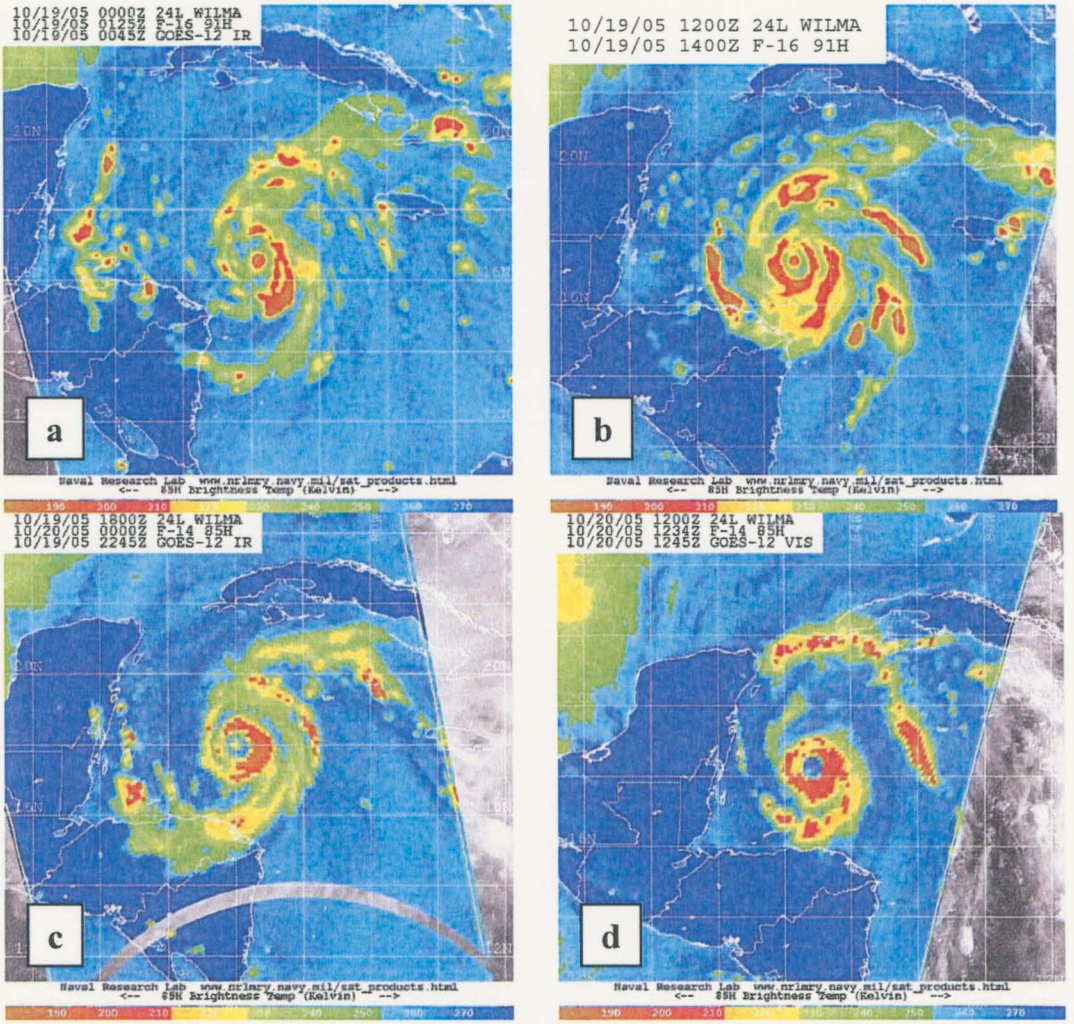

Figure 3.9(a-d): SSMIS 91 GHz and SSM/I 85H GHz microwave imagery for Hurricane Wilma (2005) illustrating an eyewall replacement cycle.

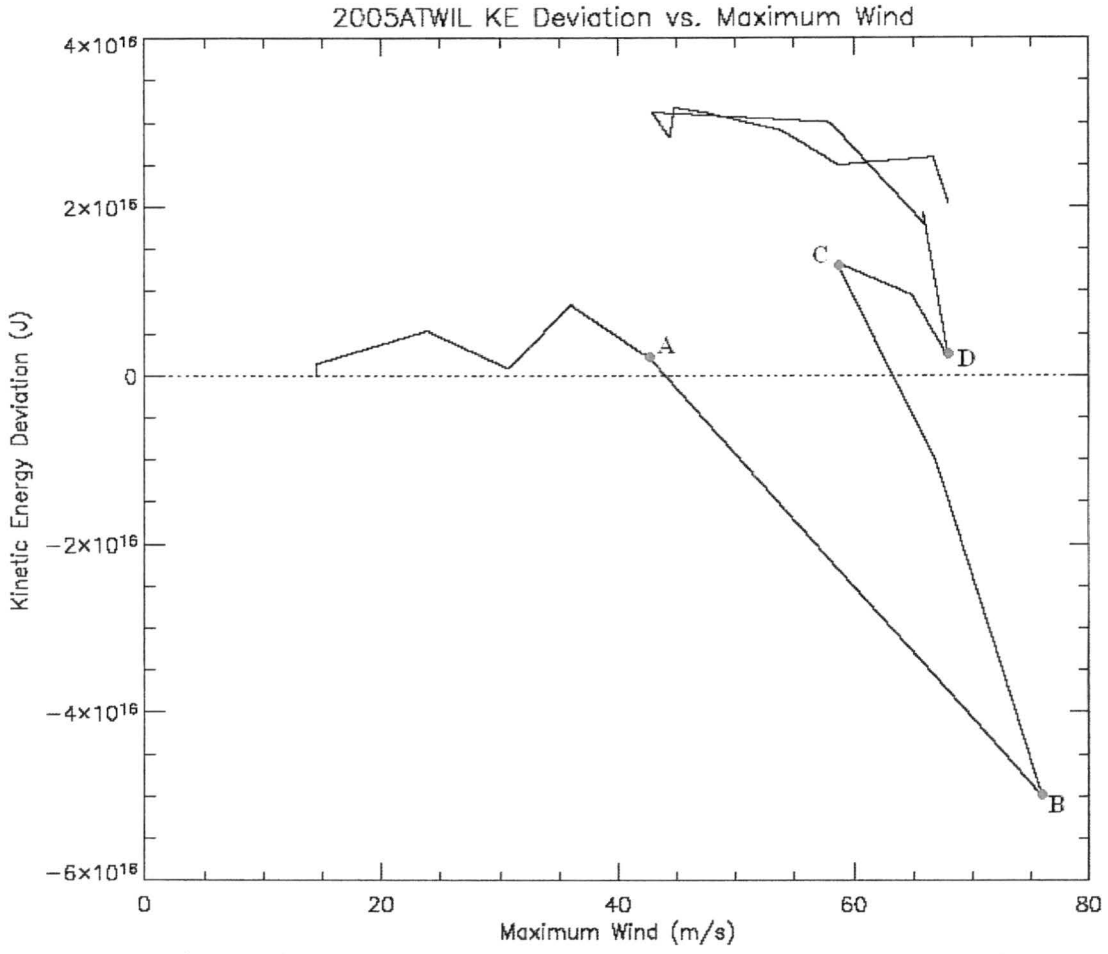

Figure 3.10: The KE deviations from the mean curve versus intensity evolution for Hurricane Wilma (2005). The labeled points A-D correspond to the storm's structure and intensity changes during an eyewall replacement cycle.

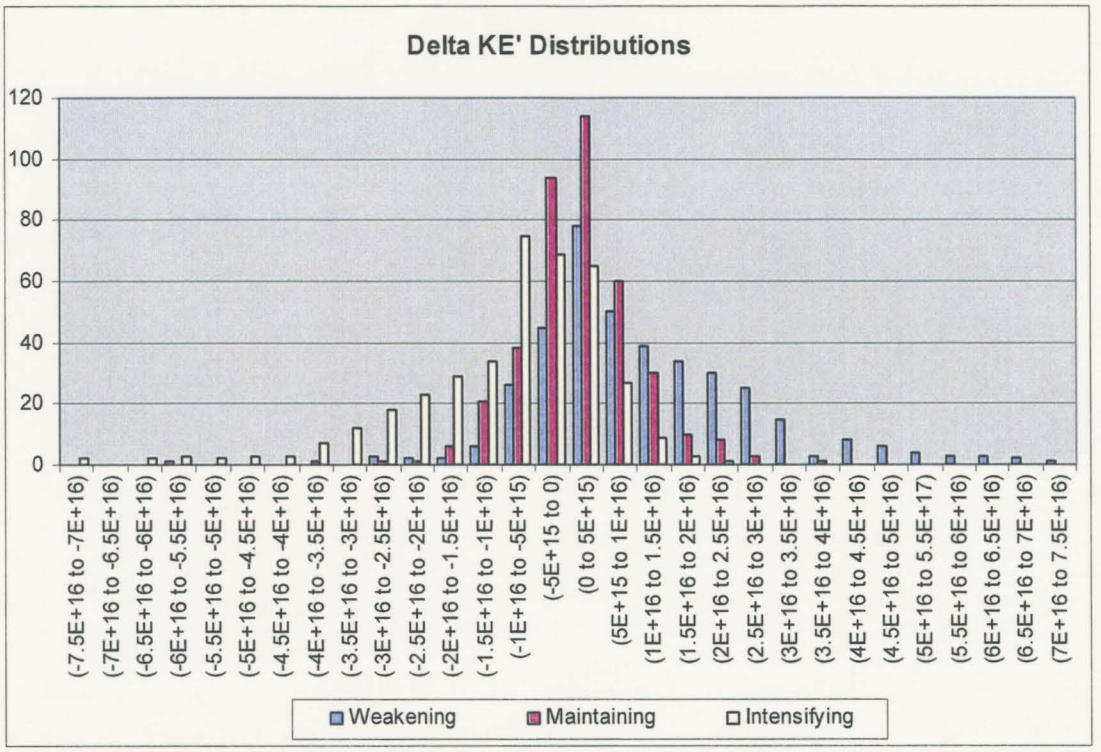

Figure 3.11: A histogram of the ΔKE' distributions for weakening, maintaining intensity, and intensifying storms

Table 3.1: The SSHS and the proposed Kinetic Energy Hurricane Scale (KEHS)

Category	SSHS (V_{max}) (kt)	Percentage (%)	KEHS ($*10^{16}$J)
0	34 – 63	53.0	< 2.84
1	64 – 82	24.4	2.84 – 5.35
2	83 – 95	10.9	5.35 – 7.09
3	96 – 113	6.5	7.09 – 8.56
4	114 – 135	4.2	8.56 – 10.0
5	> 135	1.1	> 10.0

Table 3.2: Data for all U.S. land-falling hurricanes (1995-2005) at approximately the time of land-fall

Storm Name and Year	Kinetic Energy (J)	NHC V_{max} (kt)	NHC Land-fall Location	Estimated Damages
Erin 1995 (1)	3.346E+16	75	Vero Beach, FL	$700M
Erin 1995 (2)	2.518E+16	75	Pensacola Beach, FL	
Opal 1995	4.469E+16	100	Pensacola Beach, FL	$3B
Bertha 1996	4.069E+16	90	Wilmington, NC	$270M
Fran 1996	8.826E+16	100	Cape Fear, NC	$3.2B
Danny 1997 (1)	1.232E+16	65	Empire, LA	$100M
Danny 1997 (2)	1.453E+16	65	Mullet Point, LA	
Bonnie 1998	5.343E+16	95	Wilmington, NC	$720M
Earl 1998	3.017E+16	70	Panama City, FL	$79M
Georges 1998 (1)	5.520E+16	90	Key West, FL	$5.9B
Georges 1998 (2)	6.034E+16	90	Biloxi, MS	
Bret 1999	3.960E+16	100	Padre Island, TX	$60M
Floyd 1999	6.922E+16	90	Cape Fear, NC	$3B+
Lili 2002	5.270E+16	80	Intracoastal City, LA	$860M
Claudette 2003	2.727E+16	80	Matagorda Island, TX	$180M
Isabel 2003	8.104E+16	90	Drum Inlet, NC	$3.37B
Charley 2004 (1)	2.451E+16	125	Punta Gorda, FL	$14B
Charley 2004 (2)	3.293E+16	65	N. Myrtle Beach, SC	
Gaston 2004	1.502E+16	65	Awendaw, SC	$130M

Frances 2004	7.022E+16	90	Hutchinson Island, FL	$9B
Ivan 2004	9.989E+16	105	Pine Beach, AL	$14.2B
Jeanne 2004	7.022E+16	105	Hutchinson Island, FL	$6.9B
Dennis 2005	4.039E+16	105	Santa Rosa Island, FL	$2.23B
Katrina 2005 (1)	1.991E+16	70	Broward/Miami-Dade, FL	$75B
Katrina 2005 (2)	1.135E+17	105	LA/MS border	
Rita 2005	9.558E+16	100	btwn Johnson's Bayou, LA and Sabine Pass	$10B
Wilma 2005	8.763E+16	105	Cape Romano, FL	$12.2B

Table 3.3: The number of analyses associated with each intensification/growth regime

	Weakening	**Intensifying**	**Maintaining**
Non-Growing	84 (Group 1)	275 (Group 3)	154 (Group 5)
Growing	282 (Group 2)	105 (Group 4)	223 (Group 6)

CHAPTER 4 - CONDITIONS ASSOCIATED WITH STRUCTURE CHANGES

An analysis of a number of variables and conditions determined through statistical analysis to have significant differences for growing versus non-growing storms is described in this chapter. The statistical analysis, which is used to reveal the significance of a given variable, is explained in the first section. In Section 4.2 the basic storm and storm environment conditions (the integrated variables listed in Table 2.1), the radial profiles of the inner core flight-level winds, the radial profiles of the convection from the GOES data and the two-dimensional synoptic environments are analyzed. Finally, a few specific hurricanes are reviewed in section 4.3 as a cursory validation of some of the findings from this study. It should be noted that the Eastern Pacific storms are excluded from this portion of the analysis due to limited availability of aircraft data for the Eastern Pacific basin. However, this should not affect the results as this eliminates only a few storms.

4.1 Significance Testing

The next portion of this study relies upon statistical analysis to determine the probability that a given variable is significantly different for growing versus non-growing storms in each intensification regime. The student's t-test for significantly different means from statistics is utilized. The student's t-test can be used when two distributions have similar variance, but different means (Press et al, 1986). The calculations begin by finding the standard deviation from the combined variance as shown in Equation 4.1

$$s_D = \sqrt{\frac{\sum_{i\in A}(x_i - \overline{x_A})^2 + \sum_{i\in B}(x_i - \overline{x_B})^2}{N_A + N_B - 2}\left(\frac{1}{N_A} + \frac{1}{N_B}\right)} \tag{4.1}$$

where the subscripts A and B indicate values from each sample distribution, and N_A and N_B are the sample sizes for the two distributions, respectively. The t statistic is then calculated using the difference in the means of the sample distributions divided by the standard deviation (Equation 4.2):

$$t = \frac{\overline{x_A} - \overline{x_B}}{s_D} \tag{4.2}$$

The corresponding significance of t for a distribution with $N_A - N_B$ -2 degrees of freedom is determined. This significance (p) is the probability that, for distributions with equal means, the magnitude of t could be this large or larger simply by chance. To find the probability that a given variable has significant differences between two distributions (growing versus non-growing storms, for example) is

$$Probability = 1 - p \tag{4.3}$$

A threshold of 95 percent for the probability of significant difference is used throughout the following analyses to determine what variables are worthy of further investigation.

4.2 Statistically Significant Results

A. Basic Storm and Storm Environmental Conditions

A first step is to determine what characteristics and basic environmental conditions are common to each of the groups defined in Table 3.3. Utilizing the objectively analyzed reconnaissance data, GOES brightness temperature profile data, and the SHIPS model data records (i.e. all of the variables listed in Table 2.1), information about both the storm at the time of each analysis and the associating environmental conditions are retrieved. This selection of data is then sorted into arrays based on the group classifications. A parent group is also formed which contains the data for all of the analyses. For each group the mean values of each of the variables are calculated.

How the environmental conditions for the growing versus non-growing storms in each intensification scenario compare is of particular interest. To determine these relationships the difference in the means of the growing from the non-growing storms is calculated. These values are normalized by the standard deviations of each variable from the parent group in order to obtain non-dimensional values.

The statistical significance testing is now employed using a 95% significance threshold in order to determine which variables are most important. A large number of the variables show significance, but many of these provide overlapping information. Therefore, a revised list of the environmental variables is chosen which best represents the thermodynamic, dynamic, and internal conditions common to the defined storm sub-groups. The latitude (LAT), longitude (LON), sea surface temperature (RSST), ocean heat content (RHCN), magnitude of the shear (SHRD), 850 hPa environmental vorticity (Z850), and 150 hPa temperature (T150) variables were chosen because they provide basic information about the storm environment. The relative eddy momentum flux convergence variable (REFC) is a good indicator of synoptic interactions. The GOES IR variable corresponding to the percent area within the 50-200 km radial area with brightness temperatures colder than -40°C (IR8) was chosen because this temperature is representative of the freezing level. Hence, the IR8 variable is a good measure of the storm's convection. Finally, the radius of maximum symmetric tangential wind (REC1) and tangential wind gradient outside of the radius of maximum wind (REC 6) from the aircraft reconnaissance variables were selected to provide a good estimate of both the size of the eye and the overall storm. This list along with the mean values of each variable in each sub-group is shown in Table 4.1. The normalized difference in the means and

significance for each intensity change regime is shown in Table 4.2. The highlighted values indicate where the 95% significance threshold has been met. Consider now each variable separately.

Latitude: The latitudes are significant for all intensification groups. For both the weakening and maintaining intensity cases, the growing storms are located at lower latitudes than those that are not growing. However, for storms that are intensifying the opposite is true with respect to latitude.

Longitude: The longitude is significant for the intensifying and maintaining intensity storms. For both cases the growing storms tend to be located farther west in the Atlantic basin than those that are not growing.

Sea Surface Temperature (RSST): The SSTs are statistically important for the weakening and maintaining intensity storms. For both cases the growing storms have higher SSTs than the non-growing storms.

Ocean Heat Content (RHCN): The ocean heat content (OHC) is significant for all of the forms of intensity change. The weakening and maintaining intensity cases both have higher OHC values for growing storms than for non-growing storms. Note that this is consistent with the SST tendencies previously mentioned. Intensifying storms, on the other hand, tend to have lower OHC values for growing storms than for storms that are not growing.

150 hPa Temperature (T150): This variable is a measure of the tropopause height, where lower temperatures correspond to a greater height, and higher temperatures to a lesser height. The probabilities indicate that the tropopause height is significant for both weakening and intensifying storms. For weakening storms, those that are

growing have colder 150 hPa temperatures and, hence a higher tropopause height, than non-growing storms. Intensifying storms those that are not growing tend to have colder 150 hPa temperatures than the growing storms, and therefore a higher tropopause height.

850-200 hPa Shear (SHRD): The deep shear is important for all the intensity change scenarios. For storms that are weakening or maintaining intensity the shear is greater for the storms that are not growing than those that are growing. For storms that are intensifying the shear tends to be greater for the growing storms. This implies that shear actually helps a storm to grow once it has passed its intensification stage.

850 hPa Vorticity (Z850): The environmental vorticity is a factor only for storms that are weakening. Lower environmental vorticity is associated with the storms that are not growing, and higher environmental vorticity with growing storms.

200 hPa Relative Eddy Momentum Flux Convergence (REFC): The relative eddy momentum flux convergence variable is an indicator of trough interaction. When a storm interacts with a trough an increase in the 200 hPa relative eddy momentum flux convergence is expected. It is significant only for storms that are intensifying. Those that are both intensifying and growing tend to have higher values of relative eddy momentum flux convergence than those that are intensifying but not growing. This suggests that a storm that is intensifying will be more likely to grow if it is receiving upper-level momentum flux from its outside environment.

Percent area from r=50 to 200 km with TB < -40 C (IR8): This variable provides a rough measure of the inner core convection. It is significant for both weakening and intensifying storms. Storms that are weakening tend to have more convection in the

inner core for those that are growing in size than those that are not growing. Conversely, intensifying storms that are growing tend to have less inner core convection than those that are not growing.

Radius of maximum symmetric tangential wind (REC1): The radius of maximum symmetric tangential wind is a measure of the size of the inner core of the storm. It is significant for both weakening and intensifying storms. Weakening storms that are growing in size tend to have a smaller inner core than those that are weakening and not growing. Intensifying storms on the other hand tend to have a larger inner core for those that are growing than for those that are not growing.

Tangential wind gradient outside the RMW (REC6): The tangential wind gradient outside the radius of maximum wind (RMW) is statistically important for both weakening and intensifying storms. The weakening, growing storms have a larger tangential wind gradient outside the RMW than the weakening, non-growing storms. The intensifying, growing storms have a smaller tangential wind gradient outside the RMW than the intensifying, non-growing storms.

Some overlying trends are beginning to become apparent from the data and analysis completed thus far. The KE climatology establishes that more often than not a storm will either intensify or grow, but not do both simultaneously. While this is the general development, occasionally a storm will weaken and not grow, or intensify and grow (these are termed the 'anomalous' storms). From the above findings some prevalent conditions seem to contribute to a storm becoming anomalous in its structural development.

Consider first the storms that are intensifying and growing in comparison to the typical intensifying, non-growing storms. These storms tend to be located at higher latitudes, farther west, and have lower tropopause heights. They are positioned over lower ocean heat content waters. They generally experience higher shear and higher eddy momentum flux convergence possibly suggesting trough interaction. They have less inner core convection, a larger radius of maximum symmetric tangential wind (i.e. a larger inner core), and a smaller tangential wind gradient outside the RMW. These conditions seem to indicate that trough interaction is a key component for growth in intensifying storms. The trough likely supplies the extra energy needed to support simultaneous intensification and growth. Also, many of the conditions normally associated with intensification (low shear, high SST and OHC) are less for the growing and intensifying cases. This suggests that when the environment is very favorable for intensification, the changes are more confined to the inner core, and have less impact on the storm size.

The second anomalous case involves storms that weaken and do not grow. Compared to those that weaken and grow, these storms are generally located at higher latitudes, have lower tropopause heights, and are positioned over lower SSTs and lower ocean heat content waters. They experience greater shear, and have lower values of environmental vorticity. Less inner core convection, a larger inner core, and a smaller tangential wind gradient outside the RMW are also common features of these storms. These characteristics are indicative of storms in a less favorable environment which prevents the normal growth seen in weakening storms. To better understand these

processes, a more in depth study of the wind profiles, convection, and synoptic environments is necessary.

B. Tangential and Radial Wind Profiles

A closer look is now taken at the wind profiles using the azimuthally averaged symmetric tangential and radial winds from the aircraft reconnaissance objective analyses. The tangential wind profiles should support the results of the statistical analysis of the REC1 (radius of maximum symmetric tangential wind) and REC6 (tangential wind gradient outside of the radius of maximum wind) variables. Furthermore, the radial wind profiles, which at the 700 hPa pressure level give a representation of the secondary storm circulations, should provide further insight into the dynamics of the storms.

Tangential Winds: The tangential winds show significant differences for all storm intensification cases. For weakening storms the tangential winds show statistically significant differences in the 6-82 km radial area (Fig. 4.1). In this region the growing storms have greater tangential winds. More importantly, the weakening, growing storms show a more typically tangential wind profile with a much steeper wind gradient around the eyewall. Also, the radius of maximum tangential wind is clearly smaller for the weakening, growing storms.

For intensifying storms the tangential winds have significant difference in the 6-94 km radial area (Fig. 4.2). In this region the non-growing storms have greater tangential winds and greater wind gradients around the radius of maximum tangential winds. Also, the radius of maximum tangential wind is smaller for the non-growing storms than for the growing storms. These results for the weakening and intensifying

storm cases, not surprisingly, are consistent with the findings for the REC1 and REC6 reconnaissance variables.

For storms that are approximately maintaining their intensity the tangential wind profiles show statistically significant differences in the 138-198 km radial area (Fig. 4.3). In this region the tangential winds are greater for the non-growing storms. This signifies that the maintaining, non-growing storms are larger in size than those that are growing.

Radial Winds: The radial winds show statistically significant difference for growing versus non-growing storms for both weakening and maintaining intensity storms. Note that in the radial wind profile plots positive radial wind values indicate winds which are diverging away from the center of the storm and negative values indicate winds that are converging towards the center of the storm. At the 700 hPa level the radial winds give a representation of the inflow and outflow regions of the storm's secondary circulation.

For the weakening storms the radial winds are significant at radii greater than 110 km from the center of the storm (Fig. 4.4). At these radii the growing, weakening storms have greater inflow. In fact, looking at the mean profiles it is clear that they have a more standard profile of the radial winds with outflow at smaller radii switching over to inflow farther from the center of the storm. However, the weakening, non-growing storms have a noisier profile of the radial winds with no clear point where the radial winds switch from outflow to inflow. This signifies that the secondary circulation is decaying for weakening, non-growing storms. The weakening, growing storms show a profile for the radial winds of outflow near the center of the storm and inflow past approximately 90 km from the storm-center.

For maintaining intensity storms the radial winds are significant at radii greater than 134 km from the storm-center (Fig. 4.5). The growing storms have radial winds which are converging at a greater speed at these radii. To a lesser extent, similar trends to those described for the weakening storms are seen in the profiles for the maintaining intensity storms.

C. Convective Profiles

The GOES IR brightness temperature and standard deviations in brightness temperature radial profiles are now studied in order to gain a better understanding of the structure of the inner and outer core heating in the different types of storms. Brightness temperatures reveal the structure of the convection in that colder brightness temperatures indicate higher clouds, which in a hurricane result from more intense convection. The standard deviation in brightness temperature provides a measure of the asymmetry of the convection where higher values indicate greater convective asymmetry. The brightness temperature profiles show statistically significant differences for weakening and maintaining intensity storms. These profiles of standard deviations in brightness temperature are significantly different for all storm intensity change scenarios.

For weakening storms the 2-18 km radial area in the brightness temperature profiles is significantly different for the growing versus non-growing storms (Fig. 4.6). The non-growing storms have colder cloud-tops near the center of the storm, but warmer cloud-tops through the eyewall, indicating a less convective eyewall than that of the growing storms. The profiles of the standard deviation in brightness temperature for weakening but growing versus non-growing storms exhibit significant differences in the radial areas of 6-22 km and 42-182 km (Fig. 4.7). This illustrates that weakening but

growing storms tend to have more asymmetric convection near the storm-center, and weakening but non-growing storms tend to have greater asymmetric convection outside of the eyewall. This suggests that weakening but non-growing storms have greater heating occurring in the regions outside of the eyewall, and extending to the outer regions of the inner core, than their growing counterparts.

Although the brightness temperature profiles for intensifying storms do not show significant differences in their means, there are some interesting features that are worth mentioning (Fig. 4.8). At the center of the storm the cloud-top temperatures are nearly the same, but the brightness temperature profiles diverge noticeably outwards through the eyewall. The non-growing storms exhibit colder cloud-tops through the eyewall indicating an increased convective region. The growing storms, on the other hand, show a flatter, less convective brightness temperature profile through the eyewall. The profiles of the standard deviation in brightness temperatures for intensifying storms, however, do exhibit significant differences for growing versus non-growing storms (Fig. 4.9). Near the center of the storm (6-10 km region) the non-growing storms show greater asymmetry in their convection, but closer to the eyewall and extending out to the outer rainbands (30-330 km radial area) the growing storms show greater convective asymmetry. This suggests that the intensifying, growing storms have more heating occurring outside of the eyewall and extending to the outer core of the storm, well into the rainbands, than the non-growing storms.

Storms of maintaining intensity have significantly different brightness temperature profiles in the 198-286 km radial area (Fig. 4.10). In this region the growing storms have colder brightness temperatures which suggest that they have more

convective rainbands compared to the non-growing storms. The profile of the standard deviation in brightness temperatures 14-26 km radial area shows significant differences in the storm growth profiles (Fig. 4.11). In this radial area the growing storms exhibit more asymmetric convection than the non-growing storms.

D. Synoptic Environments

Using the NCEP reanalysis data corresponding to each of the aircraft reconnaissance analyses, a composite analysis of the horizontal wind-fields is done for pressure levels of 200, 500, 700 and 850 hPa. The magnitude of the 850-200 hPa deep shear vectors are calculated using the 200 hPa and 850 hPa horizontal winds in Equation 4.4.

$$Shear = \sqrt{(u_{200} - u_{850})^2 + (v_{200} - v_{850})^2} \tag{4.4}$$

The 2-D wind-field and deep shear plots provide a more detailed view of the synoptic conditions associated with each type of storm. The mean fields for each group are computed and statistically analyzed using the methods previously described for the variable analysis, but now extended to a 2-D grid field. The significance fields for the zonal and meridional winds indicate that the intensifying and weakening storm groups have the most noteworthy synoptic features.

Consider first the 200 hPa, 850 hPa and deep shear fields for intensifying storms. The 200 hPa mean wind-fields for both the non-growing (Fig. 4.12) and growing (Fig. 4.13) storms show evidence of the upper level anticyclone. An upper level trough is evident to the west of both the growing and non-growing storms, but for the growing storms the trough is stronger and extends farther south. This stronger trough causes the anticyclone to be displaced farther east of the storm. In addition, the winds around the

anticyclone are less axisymmetric for the growing storms as a result of the trough interaction. This distortion of the wind-field indicates that the trough may be importing momentum into the storm. This supports earlier findings for the 200 hPa relative eddy momentum flux convergence (REFC) variable, which measures greater 200 hPa momentum flux in intensifying storms that are growing than in those that are not growing.

The 850 hPa wind-fields for the non-growing (Fig. 4.14) and growing (Fig. 4.15) storms are dominated primarily by the storm flow. The weak anti-cyclonic circulations directly north of the non-growing storms and northwest of the growing storms, and the cyclonic circulations southwest of both types of storms are likely representative of a synoptic environmental response to the imposed strong cyclonic circulation of the composite storm. With respect to the northern cyclonic circulation, a subtropical ridge is often seen to the north of Atlantic storms. Given the presence of a stronger upper level trough, which has been shown to displace the upper level anticyclone over the storm, the magnitude of the deep vertical shear should be greater for the intensifying, growing storms than for the intensifying, non-growing storms. Contour plots of the shear indicate that this is the case. The shear is markedly enhanced to the northwest of intensifying, growing storms (Fig. 4.16) as compared to those that are not growing (Fig. 4.17).

In weakening storms the upper level anticyclones are evident in the 200 hPa wind-field plots for both the growing (Fig. 4.18) and non-growing (Fig. 4.19) storms. The anticyclone is displaced farther east for the non-growing storms compared to the growing storms. In the region to the northwest of the storm a trough feature appears for both weakening storm groups. An analysis of the winds in this region shows that the

non-growing storms have a moderately stronger trough than the growing storms. This helps to create a more highly sheared environment, as shown by the shear fields for the non-growing (Fig. 4.20) and growing (Fig. 4.21) storms. In weakening storms a more sheared environment contributes to storm decay unlike intensifying storms which have been shown to grow in a more highly sheared environment. Note that the anticyclone circulations due to the subtropical ridge in the 850 hPa wind-fields have an eastward location with respect to the storm for the weakening but growing (Fig. 4.22) and non-growing (Fig. 4.23) storms. This is in contrast to the north and north-west locations observed in the 850 hPa wind-fields of the intensifying but non-growing and growing storms.

The 700 hPa temperature advection fields are now computed, and the mean fields generated and statistically analyzed to determine if there are significant differences in the baroclinic environments. The temperature advection ($-\vec{V}\cdot\nabla T$) is calculated using Equation (4.5):

$$-\vec{V}\cdot\nabla T = -\left(\frac{1}{a\cos\theta}\frac{\partial T}{\partial \lambda}\cdot u + \frac{1}{a}\frac{\partial T}{\partial \theta}\cdot v\right), \tag{4.5}$$

where u is the zonal component of the wind, v is the meridional component of the wind, λ is the longitude, θ is the latitude, and a is the mean radius of the earth ($6.37*10^6$ m). Spherical coordinates are used in order to ensure the accuracy of the temperature advection values at all latitudes. Using finite differencing techniques to find the temperature change across each grid point and the horizontal wind-fields, the temperature advection fields are generated. Positive temperature advection values represent regions of warm air advection, and negative values represent cold air advection.

The 700 hPa temperature advection fields for both weakening storms and intensifying storms reveal some interesting differences for the growing and non-growing storms. The intensifying, growing storms show an interesting temperature advection dipole with strong warm air advection in the northeast quadrant and cold air advection in the northwest quadrant of the storm (Fig. 4.24). This highly baroclinic environment is a factor for growth in intensifying storms. This dipole feature is not evident in the temperature advection fields for intensifying, non-growing storms (Fig. 4.25); advection features present near the center of the storm are a likely result of the compositing and not indicative of strong temperature advection. Of greater interest, a strikingly similar temperature advection dipole feature is present also for weakening, non-growing storms (Fig. 4.26). This suggests that similar baroclinic effects to those of the intensifying but growing storms are influencing weakening but non-growing storms; however, the effect with respect to growth is the opposite for weakening storms. The weakening, growing storms show less temperature advection across the storm (Fig. 4.27). To better understand the causes and effects of the temperature advection dipole feature that is prevalent in both anomalous storm types, further study is necessary through a complete energy budget analysis.

4.3 Summary of Mechanisms for Tropical Cyclone Growth

The results of statistical testing, and the subsequent analysis that has been presented on conditions associated with different types of storm structural evolution, imply that there are two ways for storms to grow. The first type is growth through eyewall replacement cycles, which were identified and discussed in Chapter 3 as mechanisms for storm growth. Eyewall replacement cycles are inner core dominated

processes which occur when a storm has reached a sufficiently intense state and is in a favorable synoptic environment. This process can cause an initial weakening in the storm's intensity as the inner eye breaks down; the new eye that then forms from the secondary eyewall is typically larger than its predecessor. The end result is a growth in the storm's circulations.

The second type of growth is induced by environmental forcing. Environmental forcing can be caused by momentum flux from trough interactions, a more highly sheared environment, temperature advection, or a combination of these features. When a storm is in a stage of intensification, interaction with a trough may import additional momentum into the core inducing growth. In this scenario, kinetic energy from the mean flow of the trough is converted into kinetic energy of the storm. The baroclinicity of the storm environment can also be a source of forcing on the storm. Tropical cyclone development is generally thought to require a vertically stacked structure (a barotropic environment). However, the formation of a more tilted vertical structure (a baroclinic environment) may stimulate growth in the storm. This vertical tilt is a likely result of shear caused by a trough or some other atmospheric disturbance. Shear can cause baroclinic instability and hence, temperature advections as the winds flow across a temperature gradient. In this situation, potential energy from the baroclinic instability might be converted into kinetic energy in the storm leading to a growth in the storm's circulations.

It is interesting to note that environmentally forced growth applies only to storms that are in an intensification stage. For weakening storms environmental forcing has a negative effect on structure. Recall the mean values of the deep shear (SHRD) variable for intensifying and weakening storms in Table 4.1. The environmental shear for both

weakening and intensifying storms that are growing is comparable (16.3 kt and 16.6 kt, respectively). However, for non-growing, weakening storms the shear is a notably higher 19.1 knots. This indicates that moderate environmental forcing may enhance a storm; however, too much forcing will cause a more rapid decay of the storm.

4.4 Case Studies

Having determined through statistical analysis that there are common features and characteristics for the various types of storm structural evolution, validation of these results is in order. A few storms have been chosen based upon the categorization of the analyses for each storm. The storm's evolution is related to the Tropical Cyclone Report for that storm from the National Hurricane Center (NHC) archive. Storms that exhibit typical and atypical structural evolution have been presented.

Hurricane Mitch (1998) is an example of a storm that experienced a fairly typical structural evolution as evidenced by the plot of KE' versus intensity (Fig. 4.28) and the time series, in Julian days from the time of the first analysis of the storm, of the intensity, environmental shear, 200 hPa eddy momentum flux convergence, and KE' (Fig. 4.29) for the storm. The analyses correspond to the period from 18 UTC October 23 to 12 UTC October 29 during Mitch's lifetime. Additionally, Fig. 4.30 shows the track of Hurricane Mitch from the NHC best-track data. The time series plots show that from 18 UTC October 23 to 12 UTC October 26, the analyses categorize the storm as intensifying and not growing, and during the period of 6 UTC October 27 to 12 UTC October 29, as weakening and growing in size. The KE' time series essentially mirrors the intensity time series (Fig. 4.29) illustrating the growth and non-growing pattern through the storm's intensification and weakening stages. The intensifying stage indicated by the

analyses encompasses the time shortly before the storm became a hurricane, located to the southwest of Jamaica, until it reached its maximum intensity on the afternoon of the 26th. During this time it underwent a rapid intensification. A reported symmetric, well-established upper-tropospheric outflow pattern evident in the satellite imagery is suggestive of a low-shear, undisruptive synoptic environment which allowed a typical intensification process (Guiney and Lawrence, 1999). On the 27th the storm passed over Swan Island and began to weaken in intensity, a process which would continue through the 29th when it made land-fall in Honduras. The minimal values of eddy momentum flux convergence shown in Fig. 4.29 indicate that the storm did not experience much environmental forcing. Aside from the land interactions, which were likely a crucial factor in the storm's weakening stages, Mitch was in an environment well-suited to host a substantial hurricane.

Hurricane Dennis (1999) was an atypical storm which experienced trough interactions that appear to have enhanced the storm's structural evolution. The KE' versus intensity plot is shown in Fig. 4.31, and the time series of the intensity, environmental shear, 200 hPa eddy momentum flux convergence, and KE' are shown in Fig. 4.32. The track of the storm from the NHC extended best-track data is shown in Fig. 4.33. The analyses for the storm correspond to the time span from August 25 00 UTC to August 31 12 UTC. Hurricane Dennis formed August 26th in the western Atlantic at the east-southeast end of a trough and in upper-level westerly shear (Beven, 2000). This environment caused the storm's convection to be asymmetric with a greater amount in its eastern portion. Furthermore, the environment prevented the storm's circulations from consolidating, as is normally seen in hurricanes, keeping the radius of maximum winds

fairly large throughout the initial intensification of the storm. The increasing shear and eddy momentum flux convergence in the first portion of Fig. 4.32 were caused by that initial trough interaction. During this period the KE' was also seen to increase indicating a growth of the wind-field. The shear decreased late on the 27th after which the storm reached its peak intensity of 90 knots on the 28th. However, a second mid-latitude trough interaction on the 28th and 29th caused a more northward movement of the storm. During this time the radius of maximum winds in the storm remained large (extending 70 to 85 nautical miles August 29-30). This second trough interaction was evident in the time series plots of the shear and eddy momentum flux convergence. Even with the increased shear and momentum flux, the storm's intensity was maintained and even increased. Furthermore, the KE' increased as well during this period as the storm's circulation grew.

The structural evolution of Hurricane Wilma (2005) can be separated into two stages. During the first stage while the storm was in the Caribbean it intensified and grew through an eyewall replacement cycle, as described in detail in Chapter 3. As the storm traveled over the Gulf of Mexico towards and across southern Florida it continued to grow and intensify, however this development was a result of synoptic forcing. A strong mid-tropospheric trough which was steering the storm along this path also created a strongly sheared environment for the storm (Pasch et al, 2006). The KE' versus intensity plot is shown in Fig. 3.5, and the time series of the intensity, environmental shear, 200 hPa eddy momentum flux convergence, and KE' are shown in Fig. 4.34. The track of the storm from the NHC extended best-track data is shown in Fig. 4.35. The analyses for the storm correspond to the time span from October 17 18 UTC to October 25 00 UTC. The eyewall replacement cycle is shown by the large increase and then drop

in the intensity and a corresponding drop and increase in the KE' in the time series plots. The trough interactions during the storm's passage over the Gulf of Mexico are evident by the increasing shear and eddy momentum flux in the latter part of the time series plots. During this time, however, the storm continued to intensify and maintain and even increase a bit in size, as is demonstrated by the KE' trend. This gives support to the hypothesis that trough interactions and more highly sheared environments can induce growth in an intensifying tropical cyclone.

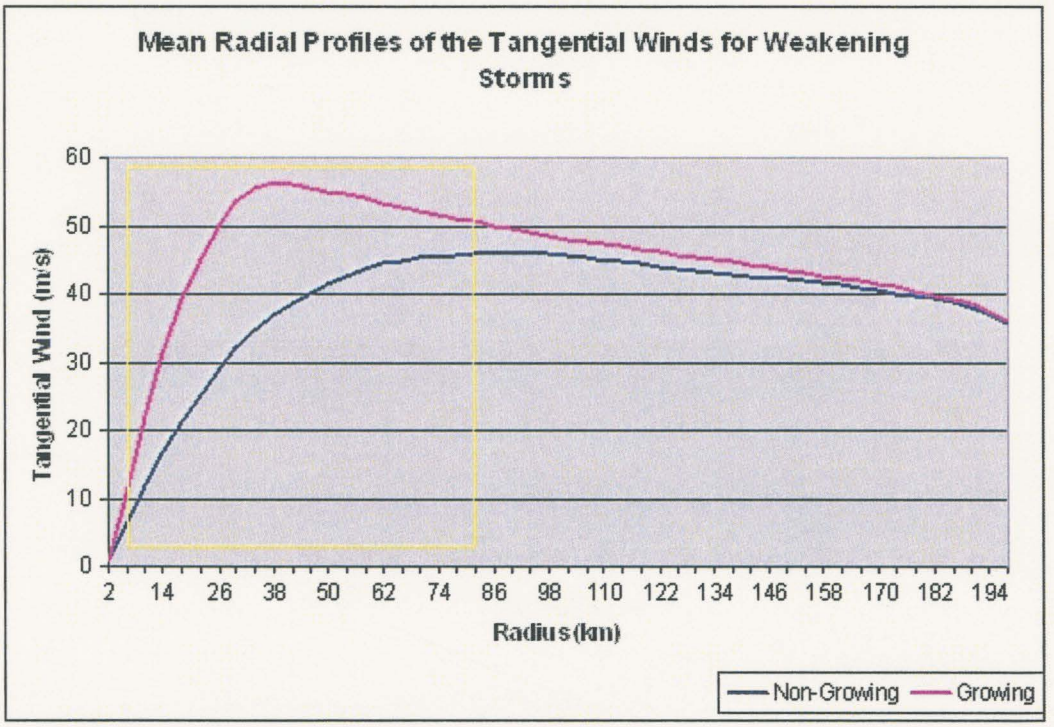

Figure 4.1: Mean radial profiles of the azimuthally averaged symmetric tangential winds for weakening storms. The yellow box denotes where there is greater than 95% probability of significant differences in the growing vs. non-growing profiles.

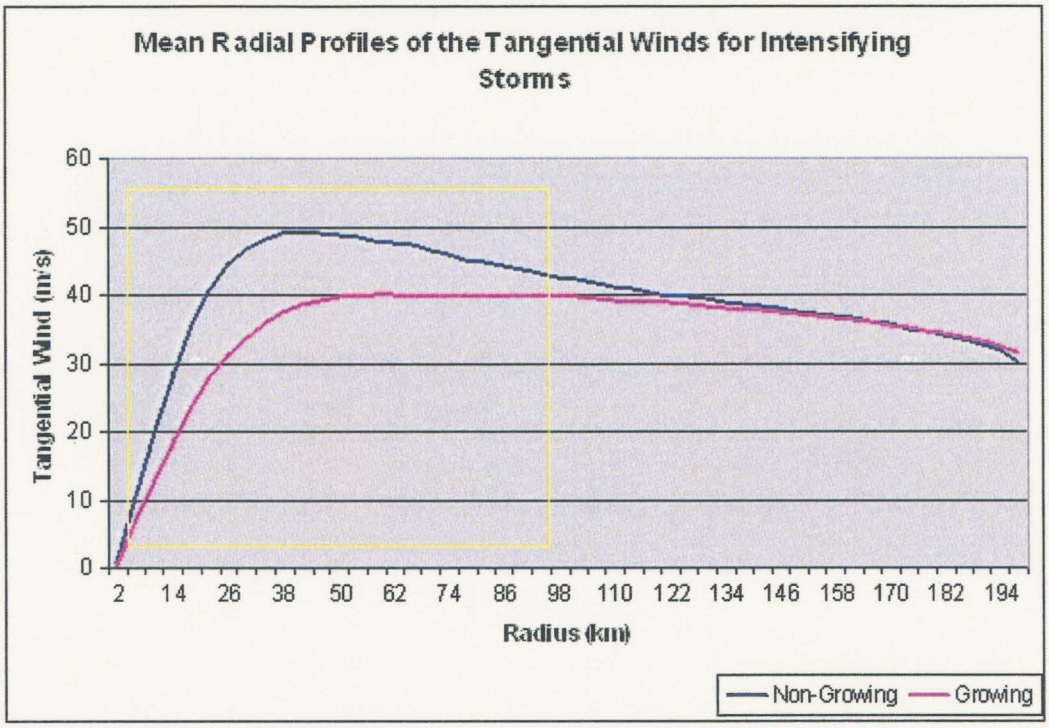

Figure 4.2: Mean radial profiles of the azimuthally averaged symmetric tangential winds for intensifying storms. The yellow box denotes where there is greater than 95% probability of significant differences in the growing vs. non-growing profiles.

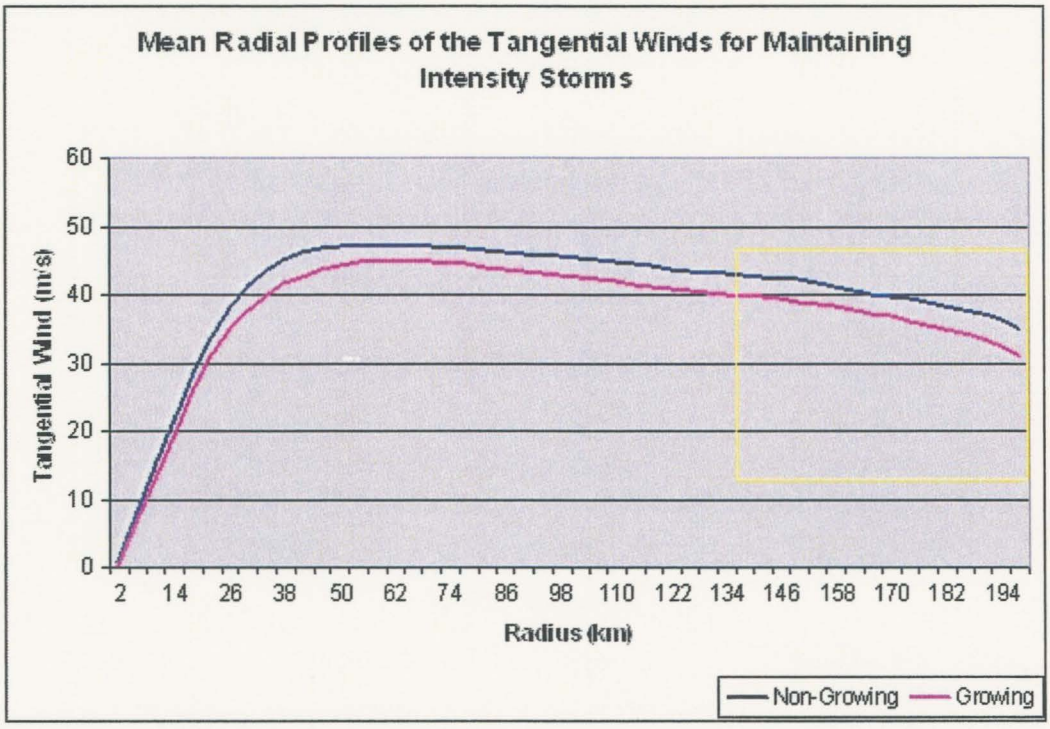

Figure 4.3: Mean radial profiles of the azimuthally averaged symmetric tangential winds for maintaining intensity storms. The yellow box denotes where there is greater than 95% probability of significant differences in the growing vs. non-growing profiles.

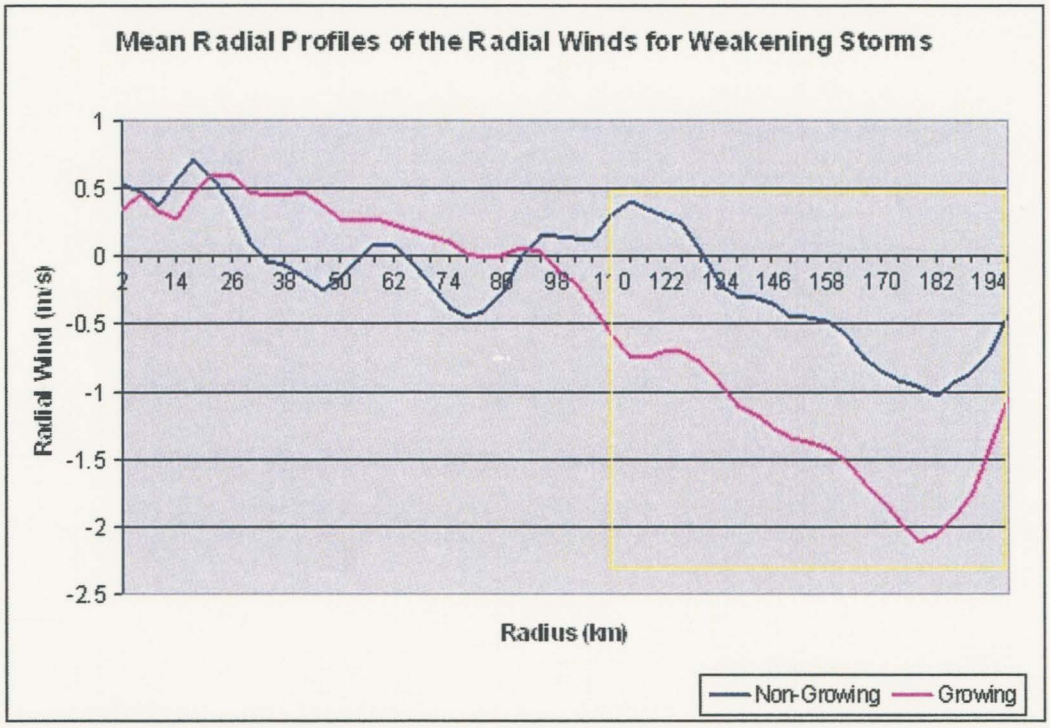

Figure 4.4: Mean radial profiles of the azimuthally averaged symmetric radial winds for weakening storms. The yellow box denotes where there is greater than 95% probability of significant differences in the growing vs. non-growing profiles.

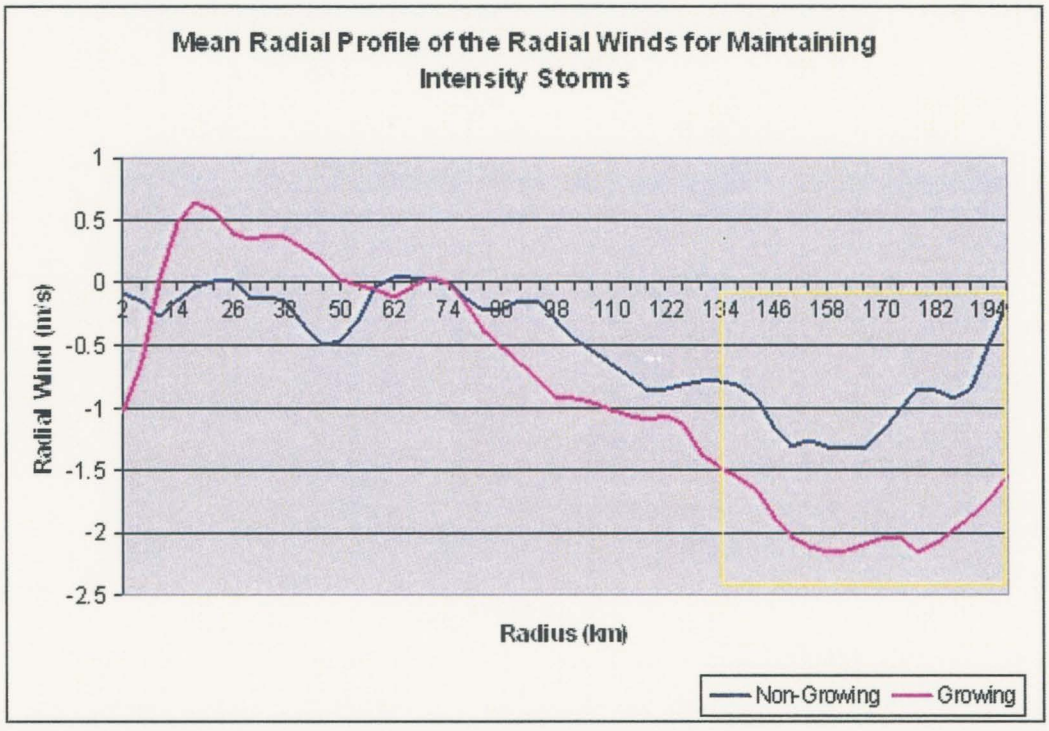

Figure 4.5: Mean radial profiles of the azimuthally averaged symmetric radial winds for maintaining intensity storms. The yellow box denotes where there is greater than 95% probability of significant differences in the growing vs. non-growing profiles.

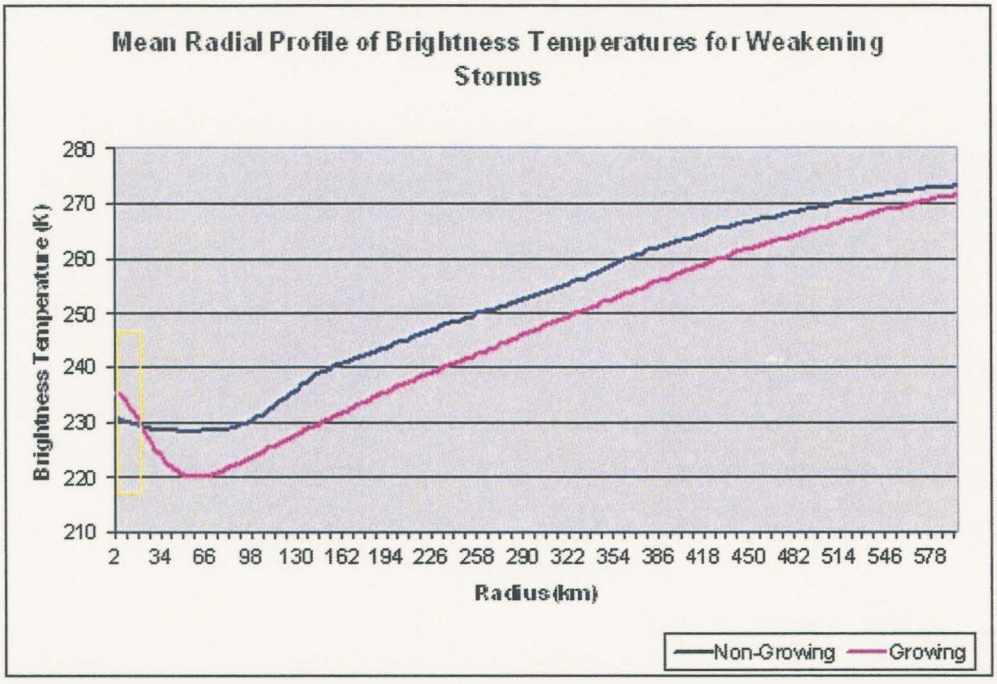

Figure 4.6: Mean radial profiles of the GOES IR brightness temperatures for weakening storms. The yellow box denotes where there is greater than 95% probability of significant differences in the growing vs. non-growing profiles.

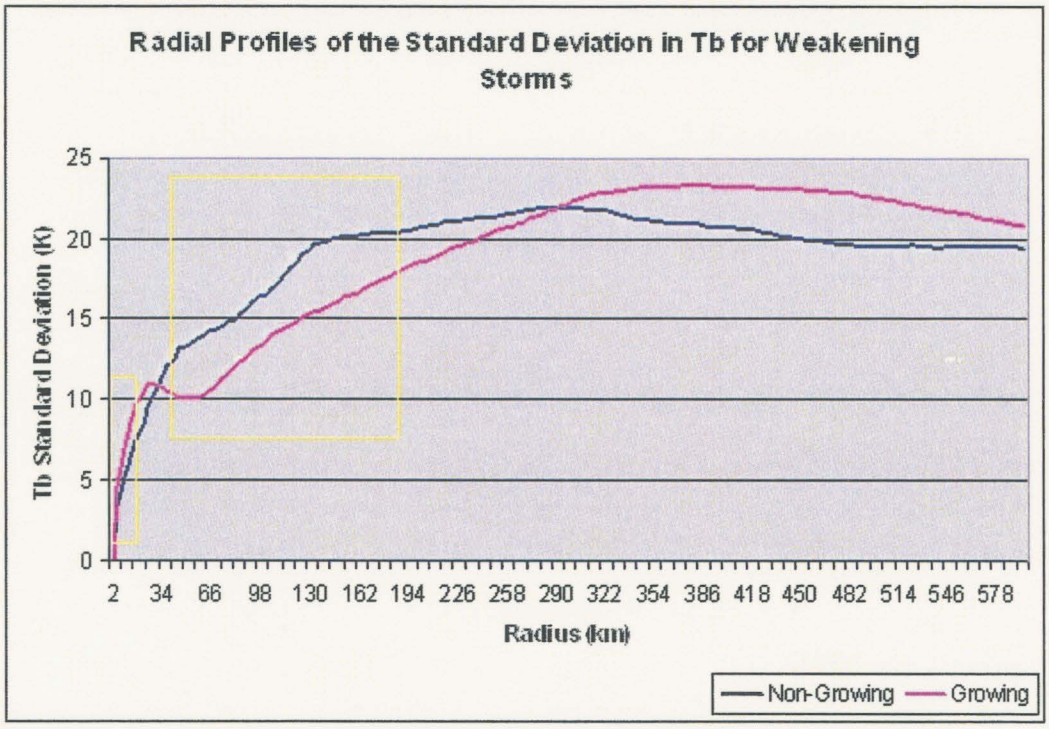

Figure 4.7: Mean radial profiles of the GOES IR brightness temperature standard deviations for weakening storms. The yellow boxes denote where there is greater than 95% probability of significant differences in the growing vs. non-growing profiles.

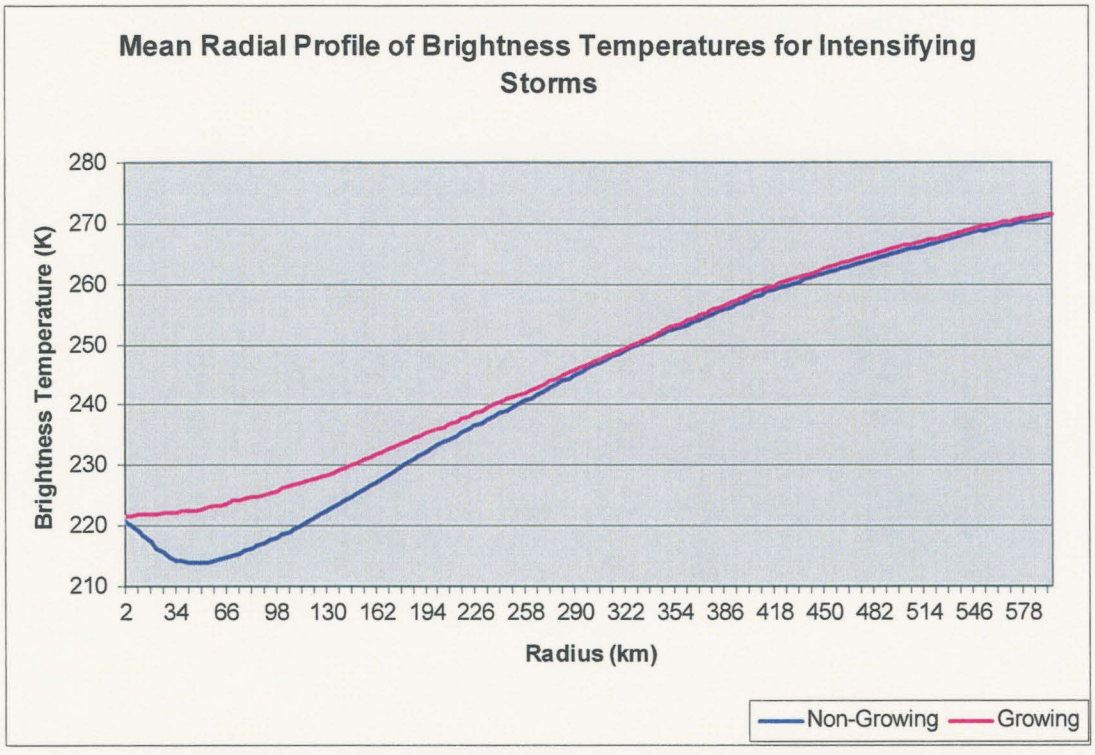

Figure 4.8: Mean radial profiles of the GOES IR brightness temperatures for intensifying storms.

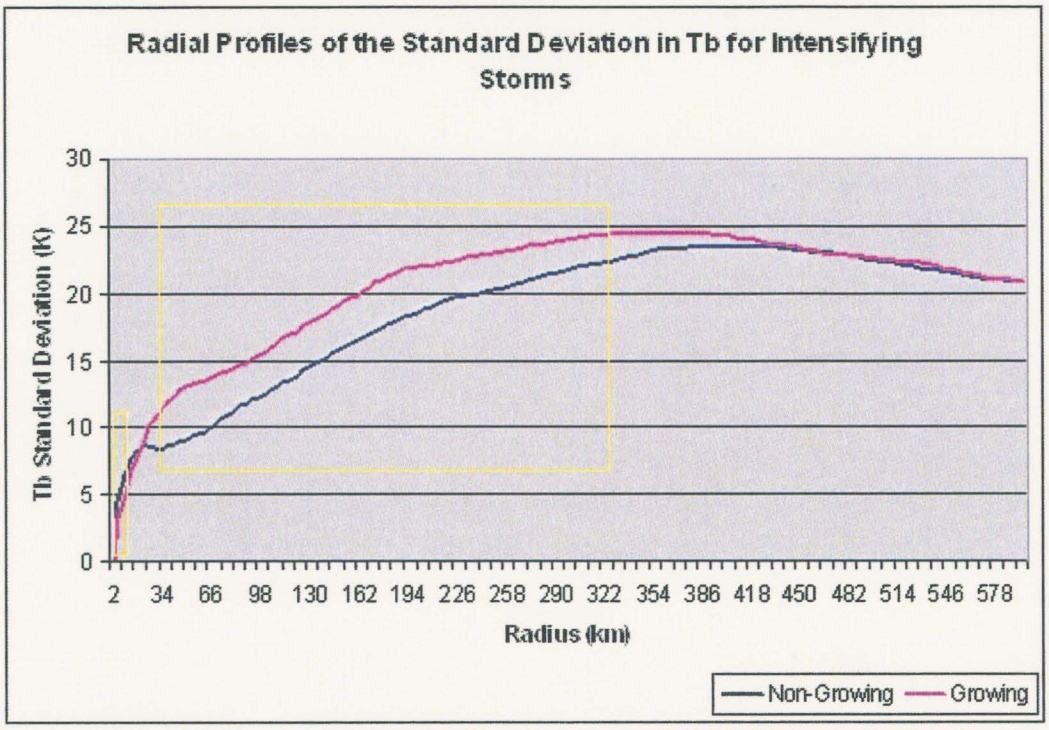

Figure 4.9: Mean radial profiles of the GOES IR brightness temperature standard deviations for intensifying storms. The yellow boxes denote where there is greater than 95% probability of significant differences in the growing vs. non-growing profiles.

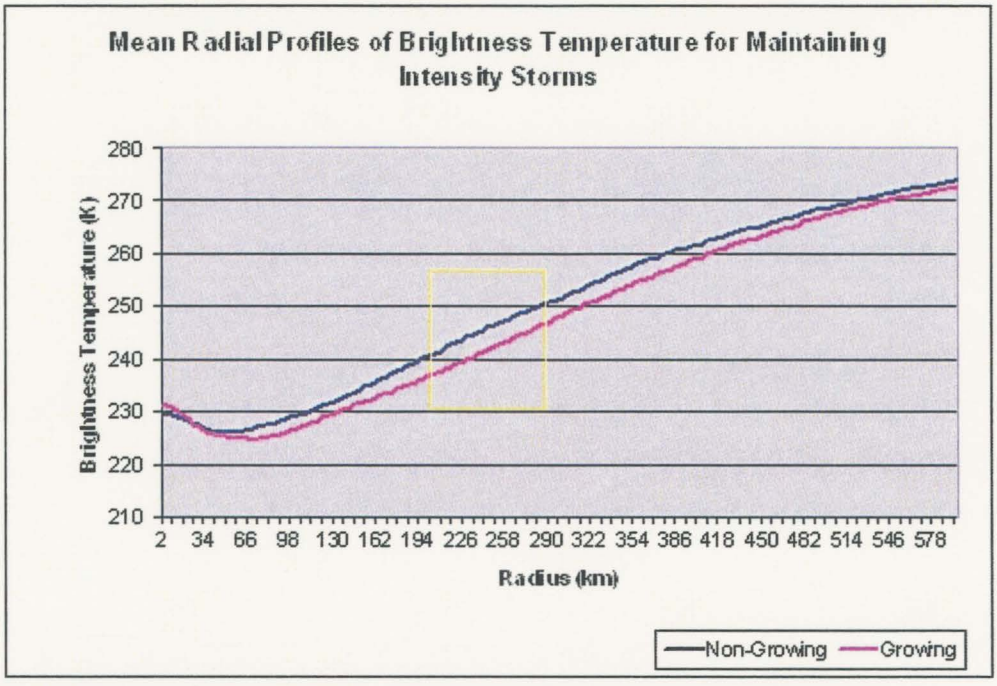

Figure 4.10: Mean radial profiles of the GOES IR brightness temperatures for maintaining intensity storms. The yellow box denotes where there is greater than 95% probability of significant differences in the growing vs. non-growing profiles.

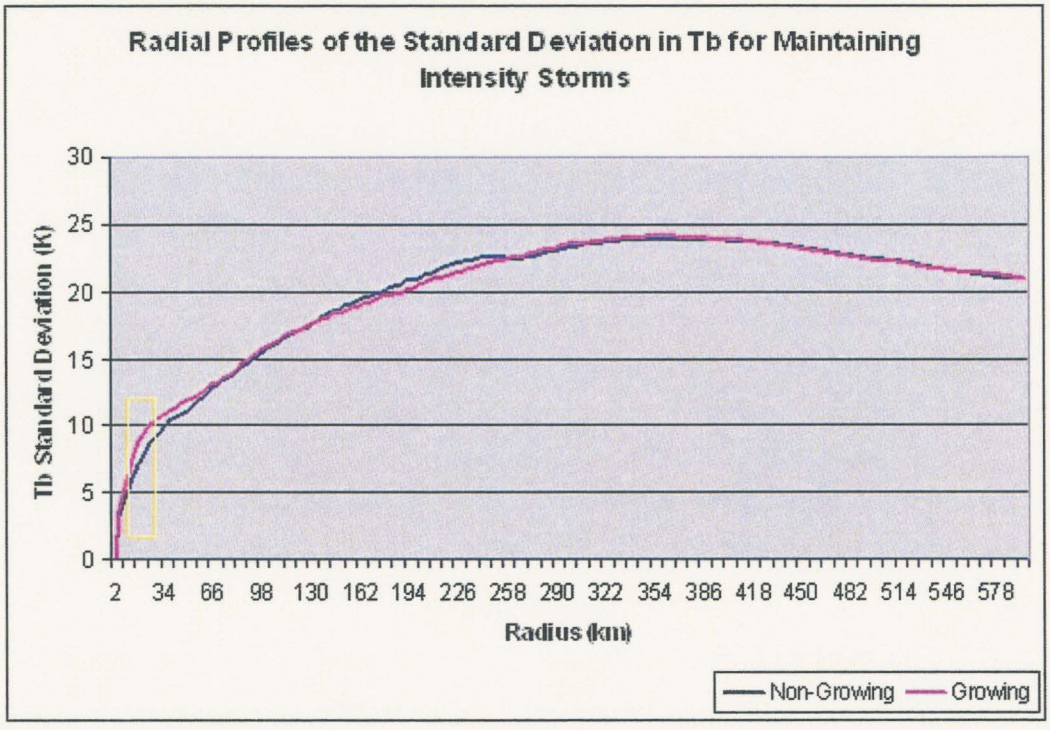

Figure 4.11: Mean radial profiles of the GOES IR brightness temperature standard deviations for maintaining intensity storms. The yellow box denotes where there is greater than 95% probability of significant differences in the growing vs. non-growing profiles.

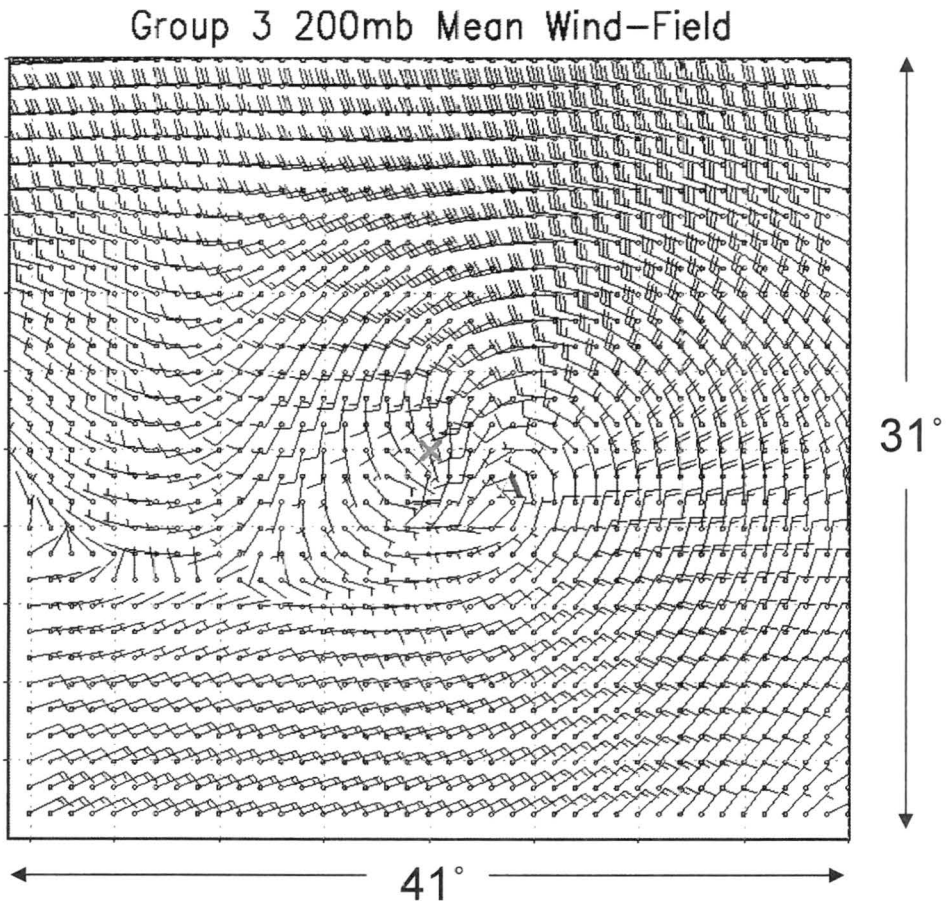

Figure 4.12: 200 hPa mean wind-field [kts] for intensifying, non-growing storms. The 'X' denotes the location of the center of the hurricane. The 'A' marks the location of the upper-level anticyclone.

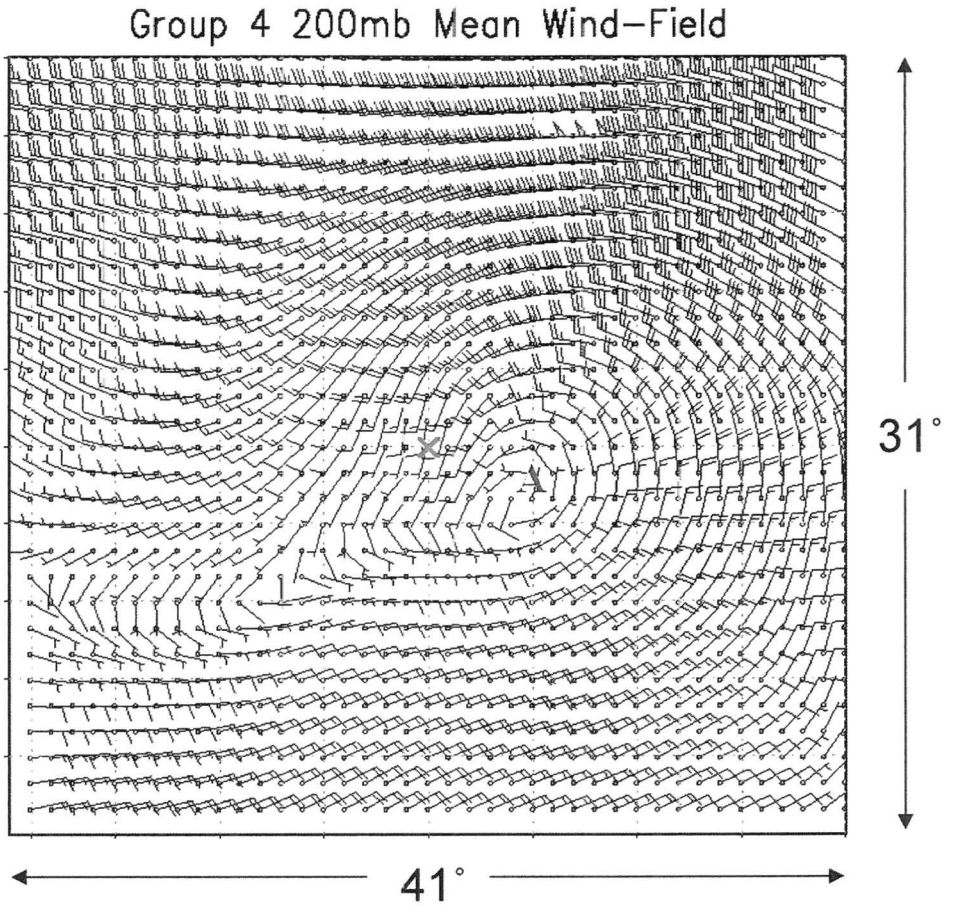

Figure 4.13: 200 hPa mean wind-field [kts] for intensifying, growing storms. The 'X' denotes the location of the center of the hurricane. The 'A' marks the location of the upper-level anticyclone.

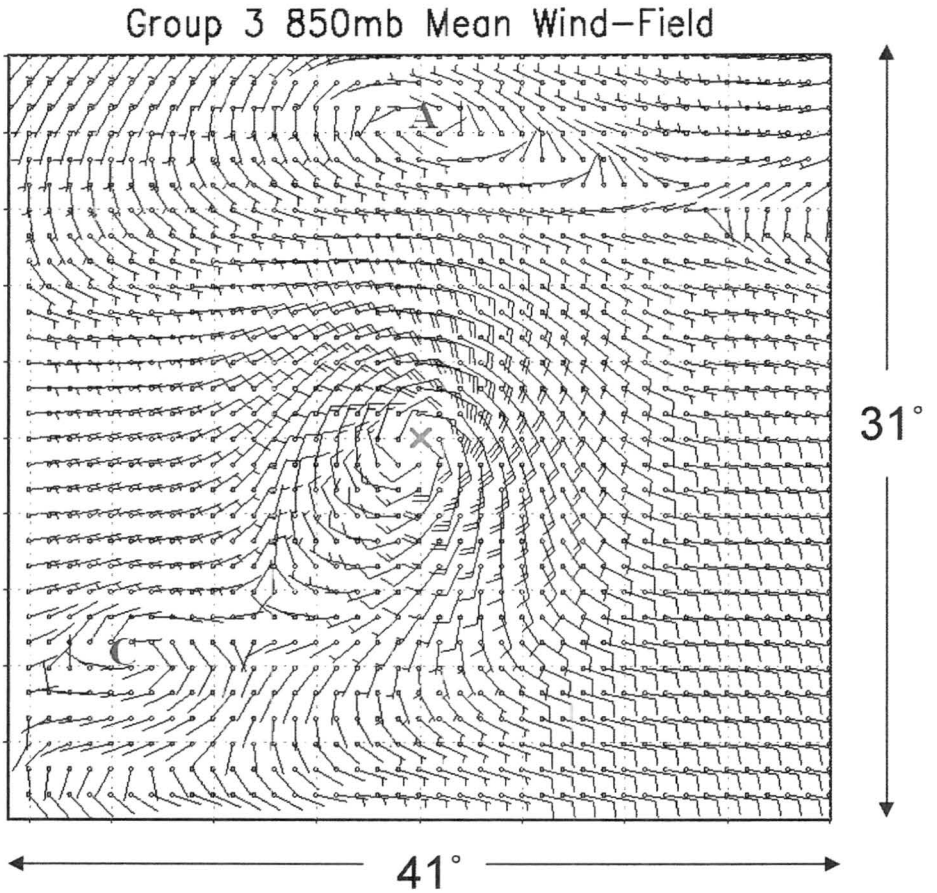

Figure 4.14: 850 hPa mean wind-field [kts] for intensifying, non-growing storms. The 'X' denotes the location of the center of the hurricane. The 'A' and 'C' mark the locations of anticyclone and cyclone circulations which represent the synoptic environmental response to the imposed strong cyclonic circulation of the composite storm.

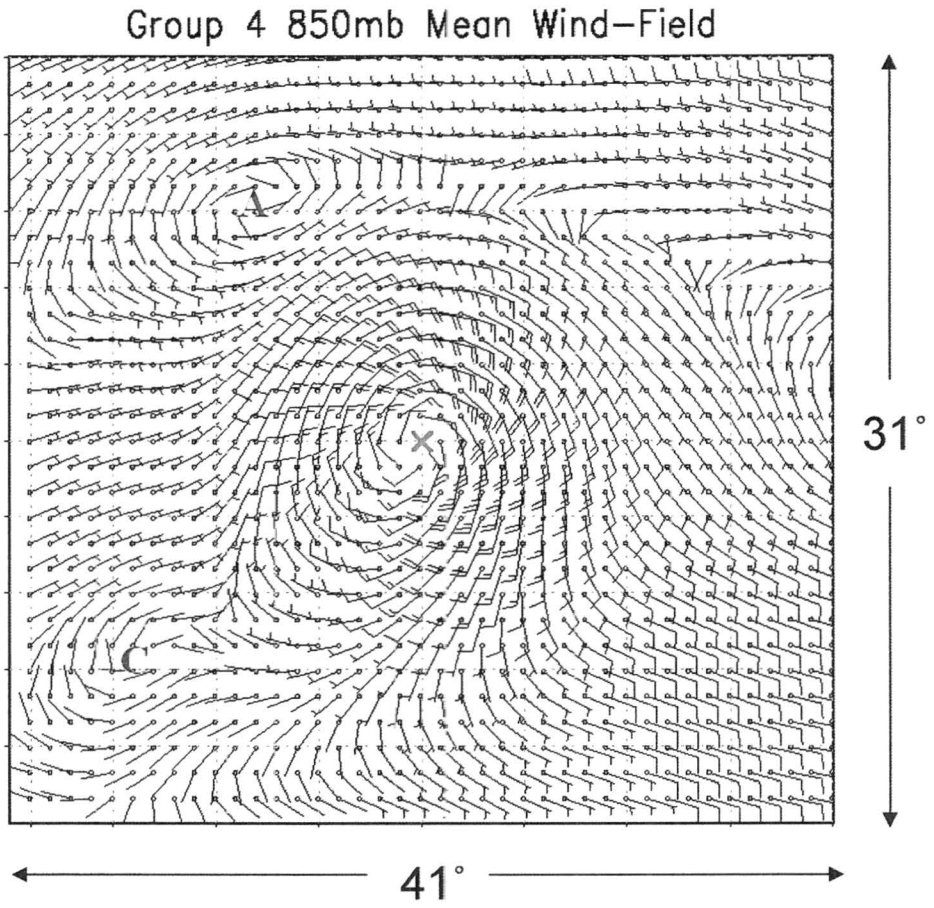

Figure 4.15: 850 hPa mean wind-field [kts] for intensifying, growing storms. The 'X' denotes the location of the center of the hurricane. The 'A' and 'C' mark the locations of anticyclone and cyclone circulations which represent the synoptic environmental response to the imposed strong cyclonic circulation of the composite storm.

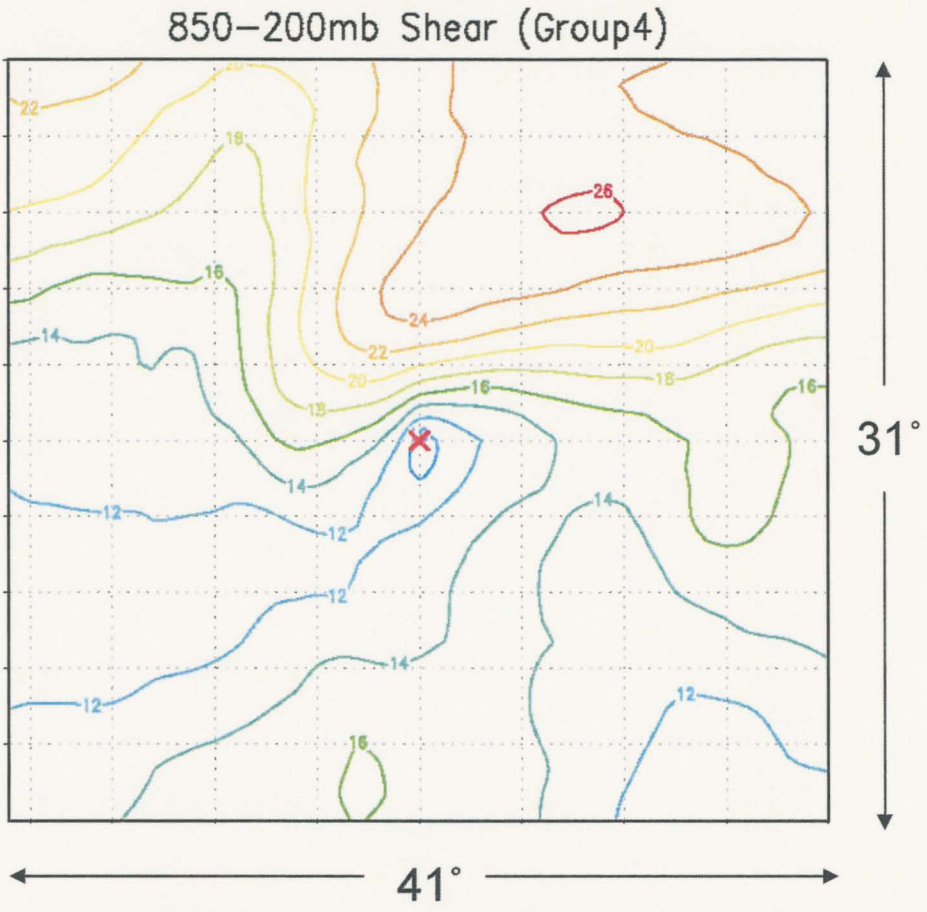

Figure 4.16: 850-200 hPa mean shear [ms^{-1}] for intensifying, growing storms. The 'X' denotes the location of the center of the hurricane.

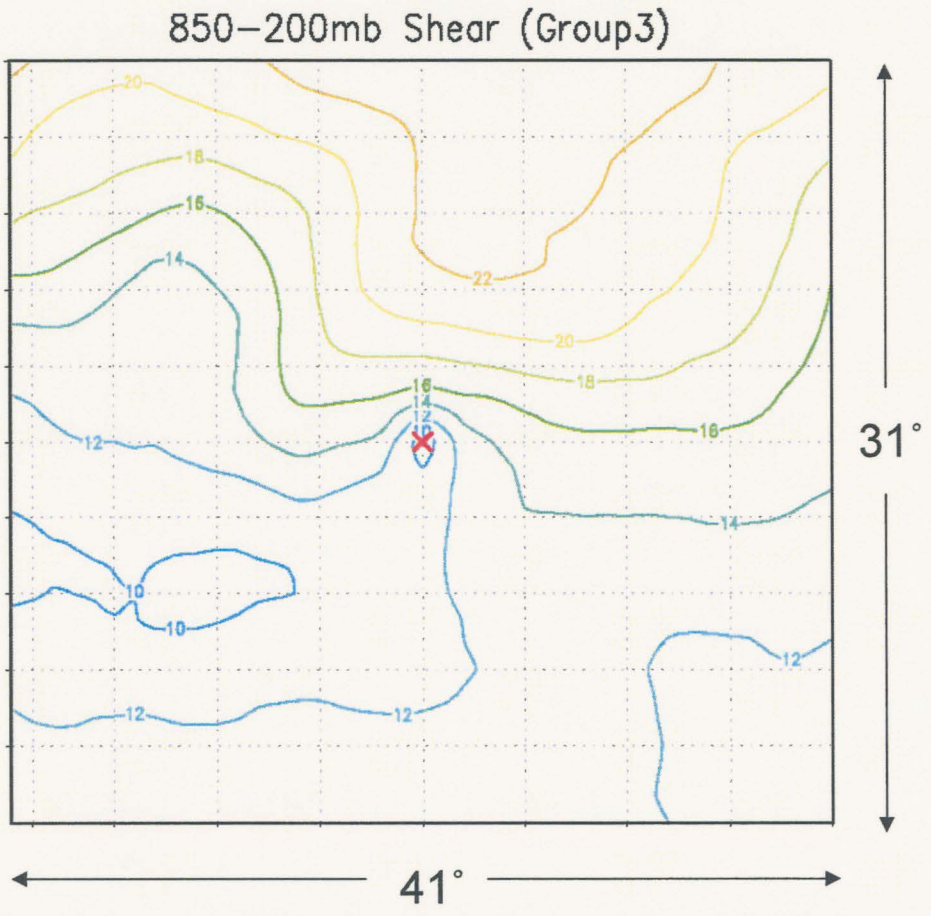

Figure 4.17: 850-200 hPa mean shear [ms^{-1}] for intensifying, non-growing storms. The 'X' denotes the location of the center of the hurricane.

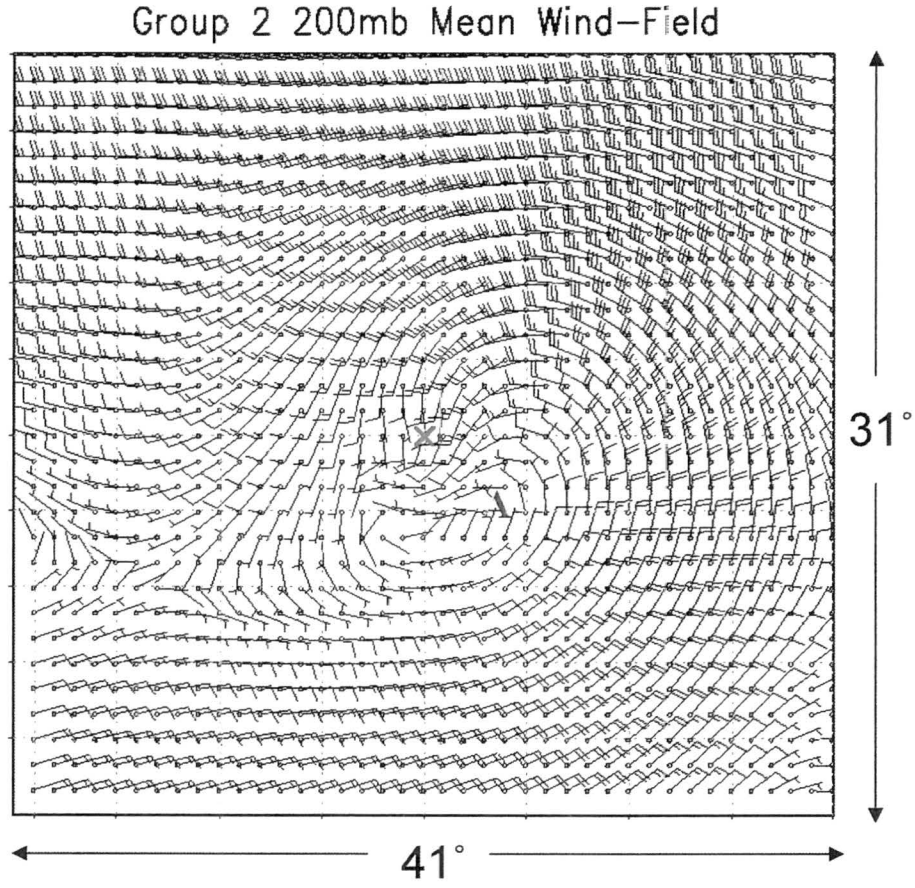

Figure 4.18: 200 hPa mean wind-field [kts] for weakening, growing storms. The 'X' denotes the location of the center of the hurricane. The 'A' marks the location of the upper-level anticyclone.

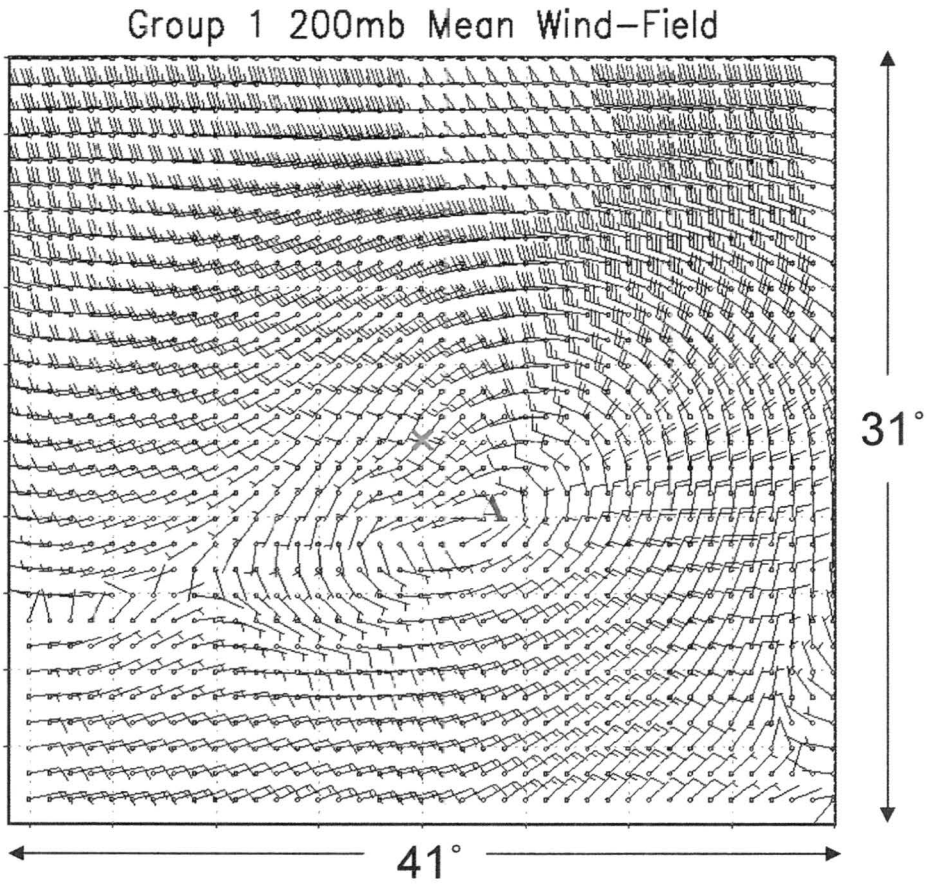

Figure 4.19: 200 hPa mean wind-field [kts] for weakening, non-growing storms. The 'X' denotes the location of the center of the hurricane. The 'A' marks the location of the upper-level anticyclone.

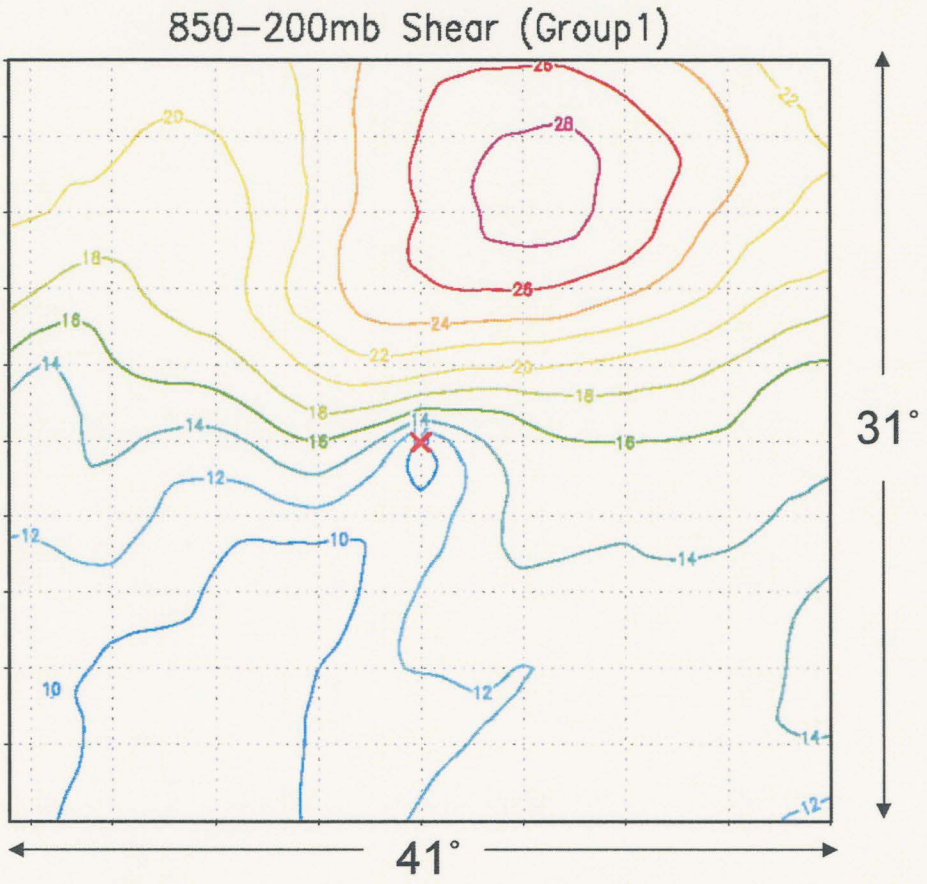

Figure 4.20: 850-200 hPa mean shear [ms^{-1}] for weakening, non-growing storms. The 'X' denotes the location of the center of the hurricane.

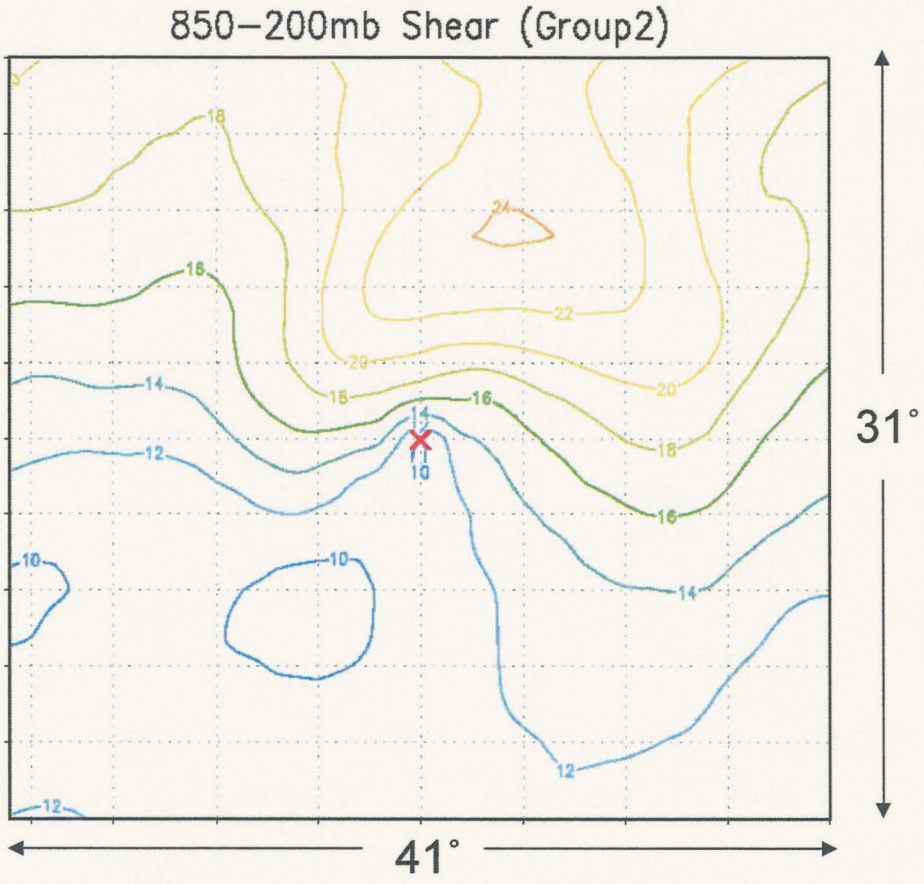

Figure 4.21: 850-200 hPa mean shear [ms^{-1}] for weakening, growing storms. The 'X' denotes the location of the center of the hurricane.

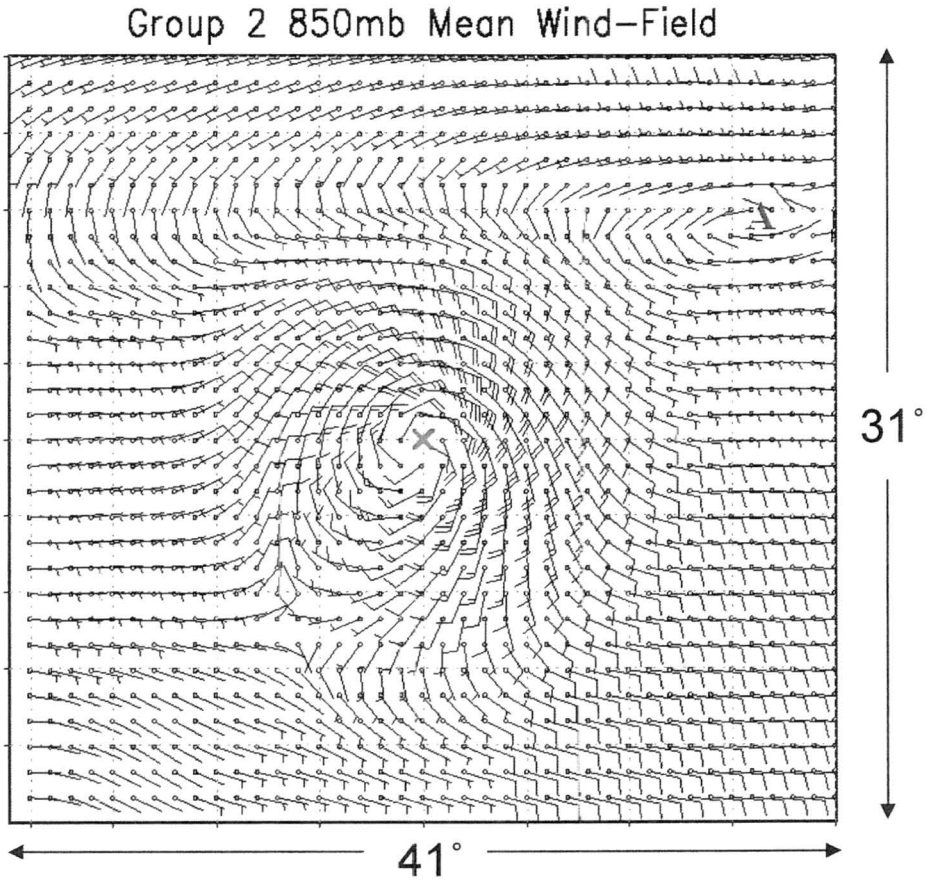

Figure 4.22: 850 hPa mean wind-field [kts] for weakening, growing storms. The 'X' denotes the location of the center of the hurricane. The 'A' marks the location of an anticyclone which is representative of the synoptic environmental response to the composite cyclone.

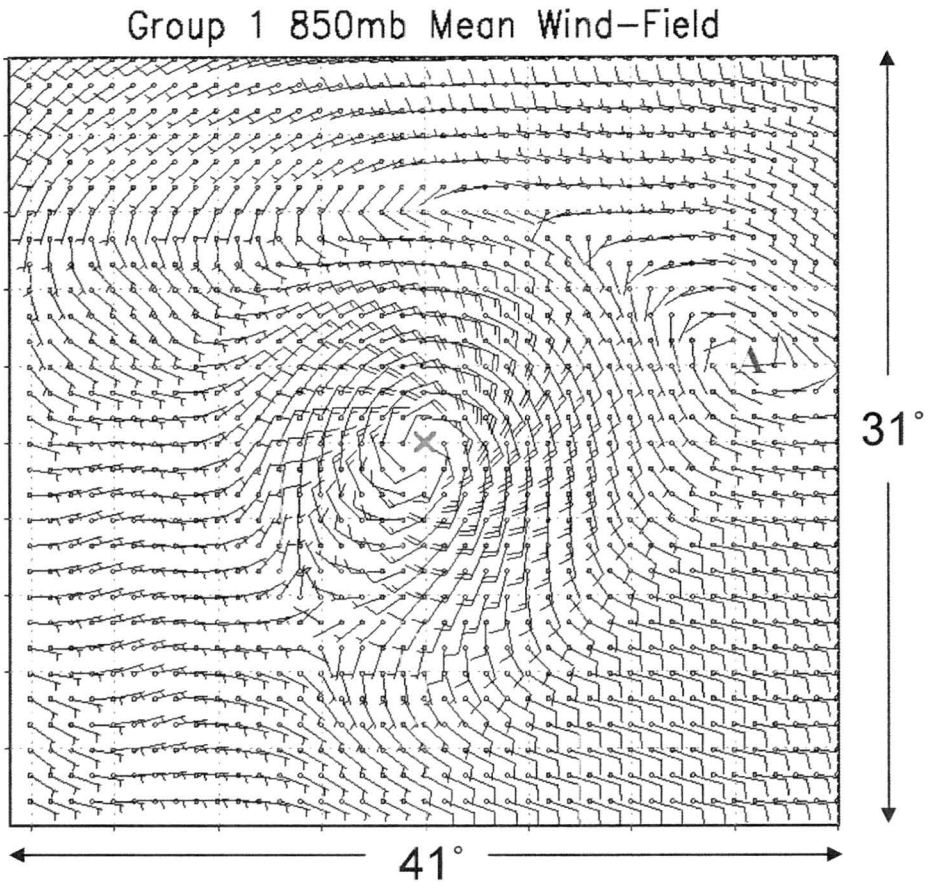

Figure 4.23: 850 hPa mean wind-field [kts] for weakening, non-growing storms. The 'X' denotes the location of the center of the hurricane. The 'A' marks the location of an anticyclone which is representative of the synoptic environmental response to the composite cyclone.

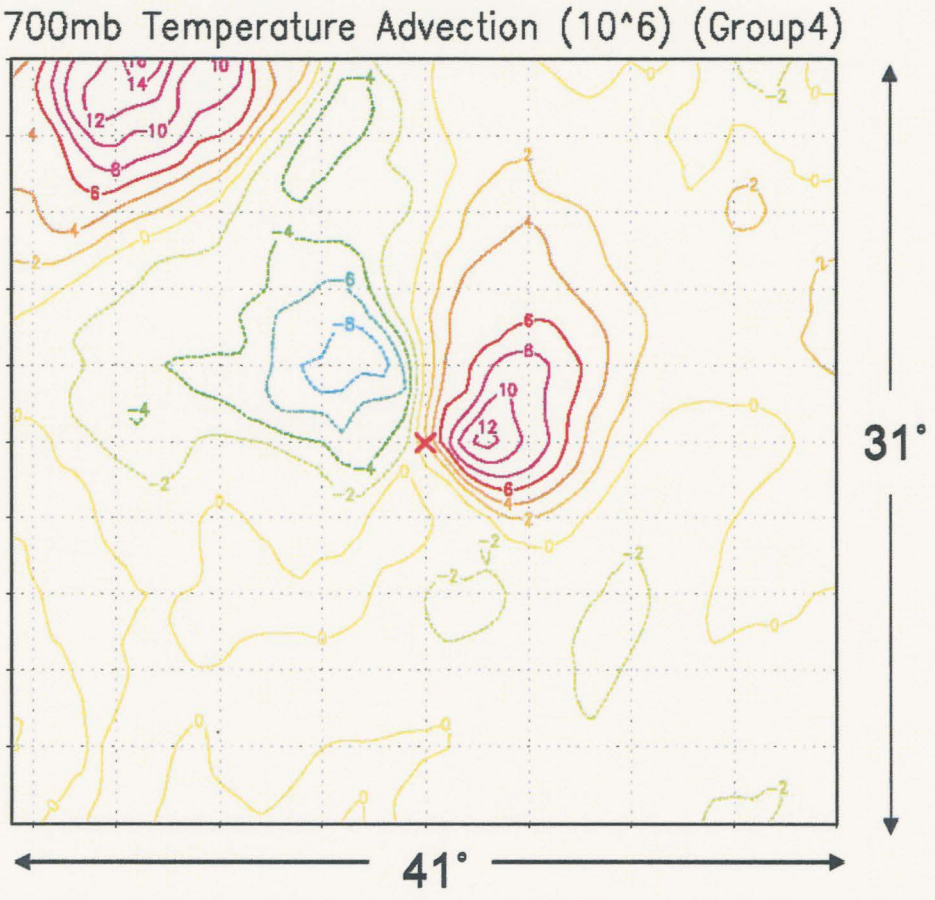

Figure 4.24: 700 hPa mean temperature advection [Ks^{-1}] for intensifying, growing storms. The 'X' denotes the location of the center of the hurricane.

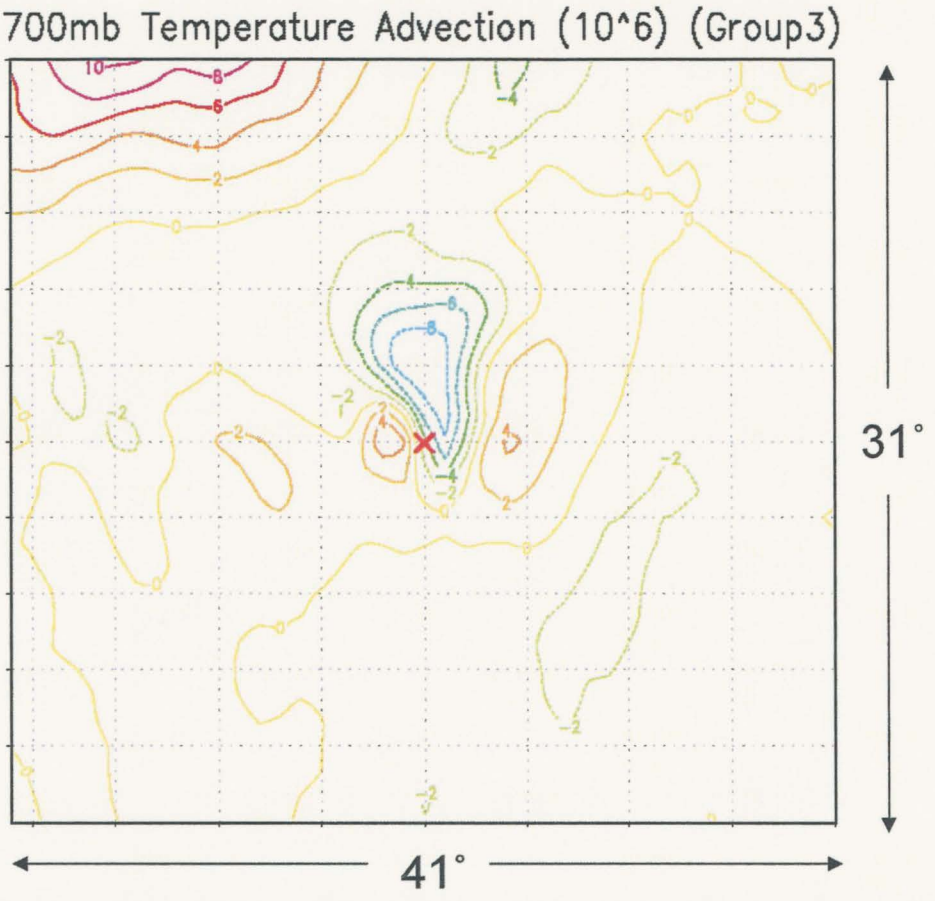

Figure 4.25: 700 hPa mean temperature advection [Ks^{-1}] for intensifying, non-growing storms. The 'X' denotes the location of the center of the hurricane.

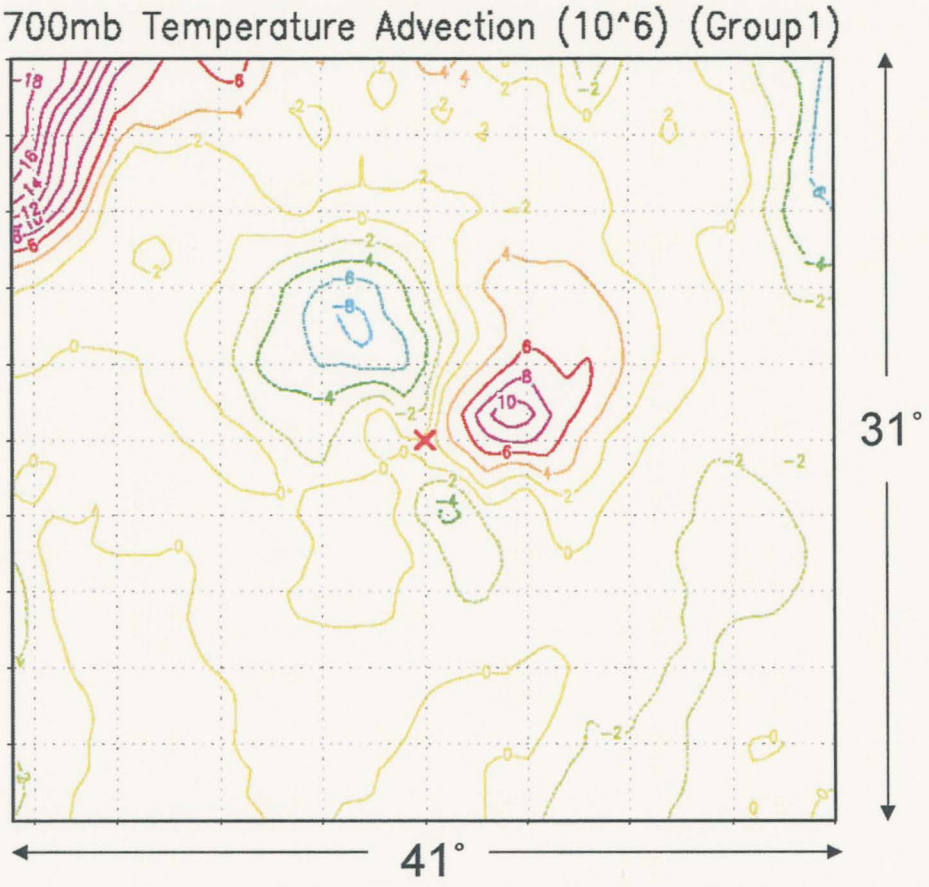

Figure 4.26: 700 hPa mean temperature advection [Ks^{-1}] for weakening, non-growing storms. The 'X' denotes the location of the center of the hurricane.

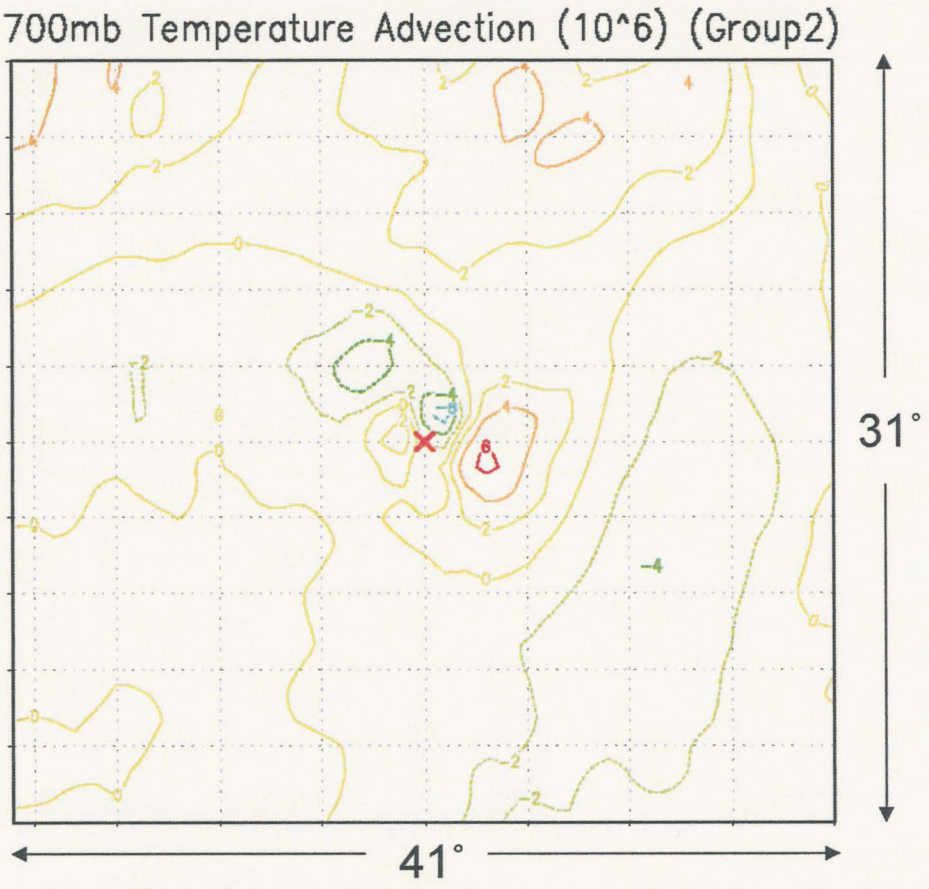

Figure 4.27: 700 hPa mean temperature advection [Ks^{-1}] for weakening, growing storms. The 'X' denotes the location of the center of the hurricane.

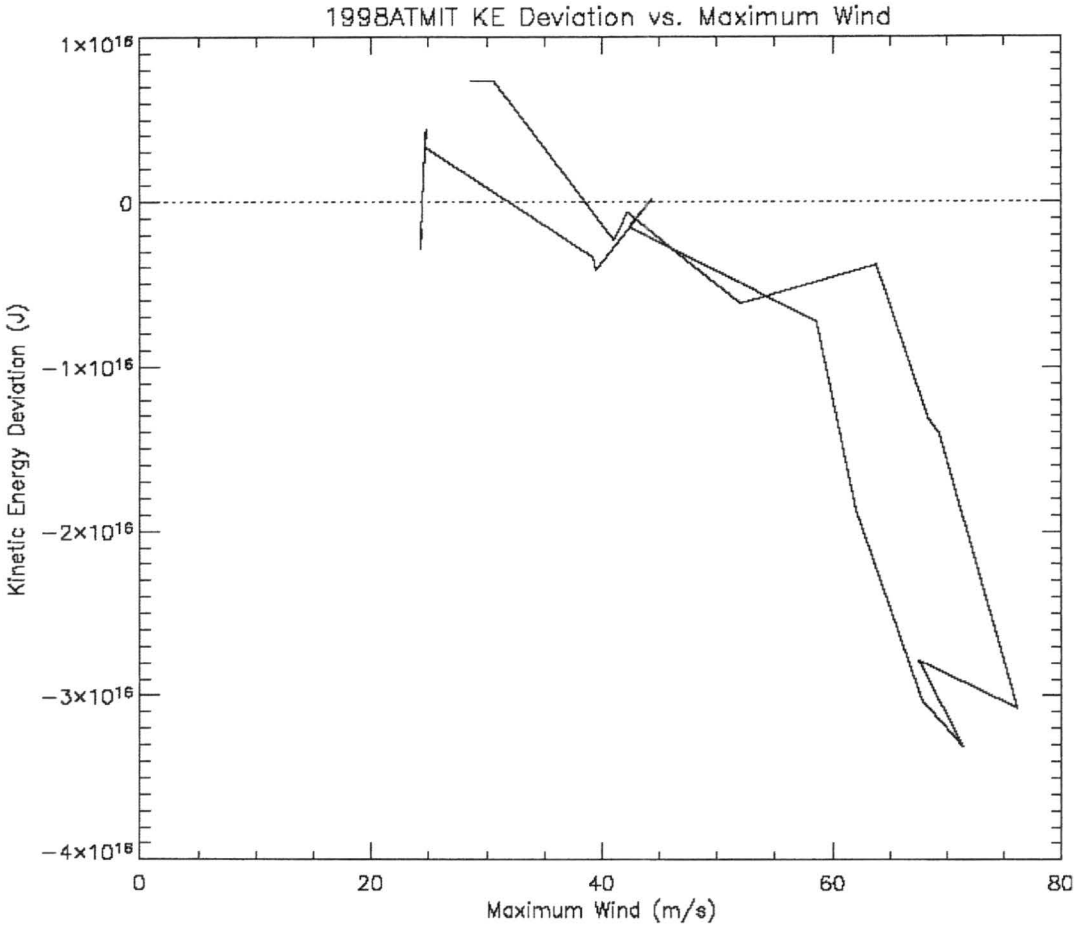

Figure 4.28: KE deviations from the mean curve versus intensity for Hurricane Mitch (1998) indicating the structural evolution of the storm.

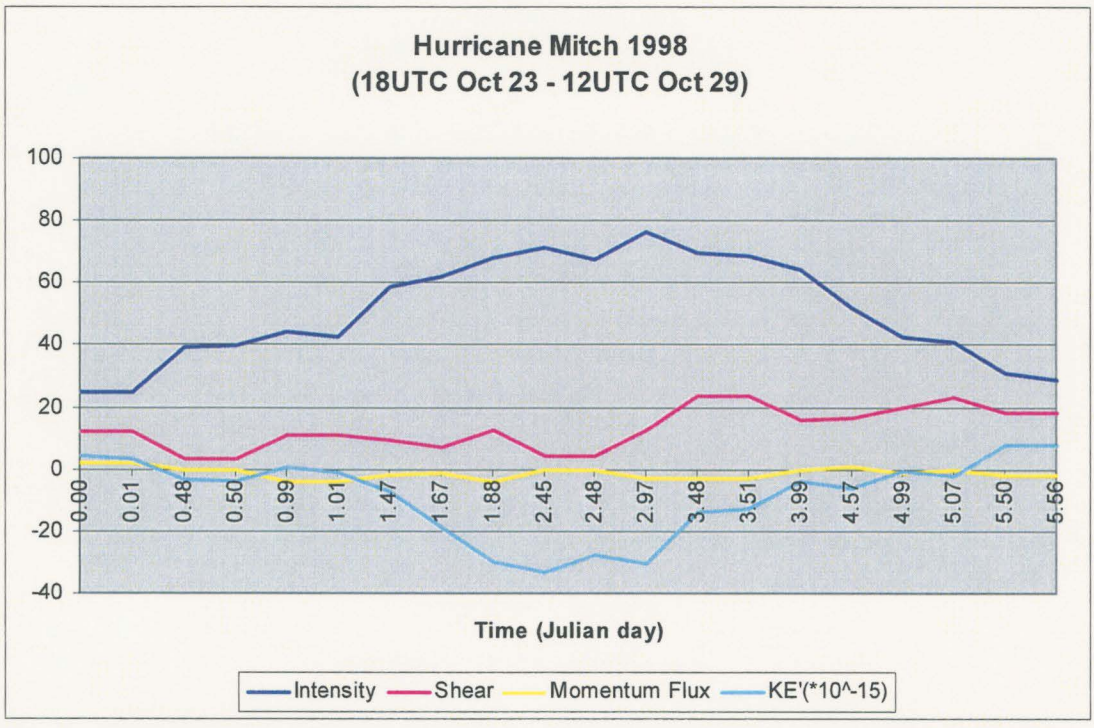

Figure 4.29: Time series of the intensity, environmental shear, 200 hPa eddy momentum flux convergence, and KE deviations from the mean curve for Hurricane Mitch (1998).

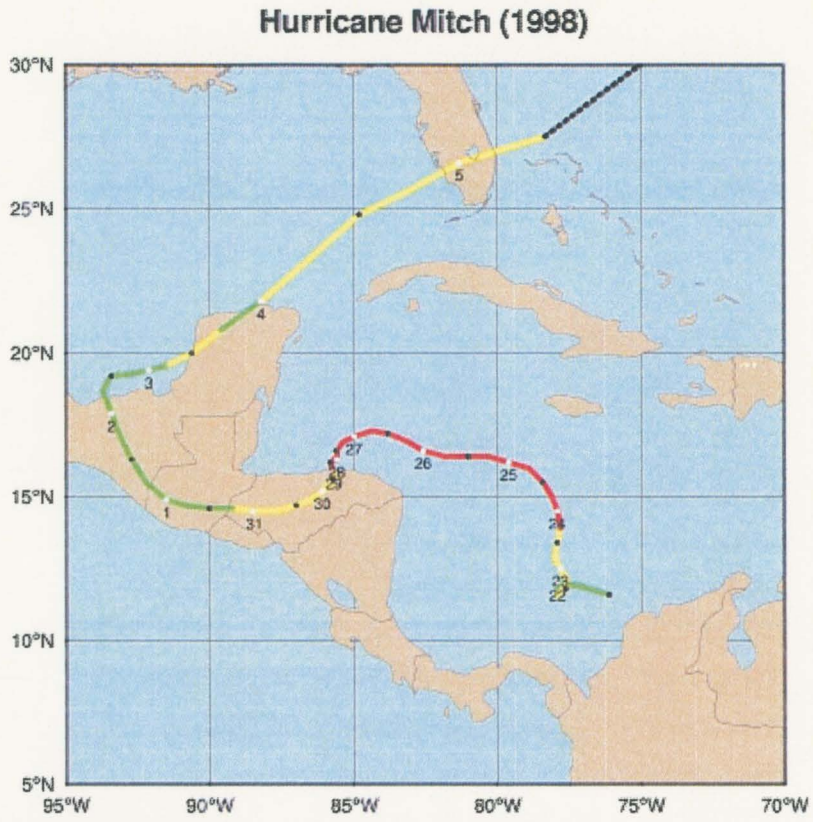

Figure 4.30: The track of Hurricane Mitch (1998) from NHC extended best-track. The colors indicate the storm's intensity throughout its lifetime and the numbered data points correspond to day of the month.

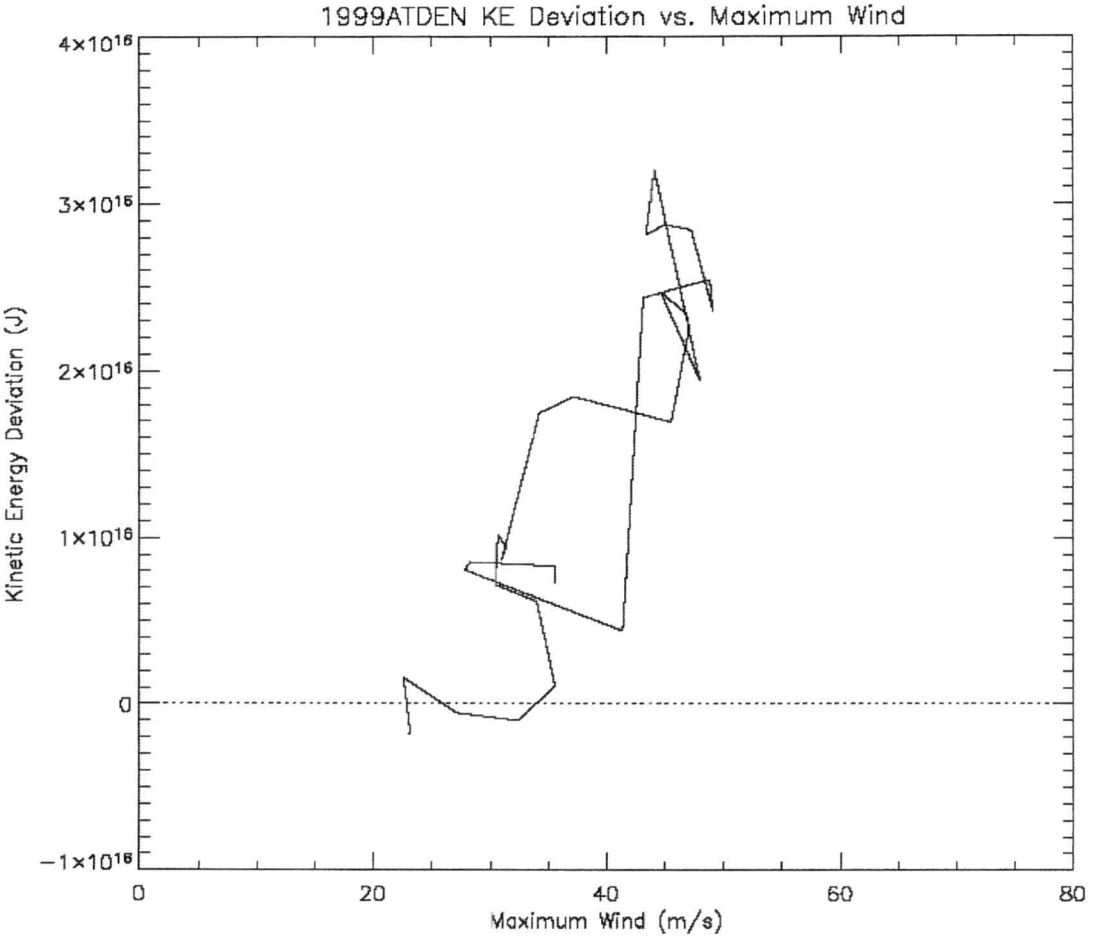

Figure 4.31: KE deviations from the mean curve versus intensity for Hurricane Dennis (1999) indicating the structural evolution of the storm.

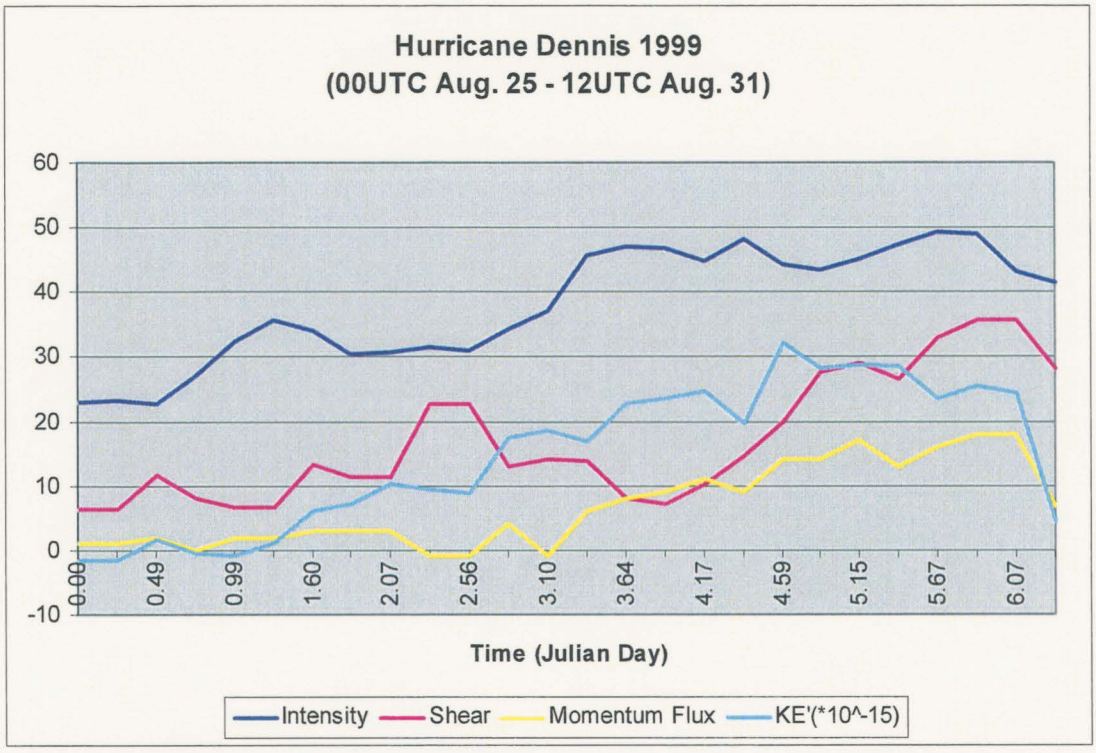

Figure 4.32: Time series of the intensity, environmental shear, 200 hPa eddy momentum flux convergence, and KE deviations from the mean curve for Hurricane Dennis (1999).

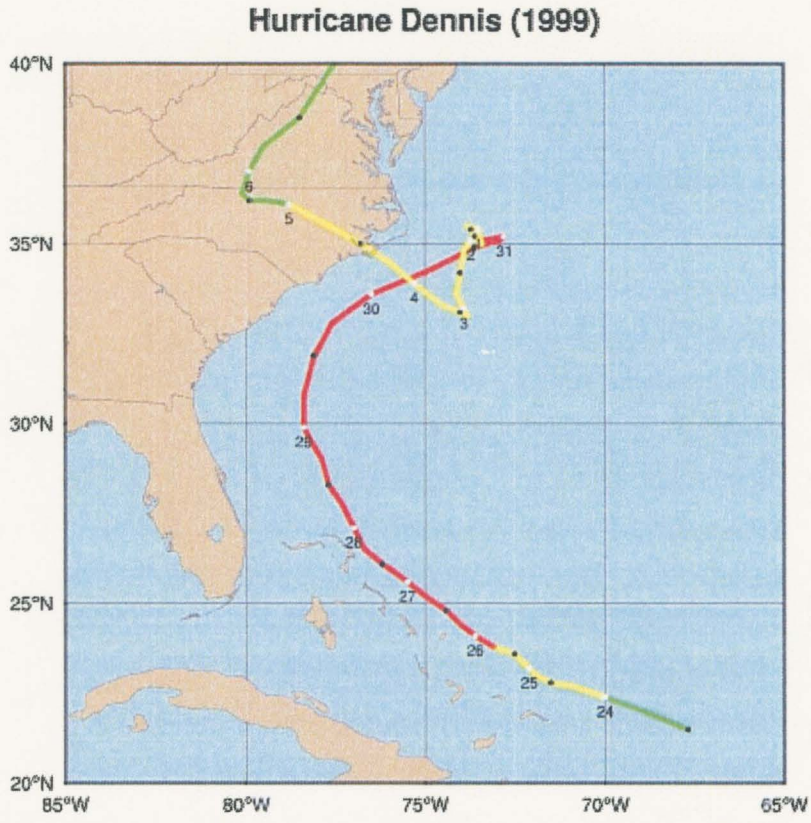

Figure 4.33: The track of Hurricane Dennis (1999) from NHC extended best-track. The colors indicate the storm's intensity throughout its lifetime and the numbered data points correspond to day of the month.

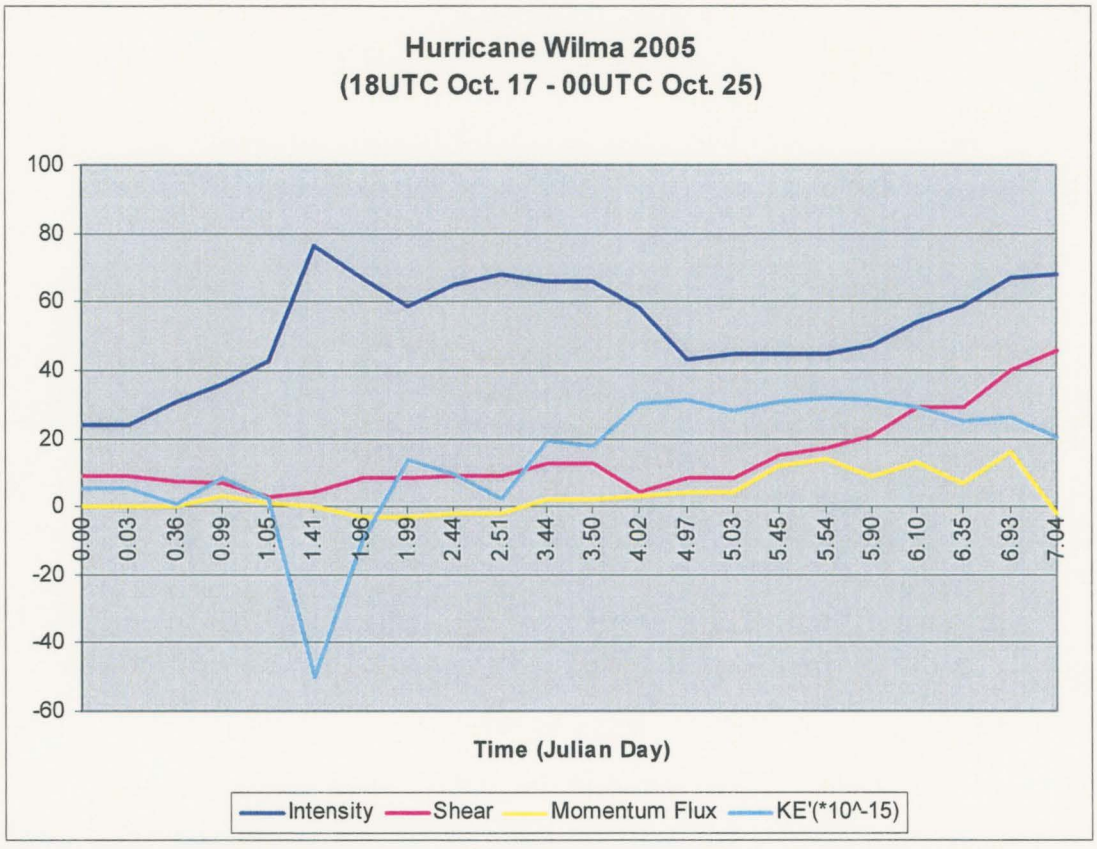

Figure 4.34: Time series of the intensity, environmental shear, 200 hPa eddy momentum flux convergence, and KE deviations from the mean curve for Hurricane Wilma (2005).

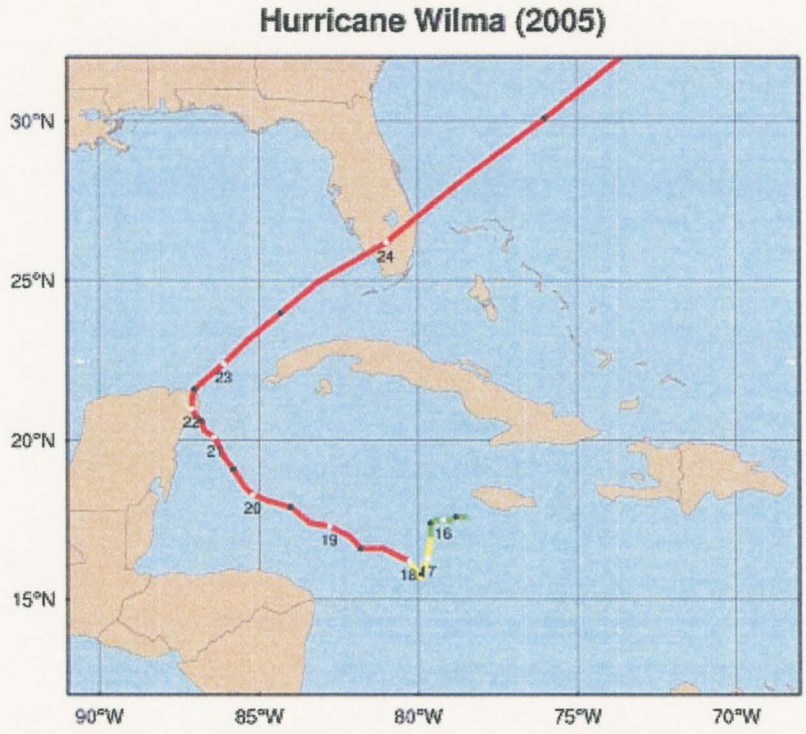

Figure 4.35: The track of Hurricane Wilma (2005) from NHC extended best-track. The colors indicate the storm's intensity throughout its lifetime and the numbered data points correspond to day of the month.

Table 4.1: Mean values for the storm/storm environment variables

	Group 0	Group 1	Group 2	Group 3	Group 4	Group 5	Group 6	Units
LAT	24	27	23.4	21.7	25.7	25.6	24.4	°N
LON	75	76.7	74.5	74.7	78.8	72.8	75.3	°W
RSST	28.5	28.1	28.5	28.8	28.6	28.1	28.7	°C
RHCN	53.7	40.4	52.8	63.2	54.2	44.1	54.9	kJ/cm2
T150	-65.8	-65.2	-65.7	-66.3	-65.5	-65.6	-65.8	°C
SHRD	16	19.1	16.3	14.7	16.6	17.8	14.8	kt
Z850	33.5	23.8	34.7	40.1	44.2	29.5	25.5	sec-1*10**5
REFC	3.4	3.0	3.5	3.0	4.4	3.3	3.5	m/sec/day, 100-600 km avg
IR8	67.1	52.8	67.4	73.9	65.3	62.6	66.7	%
REC1	70.9	91.0	60.1	58.7	81.8	77.1	81.7	km
REC6	-34.7	-18.2	-43.1	-42.9	-25.9	-27.9	-29.5	100*kt/km

Table 4.2: Probabilities and normalized differences in the means for the revised set of storm/storm environment variables

	WEAKENING		INTENSIFYING		MAINTAINING	
	Prob.	**ΔMean**	**Prob.**	**ΔMean**	**Prob.**	**ΔMean**
LAT	100.00%	-0.57	100.00%	0.63	96.88%	-0.19
LON	93.90%	-0.19	99.78%	0.35	98.12%	0.21
RSST	97.31%	0.25	90.83%	-0.14	100.00%	0.44
RHCN	99.91%	0.4	97.21%	-0.29	99.22%	0.35
T150	99.85%	-0.36	100.00%	0.51	91.75%	-0.14
SHRD	99.80%	-0.33	96.55%	0.22	99.97%	-0.35
Z850	95.76%	0.22	75.64%	0.08	78.40%	-0.08
REFC	74.35%	0.08	97.26%	0.23	65.03%	0.04
IR8	100.00%	0.44	100.00%	-0.26	93.48%	0.13
REC1	100.00%	-0.63	100.00%	0.47	89.22%	0.09
REC6	100.00%	-0.76	99.94%	0.52	65.94%	-0.05

CHAPTER 5 - CONCLUSIONS AND FUTURE WORK

5.1 Conclusions

The overall impact of a tropical cyclone is highly dependent upon the size and structure of the storm. A large storm has not only a greater area of damaging wind, but also creates a more substantial storm surge compared to a small storm of equal intensity. Evidence of this can be found by studying Hurricane Katrina (2005) and Hurricane Charley (2004). Charley was actually more intense at land-fall than Katrina, but was a much smaller storm and had significantly less storm surge than Katrina. Therefore, it is of critical importance to understand and forecast tropical cyclone structural evolution. This study aims to gain a better understanding of storm structural evolution with particular emphasis on determining the storm and environmental characteristics commonly associated with the various types of evolution.

In this study the inner core kinetic energy data recorded from 1995 through 2005 on Atlantic and East Pacific hurricanes has been used to establish a climatology of hurricane KE. A new KE hurricane scale has been presented that shows promising results in predicting hurricane destructive potential when applied to U.S. land-falling hurricanes from 1995 through 2005. This KE scale supplements the SSHS by more accurately representing the destructiveness of large hurricanes. The trends in the KE with respect to intensity and structure have also been examined and the data separated into six groups based upon storm attributes of: weakening, intensifying, or maintaining intensity, and growing or not growing size. It has been demonstrated that tropical cyclones either intensify while not growing, or weaken and growing in size. Occasionally, however, a

storm will deviate from this typical evolution and grow in a stage of intensification or not grow during a weakening stage.

To better understand the forces behind the structural changes in a storm in the different stages of intensity change, statistical testing was used to determine where significant differences exist between growing and non-growing storms for a wide range of variables and conditions. The basic environmental conditions were analyzed in a number of cases using climatological, persistence and synoptic variables which provide measures of the storm condition and environment. The structure of the heating was studied using profiles of cloud-top brightness temperatures and standard deviation in brightness temperatures from GOES IR imagery. Finally, the large-scale synoptic environments were examined using NCEP reanalysis data. Collectively these studies provide an idea of the underlying mechanisms responsible for storm structure change and growth.

Two main types of mechanisms that lead to growth in an intensifying tropical cyclone were proposed. The first method was through eyewall replacement cycles. During an eyewall replacement cycle storms initially lose intensity as the inner eyewall breaks down and is replaced by an existing secondary eyewall. The new larger eye may contract as the storm re-intensifies but generally remains larger than the previous eye. The result is a growth in the overall storm circulations. The second mechanism for growth was via environmental forcing. Forcing can be caused by momentum flux from a trough interaction where flow from an approaching trough can import momentum into the storm environment and contribute to an increase in the storm's circulations. Another source of environmental forcing could be from the baroclinic effects of a sheared

environment and/or temperature advection into a storm's inner core. A vertically sheared environment can cause the convection to be displaced to outer regions of the storm. Similarly, the advection of warm air into a storm will lead to enhanced convection in these regions of advection. An increase in the convection in the external regions of the inner core and into the outer core of the storm can cause an overall storm growth for an intensifying storm.

It is interesting to note that the conditions which create an environment most suitable for growth in an intensifying storm have the opposite effect upon the growth of a weakening storm. Without environmental forcing a storm will develop in a typical manner (intensifying/not-growing, and weakening/growing). With moderate forcing a storm may actually grow in size, but with too much forcing its circulations break down. Essentially, these conditions disrupt the normal structural evolution of a tropical cyclone causing a storm to evolve in an atypical manner such that an intensifying storm will grow in size and a weakening storm will simply fall apart.

5.2 Future Work

To gain a more substantial understanding of the causes of growth in a tropical cyclone further investigations are necessary. First of all, a more thorough look at the convective structure using the 2-dimensional GOES IR brightness temperature profiles would provide a way to determine the location of convective asymmetries. This is of particular interest in studying weakening but non-growing storms and intensifying but growing storms, both of which have more asymmetric convection than their growing/non-growing counterparts.

Also recall that previous studies, which used very simplified models, hypothesized a low-level momentum source as a means for structural change in tropical cyclones. However, this study has identified only upper-level momentum sources inducing structural changes. Further investigation of the low-level synoptic environments is necessary to determine if low-level momentum sources exist and are important. A modeling study may still be necessary if this further analysis of the low-levels is inconclusive.

The next step would be to carry out a full modeling study to better understand tropical cyclone structure change. The observed KE evolution of a few specific hurricanes in the 1995-2005 data set representing both types of structural evolution as well as the mechanisms that may contribute to tropical cyclone structural change, could be compared to WRF (Weather Research and Forecasting) model simulations of those storms. Furthermore, a complete energy budget calculation using a model study would allow the mechanisms behind tropical cyclone growth to be determined. This information could then be used to develop a prediction system for storm structure change. Such a prediction system would be a valuable tool for providing more accurate warnings to those areas in danger during the tropical cyclone seasons.

REFERENCES

Aberson, S., Black, M., Black, R., Burpee, R., Cione, J., Landsea, C., and Marks, F., 2006: Thirty Years of Tropical Cyclone Research with the NOAA P-3 Aircraft. *Bull. Amer. Meteor. Soc.*, **87**, 1039-1055.

Beven, J., cited 2006: Preliminary Report, Hurricane Dennis. [Available online at http://www.nhc.noaa.gov/1999dennis.html.]

Challa, M., and Pfeffer, R., 1980: Effects of Eddy Fluxes of Angular Momentum on Model Hurricane Development. *Journal of Atmospheric Sciences*, **37**, 1603-1618.

Cocks, S., and W. Gray, 2002: Variability of the Outer Wind Profiles of Western North Pacific Typhoons: Classification and Techniques for Analysis and Forecasting. *Monthly Weather Review*, **130**, 1989-2005.

Dunn, G.E., and B.I. Miller, 1960: Atlantic Hurricanes. *Louisiana State University Press*, 326 pp.

Eliassen, A., 1951: Slow thermally or frictionally controlled meridional circulation in a circular vortex. *Astrophys. Norv.*, **5**, 19-60.

Holland, G., 1983a: Angular momentum transports in tropical cyclones. *Quart. J. R. Met. Soc.*, **109**, 187-209.

Holland, G., and Merrill, R., 1984: On the dynamics of tropical cyclone structural changes. *Quart. J. R. Met. Soc.*, **110**, 723-745.

Guiney, J., and Lawrence, M., cited 2006: Preliminary Report, Hurricane Mitch. [Available online at http://www.nhc.noaa.gov/1998mitch.html.]

Kantha, L., 2006: Time to replace the Saffir-Simpson Hurricane Scale? *EOS,* **87**, 3-6.

Kistler, R., and Coauthors, 2001: The NCEP-NCAR 50-Year Reanalysis: Monthly means CD-ROM and documentation. *Bull. Amer. Meteor. Soc.*, **82**, 247-267.

Merrill, R.T., 1984: A comparison of large and small tropical cyclones. *Mon. Wea. Rev.*, **112**, 1408-1418.

Mueller, K., DeMaria, M., Knaff, J.A., and Vonder Haar T.H., 2006: Objective Estimation of Tropical Cyclone Wind Structure from Infrared Satellite Data. *Wea. Forecasting*, **21**, in press.

Pasch, R., Black, E., Cobb, H., and Roberts, D., cited 2006: Tropical Cyclone Report, Hurricane Wilma. [Available online at http://www.nhc.noaa.gov/pdf/TCR-AL252005_Wilma.pdf.]

Press, W., Teukolsky, S., Vetterling, W., and Flannery, B., 1986: Numerical Recipes in Fortran 77. *Cambridge University Press*, 610-613.

Riehl, H., 1979: Climate and Weather in the Tropics. *Academic Press*, 611 pp.

Shapiro, L., and Willoughby, H., 1982: The response of balanced hurricanes to local sources of heat and momentum. *Journal of Atmospheric Sciences*, **39**, 378-394.

Sundqvist, H., 1970: Numerical simulation of the development of tropical cyclones with a ten-level model. Part 1. *Tellus*, **22**, 369-390.

U.S. Air Force 53rd Weather Reconnaissance Squadron, cited 2006: Fact Sheets. [Available online at http://www.hurricanehunters.com/fact.htm.]

Weatherford, C., and W.M. Gray, 1988: Typhoon structure as revealed by aircraft reconnaissance. Part I: Data analysis and climatology. *Mon. Wea. Rev.*, **116**, 1032-1043.

Weatherford, C., and W.M. Gray, 1988: Typhoon structure as revealed by aircraft reconnaissance. Part II: Structural variability. *Mon. Wea. Rev.*, **116**, 1044-1056.

Willoughby, H., Clos, J., and Shoreibah, M., 1982: Concentric Eye Walls, Secondary Wind Maxima, and the Evolution of the Hurricane Vortex. *Journal of Atmospheric Sciences*, **39**, 395-411.

Zehr, R. M., 2000: Tropical cyclone research using large infrared image data sets. *Proc. 24th Conf. on Hurricanes and Tropical Meteorology*. Fort Lauderdale, FL, Amer. Meteor. Soc. 486-487.